

---

**UNIVERSITAT POLITÈCNICA DE CATALUNYA**  
**DEPARTAMENT D'ENGINYERIA DEL TERRENY, GEOFISICA I**  
**CARTOGRÁFICA**  
**ESCOLA TÈCNICA SUPERIOR D'ENGINYERS DE CAMINS,**  
**CANALS I PORTS**

---

**METODOLOGÍA PARA LA MODELACIÓN**  
**HIDROGEOLÓGICA DE MEDIOS FRACTURADOS**

TESIS DOCTORAL

PRESENTADA POR:

**LURDES MARTINEZ LANDA**

DIRIGIDA POR:

**JESÚS CARRERA RAMÍREZ**

**AGUSTÍN MEDINA SIERRA**

---

BARCELONA Diciembre 2004

---



## RESUMEN

Low permeability fractured media (LFFM) can be viewed as consisting of a virtually impervious matrix transversed by more or less conductive fractures. Experience dictates that a few of these concentrate most of the flow, this controlling the overall behaviour of the medium. Therefore, they need to be characterized for proper understanding of the system. Unfortunately, no widely accepted methodology is available to this end. In this context the objective of this thesis is three fold:

1. Define a methodology to model this type of media.
2. Explain how the explicit modeling of hydraulically dominant fracture helps in explaining scale effects.
3. Apply the methodology to two real case studies: the FEBEX at Grimsel and the Ratones mine.

The thesis consists of three independent but complementary papers. They are described below.

First, I present a methodology to identify the most significant water conductive fractures. The method is based on the interpretation of cross-hole tests, and is supported by geology, geophysics and hydraulic data. This methodology has been applied to the hydrogeological characterization of a granitic block within FEBEX experiment, Switzerland. Characterising this medium starts by achieving a geometrical identification of the fractures, which demands mainly geological and geophysical data. Single borehole hydraulic tests help in neglecting those transmissive fractures, but the only means to assess the connectivity between points and the fractures extent consists of conducting cross-hole tests. The resulting geometry is later implemented into a 3D finite element mesh, where the fractures are simulated as 2D elements that are embedded into a 3D porous media that includes the effect of minor fractures. Hydraulic parameters have been obtained from the joint interpretation of cross-hole tests with 3D numerical models, using automatic calibration techniques and adjusting all the measurements simultaneously. This methodology has proved capable of reproducing steady state heads, and also of quantifying groundwater flow to the experimental area of the FEBEX tunnel.

---

Different types of hydraulic tests (pulse, recovery, cross-hole and tunnel inflow measurements) have been performed in low permeability fractured granite around the FEBEX tunnel in Grimsel (Switzerland). We have interpreted the tests using conventional methods that treat the medium as a homogeneous one. Results display scale effects. Hydraulic conductivities increase, by orders of magnitude, with the volume of rock tested (from pulse to cross-hole tests). The objective of our work is to show that this scale effect is apparent. It reflects the limitations of the equivalent hydraulic conductivity derived from the homogeneous model interpretation of the tests. For this purpose, we have used the methodology described in the first paper. Transmissivity values used in the model to represent fractures are consistent with those derived from cross-hole tests, and the few single-hole tests at intervals intersecting fractures. On the other hand, matrix hydraulic conductivities are consistent with the remaining single-hole, short-time tests. This model can also be used to simulate observed heads and tunnel inflows. In summary, the final model is consistent with all the relevant measurements, taken at different support scales. This provides some insight into the issue of scale effects, which has been a topic of debate in the literature. In essence, the majority of small scale tests are performed in matrix intervals. Thus, any averaging of these values would suggest relatively small effective permeability. Yet large scale permeability of the rock is controlled by a few fractures, which provide high connectivity to the system, but are intersected by few testing intervals. As a result, large scale permeability is qualitatively different and quantitatively larger than small scale permeability.

Finally, the proposed methodology is applied to the hydraulic characterization of the “Los Ratones” uranium mine. The identification of the main heterogeneities in this case has been made by means of a combination of several techniques. Structural geology, together with borehole samples, geophysics, hydrogeochemistry and local hydraulic tests aided to locate all structures. Cross-hole tests were conducted to determine actually conductive fractures. When integrating all these data, a conceptual model is defined, which is used to calibrate cross-hole tests. From the results of the calibrations (cross-hole and other pumping tests), a set of model parameters that is consistent with all the observations is obtained. To verify that the site characterization is satisfactory, a blind-prediction has been carried out with the data recorded during a large-scale pumping test from the mine. This prediction has been done with the same

---

model parameters, grid and conceptual model that were calibrated with the previous tests, without modifying them. The results obtained with this simulation show a good response to the mine pumping, so that both the robustness and reliability of the model are confirmed.



## ACKNOWLEDGEMENTS

Esta es una de las partes de la tesis que más me cuesta escribir, y no es por ser desagradecida, sino por timidez y por que inevitablemente acabas olvidando a gente que ha sido importante durante el largo proceso que dura una tesis.

Por orden, para no perderme por las nubes, comienzo por mi director de tesis, Jesús Carrera. Realmente agradezco el tiempo que me ha dedicado, aunque a veces no lo parezca.

A la gente con la que he trabajado en el campo, Felip, Elena, Gustavo, Paloma, M<sup>a</sup>José, Andrés...en fin a la gente de AITEMIN, CIEMAT, ENRESA, IJA-CISC.

A Jordi Guimerà, con quien comencé en esta rama de la hidrogeología, y que pronto se marchó de la UPC y me dejó sola ante el peligro. A Luis Vives, con quien aprendí a hacer mallas. A Agustín Medina por escucharme y hacerme todos los cambios que le sugería en los programas.

También ha sido muy importante toda la gente con la que he convivido en la universidad a lo largo de todo este tiempo, Maite, Leo, Javi, Esther (y Carlitos), Jorge, Marisol, Enric, Imma, Peter, Paulino....

En especial a mi familia, (padres, hermanos, cuñados), en particular a mi tía Txaro y mi prima Enara que a veces parecen más entusiasmadas que yo, y que sí, si que podéis venir a la defensa... Y por supuesto, a Alfredo, por tu INMENSA PACIENCIA conmigo, por aguantar mis cambios de humor (y todo lo demás). Y mi peque Irati, con la que he compartido el final de mi tesis y a la que más le ha afectado esta recta final, (igual, inconscientemente, le ha llegado algo a través del cordón umbilical, su primera palabra ha sido “agua”, ¡pobreta!).





---

**TABLE OF CONTENTS**

RESUMEN .....	i
ACKNOWLEDGEMENTS .....	v
TABLE OF CONTENTS.....	vii
LIST OF FIGURES .....	ix
LIST OF TABLES.....	xvii
INTRODUCTION.....	xix

**Paper I: A METHODOLOGY TO INTERPRET CROSS-HOLE TESTS  
IN A GRANITE BLOCK**

1. INTRODUCTION .....	PI-3
2. METHODOLOGY .....	PI-6
2.1. Structural geology.....	PI-6
2.2. Hydraulic testing and preliminary interpretation.....	PI-6
2.3. Selection of conducting features. Geometrical conceptual model.....	PI-7
2.4. Numerical modelling .....	PI-8
3. APPLICATION TO FEBEX SITE.....	PI-8
3.1. FEBEX site description .....	PI-9
3.2. Identification of main structures.....	PI-11
3.3. Hydraulic testing.....	PI-13
3.4. Integrated interpretation of cross-hole tests.....	PI-16
3.5. Large scale model .....	PI-22
4. DISCUSSION AND CONCLUSIONS .....	PI-23

**Paper II: AN ANALYSIS OF HYDRAULIC CONDUCTIVITY SCALE  
EFFECTS IN GRANITE (FEBEX Experiment, Grimsel,  
Switzerland)**

1. INTRODUCTION .....	PII-3
2. SITE DESCRIPTION.....	PII-5
3. HYDRAULIC TESTING AND INTERPRETATION .....	PII-8
3.1. Pulse tests.....	PII-9
3.2. Recovery tests.....	PII-11
3.3. Integrated flowrate measures .....	PII-12

---

TABLE OF CONTENTS

---

3.4. Cross-hole tests ..... PII-13  
3.5. Cross-hole numerical interpretation (heterogeneous models) ..... PII-14  
3.6. Large scale numerical model ..... PII-17  
4. RESULTS AND DISCUSSION ..... PII-18  
5. CONCLUSIONS ..... PII-21

Paper III: A HYDROGEOLOGIC MODEL OF GRANITE ROCK AS A  
SUPPORT TO A MINE RESTORATION

1. INTRODUCTION ..... PIII-3  
2. TEST SITE ..... PIII-6  
3. HYDRAULIC CHARACTERIZATION ..... PIII-9  
    3.1. Scale effect..... PIII-12  
4. NUMERICAL MODEL ..... PIII-14  
    4.1. Model calibration of the cross-hole south test ..... PIII-17  
    4.2. Prediction of pumping from the mine..... PIII-19  
5. DISCUSSION AND CONCLUSIONS ..... PIII-22

GENERAL CONCLUSIONS ..... C-1  
REFERENCES ..... Ref-1

---

**LIST OF FIGURES**
**PAPER I: A METHODOLOGY TO INTERPRET CROSS-HOLE TESTS IN A GRANITE (FEBEX, GTS).**

- Figure 1: Drawdowns observed in response to pumping interval I2-1. Notice that  $\log(t/r^2)$  is used as horizontal axis (where  $r$  is distance to the pumping point). Fast responses suggest good connectivity. In this case F22-2 is likely to be connected to I2-1 (pumping borehole) through a flowing fracture.....PI-8
- Figure 2: Physical situation of the experiment. The Grimsel Test Site (GTS) is situated in Switzerland; the site corresponds to the Northeast tunnel within the experimental network of galleries. The radial boreholes are located at the end of the FEBEX tunnel, surrounding the experimental site. The cross-hole tests were conducted at these boreholes.....PI-10
- Figure 3: Borehole instrumentation. All the boreholes that surround the FEBEX tunnel are isolated into intervals by means of packers. Each interval is equipped with a packer pressure line, an interval pressure line and a water recirculation line. Pressure lines are connected using a tube with a pressure transducer, which is located at the FEBEX tunnel (outside the experimental zone). The five pumping intervals are drawn in black.....PI-11
- Figure 4: Definition of geometry. This figure shows that just a few of the mapped structures in the tunnel (above, Pardillo et al., 1997) are hydraulically relevant so as to treat them individually. Hydraulically important structures are shown in the lower part of the figure (lamprophyre, Fr-1, Fr-2, Fr-5 and Fr-7). These structures are the only ones included explicitly in the model. The remaining structures are treated as part of an equivalent porous medium.....PI-12
- Figure 5: Opportunistic methods to identify hydraulically relevant structures. On the left, pressure variations for intervals 3 and 4 of borehole FBX 95-002 are plotted, representing the response to the tunnel borehole machine (TBM) advance. When the TBM is working, pressure increases at the intervals. If a structure (Fr-2, lamprophyre) connecting the tunnel with the interval is intercepted, then water flows towards the tunnel
-

and pressure diminishes (peaks in pressure curves at borehole FBX 95-002-4). On the right, the response to ventilation of the tunnel are represented. It is not possible to identify any particular structure, because results account for the integrated response of the whole domain (matrix + fractures). Ventilation effects are analogous to a pumping test. The observation points in the picture are located at 2 m-distance from the FEBEX tunnel wall..... PI-13

Figure 6: Intervals may need several days to reach equilibrium conditions after borehole instrumentation. Once this happens, pressure is not constant but exhibits a natural evolution. In order to interpret the hydraulic tests at these points, it is necessary to filter any effect that has not been caused by the test. .... PI-14

Figure 7: Interpretation of cross-hole test pumping at point I2-1, showing the observation points with a larger response to the test. Transmissivities (T) estimated under the hypothesis of a homogeneous model are very similar for all points (from 0.7 up to  $1.4 \cdot 10^{-9} \text{ m}^2 \cdot \text{s}^{-1}$ ), whilst apparent storage coefficients (S) are highly variable (from 0.01 up to  $15 \cdot 10^{-6}$ ). This variability reflects the connectivity between pumping and observation points. A high S is an indication of low connectivity and, conversely, low apparent S indicates high connectivity (Meier et al., 1998)..... PI-15

Figure 8: Simplified mesh and three-dimensional geometry. The 3D mesh is built by replicating the 2D mesh along the third dimension (3D blocks delimited by not necessarily parallel layers). Then, all the elements of the geometry are projected onto this 2D mesh. Those geometrical elements –fractures (2D elements), boreholes (1D elements)– are embedded at their true position within the 3D elements (below, right). All of them are connected by the nodes that share with other finite elements of the mesh..... PI-17

Figure 9: Geometry of cross-hole tests model. a) View of the 3D mesh (notice the lamprophyre dyke). b) Zoom of a horizontal section of the experimental zone (notice the intersections of hydraulically relevant features: lamprophyre, fractures Fr-1, Fr-2 and Fr-5) and the observation points that are situated in the horizontal boreholes. This mesh corresponds to the cross-hole test conducted at the pumping interval I2-1, where the

- 
- discretization is finer and the size of the elements is of the order of 0.5 m. c) 3D perspective of the main fractures at the experimental scale. .... PI-18
- Figure 10: Fits obtained through joint interpretation pressure build-ups in test I2-1 using the grid of Figure 9. Structures included explicitly in the model are shown in the plan view above. It can be seen that injection is channelized by the lamprophyre. Response is marked at intervals intersected by, or close to, the lamprophyre (such as F12·3 or F22·3), specially F22·2, wich required a highly conductive channel (Fr-7). The response dies away form the lamprophyre dike (F22·1, F12·2, F12·1). It is distance to the lamprophyre, rather than to the pumping interval, what controls response..... PI-21
- Figure 11: Geometry of the large scale model. The dashed portion represents the area that was characterized in detail. As the effect of relatively small fractures was modeled in detail, the hydraulic conductivity of the 3D blocks in this portion is much smaller than in the remaining. ....PI-22
- PAPER II: AN ANALYSIS OF HYDRAULIC CONDUCTIVITY SCALE EFFECTS IN GRANITE (FEBEX Experiment, Grimsel, Switzerland)**
- Figure 1: Location of the Grimsel Test Site (GTS), Switzerland, including the tunnel where FEBEX experiments were conducted. Four boreholes (between 70 and 150 m-long) were drilled from the main tunnel around the experimental site (BOUS 85·001 and 002, FEBEX 95·001 and 002). 19 boreholes, averaging 15-m length, were drilled according to a radial distribution from the FEBEX tunnel (inset in the upper right corner).....PII-6
- Figure 2: View of the 23 control boreholes in the test area. They are divided into intervals by means of packers. Each interval is equipped with a pressure intake, which is connected to an outer pressure transducer, and with a water recirculation intake for performing hydrochemical sampling and hydraulic tests. This leads to a total of 64 observation points.....PII-7
- Figure 3: Pressure records at one of the observation points, from the beginning of the borehole instrumentation, displaying the interval history. The packers' position, in this borehole, has
-

been changed three times. The picture shows how pressure recoveries within the tested interval after each instrumentation change, and also as a response to tests and other events, such as drilling of FEBEX tunnel, ventilation of the tunnel, hydraulic tests conducted at other points. The effect of pulse-tests can not be identified at this scale (one data point per day), because they cause short-time perturbations.....PII-8

Figure 4: Interpretation of the recovery to three typical pulse tests. Shown are the fitted response (continuous line) and some measured data (dots, most points have been deleted for clarity). Responses depend on the geological structures within the vicinity of the boreholes. B23-2 lies in the rock matrix, thereby presenting a higher drawdown and a slower recovery. The other two tests were performed in intervals intersecting fractures, which imply a lower drawdown and a faster recovery. Notice the difference in the shape of the recovery curves when compared to that of B23-2.....PII-10

Figure 5: Recoveries in response to the instrumentation of the boreholes were interpreted using Horner's method (Horner 1951). .....PII-11

Figure 6: Schematic descriptions of methods used to estimate inflow rates to the experiment zone. (1) pressure values recorded at borehole Fbx95-002 and within the tunnel are used to obtain a pressure gradient, which yields an estimate of the inflow rate under the assumption of radial flow. (2) consists of gauging directly the drainage to the tunnel. Method 3 is represented in the third part of the figure, which contains the geological map after a long period without ventilation of the tunnel (Guimerà et al., 1998). This method consists of placing cellulose plates to quantify the inflow rate towards the tunnel walls. Plates were situated at seepage points within the tunnel.....PII-12

Figure 7: Results of analytical interpretation of the cross-hole test carried out at point Fbx2-4. Responses are interpreted by assuming homogeneous media and fitting the build-up curves for each point separately. The resulting transmissivity and storativity are shown for each interval. Notice that transmissivity variations are minimal (ranging between  $8.3E-10$  and  $16E-10 \text{ m}^2 \cdot \text{s}^{-1}$ ), whereas the storage coefficient varies by orders of magnitude (from  $2.6E-07$  up to  $54E-07$ ). This gives

- insight into the heterogeneity of the medium, since intervals that have an apparent low storage coefficient are well connected to the pumping well (Meier et al., 1998; Sánchez-Vila et al., 1999).....PII-14
- Figure 8: Results of numerical inverse interpretation of Fbx2.4 cross-hole test with a mixed model that includes hydraulically relevant fractures embedded in a 3D homogeneous medium that includes matrix and minor fractures.....PII-15
- Figure 9: Hydraulic conductivities obtained from interpretation of hydraulic tests versus test scale. The horizontal axis represents a qualitative evaluation of the size of the rock affected by each test type. Within each test type, the ranking is arbitrary. The values of equivalent hydraulic conductivity increase with the volume of rock sampled in the test. Each of the columns (for cross-hole tests) refers to a different test, with a total of 5 tests. The geometric mean ( $K_G$ ), effective 3-D conductivity ( $K_{eff3D}$ ) and the median ( $K_M$ ) have been calculated for each type of test. There is an increase of all these values with the scale of the test. The two last columns represent the results of 3D numerical models used to interpret cross-hole tests and large-scale FEBEX data, respectively. In these columns, symbols identify hydraulically relevant fractures (values between  $10^{-10}$  and  $10^{-7}$  m/s) and minor fractures lumped with the matrix (values below  $10^{-11}$  m/s).....PII-18
- PAPER III: A HYDROGEOLOGIC MODEL OF GRANITE ROCK AS A SUPPORT TO A MINE RESTORATION**
- Figure 1: Geological map of Albalá Granitic Pluton with location of the Mina Ratones area (ENRESA, 1996; Escuder Viruete and Pérez Estaún, 1998).....PIII-6
- Figure 2: Fault zone architecture of Mina Ratones area obtained from structural, seismic, core and well log data (Escuder Viruete and Pérez Estaún, 1998; Carbonell et al., 1999; Escuder Viruete, 1999; Pérez Estaún, 1999). The main identified structures are the North Fault, the South Fault and the 27 and 27' Dykes. Other relevant brittle structures of minor size are 474, 478, 285 and 220 Faults.....PIII-7
- Figure 3: Chemical and geophysical logs at the boreholes. This figure shows some of the records obtained for borehole SR1, which

have helped to identify two structures: dyke 27 and fracture SR1-3. The upper logs only display the effect of dyke 27, because water flowing through SR1-3 has circulated previously through the mine, which causes water to acquire the typical properties of mine water. In the lower logs, however, the effect of both structures can be noticed, especially in the gamma log, due to the fractures fillings. Flowmeter measurements at the borehole vertical, with an upwards flow of 3 rpm (pumping) indicate that, below 56 m depth, there is little water movement up to the intersection with dyke 27. This provokes a water inflow with upwards circulation. The same applies to a lesser extent to when intercepting fracture SR1-3. ....PIII-8

Figure 4: Results from preliminary interpretation of the South cross-hole test (pumping at SR4-1). Transmissivity and storativity are derived by fitting each borehole drawdowns, one-at-a-time, using Theis' model. Degree of connectivity is derived from the estimates of storage coefficients. T varies from 4 to  $64 \cdot 10^{-5} \text{ m}^2 \cdot \text{s}^{-1}$ , while S ranges from 1 to 53. We take S estimates to reflect connectivity. A small S (fast response) implies good hydraulic connection between pumping and observation wells. This suggest that best connections take place between the pumping interval and points S10 and SR1-3, whilst points S5 and SR1-2, and, especially point PM, were damped by the mine influence (which behaves as a constant head boundary). ....PIII-11

Figure 5: Transmissivity values obtained from interpretation of hydraulic tests performed at varying scales in different holes and intervals. In general, transmissivity grows with the scale, except for the cross-hole test, which was performed in the highly transmissive portion of the site. ....PIII-13

Figure 6: Model geometry. The model consists of two areas The "hydraulic models matrix" is the area where are concentrated the knowledge, the matrix is treated as equivalent porous media with the main structures inside. The "external matrix" is just an extension towards the boundaries, equivalent porous media without identified fractures. The hydraulic conductivity of the latter will be higher, since it is treated as an equivalent porous medium, where the main structures have not been identified. At the local level (right picture), the main



---

structures are explicitly taken into account, including the fractures, dykes 27, 27' and SR3, and the mine itself, which is excavated in both dykes. The structures are represented by means of two-dimensional elements. The Maderos creek is embedded in the Southern fault. Projections of the boreholes that are closer to the mine are represented by a black dot on surface and by an arrow at the borehole end. ....PIII-14

Figure 7: Schematic vertical section representing variations in data derived from the hydraulic characterization of borehole SR5 (500-m deep) indicate that hydraulic conductivity changes with depth. This fact was studied by Stober (1997). The model uses a modification of Stober's equation: hydraulic conductivity is kept constant up to the base of the fractured granitic unit (200 m), then changes with depth down to 350 m. From there, it remains constant down to the model bottom. ....PIII-15

Figure 8: Main structures implemented in the model as planar structures. They are defined by two-dimensional elements. The model honors surface traces and dips. Downwards extension of these structures is performed with the aid of geophysics, structural geology and intersections at boreholes. The Northern fault is the more vertical one at its upper section, and it is cut and disconnected by faults 474 and 285 towards the South. The mine is also represented by means of two-dimensional elements, because it results from the exploitation of the dykes. The Southern fault is zoned at the surface, in order to reproduce the altered zone in which the stream is embedded, where most of the water flows. ....PIII-17

Figure 9: Results (line) obtained after calibrating the SR4-1 cross-hole test data (dots) with the three-dimensional model. ....PIII-19

Figure 10: Blind prediction of the long term pumping of the mine (point PM), using calibrated with the SR4-1 cross-hole test. This pumping lasted for four months, and its influence reached all the observation points. ....PIII-20

Figure 11: Fits obtained from the pumping test calibration model. ....PIII-21

Figure 12: Comparison between altered unit observation points at the prediction and calibration. ....PIII-22

---



---

**LIST OF TABLES**
**PAPER I: A METHODOLOGY TO INTERPRET CROSS-HOLE TESTS  
IN A GRANITE (FEBEX, GTS)**

Table I: Structures considered in each of the independent calibrations of cross-hole tests. Three of these structures were only affected by one test (Fr-1, Fr-5 and Fr-7). .....PI-19

Table II: Flowrate through the dominant structures at different scales. As the model scale increase, it is likely to intersect longer and more transmissive fractures, causing increasing flow rates .....PI-23

**PAPER II: AN ANALYSIS OF HYDRAULIC CONDUCTIVITY SCALE  
EFFECTS IN GRANITE (FEBEX Experiment, Grimsel,  
Switzerland)**

Table I: Statistics of the Fbx2-4 cross-hole test. The error units are meters.....PII-16

**PAPER III: A HYDROGEOLOGIC MODEL OF GRANITE ROCK AS A SUPPORT  
TO A MINE RESTORATION**

Table I: Parameters obtained after calibration of the South cross-hole test. Units are written in m and sec, but the right dimensions (associated to the scale of each structure in the model) are explicitly defined. Transmissivity values indicate which it changes with depth: the first value holds for the upper 250m (constant parameter), the second value applies to the bottom of the domain -both for the matrix and the fractured belts. The storativity of the "fractured belts lehm" is negligible in the model ( $1.0 \cdot 10^{-30}$ ), to prevent the artefact that water might be withdrawn from that zone.....PIII-18



## INTRODUCTION

### 1.1. Motivation

Low permeability fractured media (LPFM) have been traditionally ignored in hydrogeology because they are not good sources of water. However, the situation has changed in recent years because LPFM are candidates to host wastes; they may be the only reliable source of water in some areas and they may feed wetlands and other aquatic environments. As a result, interest in LPFM has increased.

Unfortunately, LPFM are complex. The rock matrix is virtually impervious and most fractures do not carry water. In fact, it is frequently observed that one or two fractures conduct more water than all the rest together. This occurs at all scales and there is a chance that finding increasingly permeable areas may grow with the scale of the problem. As a result, effective permeability also increases. This is termed scale effect and contributes to the halo of mystery that surrounds LPFM. Hence, it is not surprising that no widely accepted methodology is available to treat them. In fact, numerous approaches are available. However, most of them can be viewed as combinations of equivalent and discrete fracture networks described below.

There are several approaches to modeling this type of media, but they can be summarized in two main methods: continuum media models and discrete fracture models.

Continuum media models adopt Darcy's law in the whole domain. They are characterized because of an apparent simplicity, but it is not direct to obtain the properties of a continuum medium from measurements made within the fractures. Homogeneous continuum medium models are usually used for a preliminary interpretation of hydraulic tests. If we accept that water is more accessible in the best connected fractures rather than within the matrix, multiple conceptualizations of the continuum medium can be proposed. The application of continuum stochastic models (Neuman, 1988; Vesselinov et al, 2001; Ando et al., 2003) aids at reproducing the heterogeneity of the medium.

Discrete fracture network models assume that the fractured medium can be represented by a fracture network embedded into an impervious matrix. The hydraulic

---

behaviour of the medium is thus controlled by the fracture network properties. These models are essentially stochastic in nature (Long et al., 1982; Dershowitz, 1984; Smith and Schwarz, 1984; Cacas et al., 1990; Anderson and Thunvik, 1986). Only a fraction of all existing fractures contributes to groundwater flow, which makes it complicated to identify the dominating structures. In fact, just a small fraction of the fractures plane plays a relevant role. This has led to developing the concept of channel networks (Moreno and Neretnieks, 1993).

Fracture network models may be useful for synthetic cases, i.e. performance assessment analyses. But it is necessary to determine which are the important fractures and where are located when a decision has to be taken in real situations, such as the choice of an underground repository. Mixed models represent an intermediate approximation between discrete fracture network and continuum medium models (Gomez-Hernandez et al., 2000). The approximation consists basically of identifying the dominating fractures and including them explicitly, whilst the matrix is treated as a porous equivalent medium that accounts for the effect of minor fracturing too. This concept has the double advantage of the simplicity associated to continuum models and the precision of counting on the dominating fractures. But it has also some problems, such as the difficulty to identify the main hydraulic structures. This is done from detailed geological data. The fractures are implemented in the model in a deterministic way, whilst the remaining fracturing is accounted for in a stochastic way.

We have opted by integrating all the available information (geology, geophysics, hydraulic tests) to achieve a better identification of those dominant structures. Fractures are represented in a deterministic way as bidimensional planes that are embedded in a 3D homogeneous matrix which includes the effect of minor fractures. The methodology has been applied to two real cases that are presented in the thesis.

## **1.2. Objectives**

The main objective of this thesis is to develop a methodology to model low permeability fractured media. This motivates three subsidiary objectives, namely:

1. To prove that it can be applied to real situations
2. To analyze whether it can explain scale effects
3. To test if the methodology can yield predictive models

### 1.3. Structure

The above objectives constitute the main topics of the three subsequent chapters. In fact, they are papers that complement each other, but they can be read independently.

The first paper presents the proposed methodology to modelling LPFM. Characterising this media starts by achieving a geometrical identification of the main fractures. Single borehole hydraulic tests help in neglecting low transmissive fractures, but the only mean to assess the connectivity between points and the fractures extent consists of conducting cross-hole tests. Geological, geophysical and hydraulic data are used to complete the characterisation of the medium. This methodology has been applied to the hydraulic characterization of a granitic block within FEBEX experiment, in Switzerland.

The second paper focuses on the scale effect problem, which consists of the apparent increase of the equivalent hydraulic conductivity with the scale of the test. We have performed several types of hydraulic tests at the same FEBEX experiment, and interpreted the measurements by means of homogeneous conventional models. The results show that the scale effect appears. In essence, most small scale tests affect only the matrix. Thus, any averaging of the hydraulic conductivity parameters would result in a relatively small effective permeability. Large scale permeability of the rock is controlled by a few fractures, which provide high connectivity to the system, but are intersected by few testing intervals. Using the above described methodology allows to remove this effect and to interpret the tests at different scales.

The last paper presents the application of the methodology to the Mina Ratones granitic area (Cáceres, Spain). The identification of the dominant fractures has been made using the geological, geophysical, hydrochemical and hydraulic testing data. The construction of the model has been made by integrating all these data. To verify that the site characterization is satisfactory, a blind-prediction has been carried out with the data recorded during a large-scale pumping test from the mine. The results obtained with this simulation show a good response to the mine pumping, so that both the robustness and reliability of the model are confirmed.





---

PAPER I

**A METHODOLOGY TO INTERPRET CROSS-HOLE TESTS IN A  
GRANITE BLOCK**

Lurdes Martínez-Landa and Jesús Carrera

Submitted to

Journal of Hydrology



---

## 1. INTRODUCTION

Hydrogeology of low-permeability fractured media has received an increasing attention during recent years, especially because of their potential as geologic barriers for the storage of radioactive wastes (Berkowitz, 2002; Neuman, 2005). As a result, a large number of experiments have been carried out in these formations: Äspö in Sweden (Tsang et al., 1996; Svenson, 2001b); Grimsel in Switzerland (Davey Mauldon et al., 1993; Martinez-Landa and Carrera, 2005a), Fanay-Augères in France (Cacas et al., (1990)); Mirror Lake in Utah, USA (Shapiro and Hsieh 1991; Day-Lewis et al., 2000); El Berrocal (Guimerà et al., 1995) and Ratones mine (Martinez-Landa et al., 2005b), both in Spain. In particular, the FEBEX experiment (Full scale Engineered Barrier Experiment) aims at studying the engineered barrier surrounding the waste and its interaction with the host rock (granodiorite) (ENRESA 1998). The experiment has been carried-out at the Grimsel Test Site (GTS) in the Swiss Alps. A number of tests have been carried-out at different scales around the experimental tunnel. Our work is motivated by the need to use these experiments to characterize the rock in detail. Our model was to be used by other teams working with the barrier.

Characterising low permeability fractured media is a complex task because hydraulic conductivity can vary over several orders of magnitude within short distances. Variability is caused by fractures or fractured zones that are interconnected and strongly condition groundwater flow, as most of the flow is carried through a limited number of major fractures. Their location and connectivity must be known in order to determine accurately the hydraulic behaviour of the medium. Since this is difficult, a number of approaches have been developed (Selroos et al., 2002; Bodin et al., 2003; Knudby and Carrera 2005a). They can be classified in three groups, as outlined below.

The first approach, continuum porous model consists of accepting from the outset that the fracture geometry cannot be described with sufficient accuracy. Instead, its effect can be obtained from hydraulic tests. In fact, the simplest version of this approach is widely used for a preliminary interpretation of hydraulic tests, since they assimilate the domain to a homogeneous medium by means of an equivalent hydraulic conductivity (Hsieh and Neuman, 1985). Acknowledging the role of fractures may require the use of stochastic methods. Ideally, if sufficient data have been collected one should be able to represent its variability accurately (Neuman, 1988; Vesselinov et al.

---

2001; Vesselinov and Neuman, 2001; Ando et al., 2003). It is not clear, however, that standard geostatistical methods can handle the continuity imposed by fractures. In fact, Neuman (1988) argues for deterministic incorporation of dominant fractures whose geometry is well known.

The second type of models takes the opposite view and consists of reproducing all fractures while usually ignoring the matrix. Discrete fracture network models represent the heterogeneity that is inherent to fractured media through networks of fracture planes. The basic assumption is that flow takes place mainly through such planes and, therefore, that flow through the rock matrix is negligible (Long et al., 1982; Dershowitz, 1984; Smith and Schwarz, 1984; Anderson and Thunkvik, 1986; Dverstop and Anderson, 1989; Cacas et al., 1990; Dershowitz et al., 1991). This hypothesis involves some limitations, since few of the fractures are hydraulically relevant. Furthermore, their location and extension is highly uncertain. Therefore, rather than simulating the actual network, DFNMs are based on stochastic simulation of the location, extension and properties of the fractures. As such, they may be more useful for risk evaluations, which emphasize uncertainty, than for site-specific models, which seek close reproduction of site conditions. Following Neretnieks (1983), it has become increasingly apparent that even within a fracture, water flow tends to concentrate through channels, which occupy a relatively small portion of the aquifer (Neretnieks, 1993; Tsang and Neretnieks, 1998). This led to the definition of channel network models, which can be viewed as a particular example of fracture network models, where preferential flow paths within fracture planes are represented through channels (Neretnieks, 1983; Moreno and Neretnieks, 1993; Gylling et al., 1999). Moreno and Tsang (1994) showed that channelling can be caused by multigaussian (i.e., without explicit connectivity) heterogeneity. This will cause channels to shift as the hydraulic gradient changes with time. Channels can also be caused by continuous zones of high transmissivity within a fracture plane, generated by rock deformation, but these are difficult to characterize (Meier et al., 2001). As a result, while acknowledging that channels may be needed to understand transport, they are hard to use to represent site specific conditions.

Site specific models require a proper description of connectivity (Knudby and Carrera, 2005a and b). This, together with the observation that most of the flux takes place through a few fractures, has prompted the development of a mixed or intermediate

---

approach. It consists of explicitly modelling hydraulically dominant fractures that are embedded in a 3-D continuum model representing minor fractures. Both the continuum and the fracture planes can be treated as heterogeneous. This concept has been adopted by several authors because of the simplicity of simulating a continuum domain, while taking into account the main fractures or fractured zones which carry most of the water (Kimmeier et al., 1985; Kiraly 1985, Carrera and Heredia, 1988; Shapiro and Hsieh, 1991; Day-Lewis et al, 2000, Carrera and Martínez-Landa, 1999). The problem with this concept is how to define and characterize these dominant fractures.

Fracture generation can be done stochastically (generating permeability fields) or in a deterministic way. Some authors identify structures based on borehole information, by assessing the connectivity among points with the results obtained from hydraulic tests (Day-Lewis et al, 2000; Svenson, 2001a and b). Gómez-Hernández et al (2000) and Hendriks and Gomez-Hernández (2002) add the geologic knowledge derived from detailed studies. This allows one to reproduce the structures that were identified by deterministic methods and to include the rest of fractures stochastically. Martínez-Landa et al. (2000) also identify the main fractures by combining all available data (detailed geology, hydraulic tests), but they represent the fractures by means of 2D planes, whilst the rest of unidentified fractures are implicitly included in the 3D rock porous background and not accounted for individually. Despite these efforts, a methodology for identifying and characterizing dominant fractures is lacking.

The objective of this work is precisely to present a methodology to achieve that goal. This methodology is based on the knowledge of structural geology, at different scales, combined with geophysics and hydraulic data, to identify the main fractures. Cross-hole hydraulic tests are used to define the fracture extension and hydraulic connectivities.

The article begins with the description of a general methodology to model low-permeability fractured media. Then, this methodology is applied to the FEBEX project, which is described prior to explaining the hydraulic tests interpretation, the process of identifying the main structures and their implementation in a 3D numerical model. Finally, some conclusions of the whole modelling approach are presented.

## 2. METHODOLOGY

The steps to be followed to identify the fractures that control groundwater flow in low-permeability fractured media are described in this section. The scope is limited to relatively small rock blocks (about 1 km at most). At larger scales, a full hydrogeological study ought to be carried out, possibly including piezometric mapping, mass balance, water chemistry and isotopes.

### 2.1. Structural geology

Obtaining an accurate description of structural geology is probably the most important step for the objective of this work. Identification of main fractures must be done after a detailed analysis at different scales, possibly starting at the regional scale (pluton) and going on to the most local scale (borehole).

At the regional scale, the geological structure of a pluton is conditioned by its own genesis –such as cooling or intrusion– and by the different fracturing processes that it has been subjected to. Moreover, establishing its current stress state may help to identify open structures by their orientation with respect to the direction of the current stress tensor. Structures that are perpendicular to the direction of minimum compressive stress or, in general, are close to failure, will tend to be open, and are likely to act as preferential flow directions (Talbot and Sirat, 2001; Gudmundsson, 2000).

These structures are identified, at the pluton scale, by means of geologic mapping (in order to describe them geometrically) and a detailed study of the fracture planes (to study the movement of the structures). Geophysical techniques may help to identify some dykes, or geological structures, with a differentiated physical behavior. Radar and tomography logs do not have enough resolution to identify single fractures, but they could identify a dyke into a granitic body (Blümling and Sattel, 1988; Pratt 1995). Combining 3D seismic tomography, outcrop and core mappings, with geostatistical modeling may also help to determine the architecture of fractured granite (Escuder-Virue et al, 2003).

At the borehole scale, analyzing fissure fillings helps to determine the potential fluid circulation along fracture planes (Perez del Villar et al., 1999). Breakouts allow one to determine the local stress direction (Jurado 1999, Zoback et al., 2003). This information leads to the assessment of the deformation history, and thus to a

---

preliminary identification of the a priori hydraulically most active structures (Perez-Estaún 1999; Pardillo et al., 1997).

## **2.2. Hydraulic testing and preliminary interpretation**

Hydraulic test interpretation is best performed in terms of drawdowns, so that all boundary conditions are homogeneous (zero flux for Neumann boundaries and zero head for Dirichlet boundaries). Obtaining drawdowns may require filtering natural head trends. Response to pumping in low-permeability media is small, but may last for a long time. As a result, spurious effects not induced by the test itself may affect results. These include the natural hydraulic trends, pressure build-up after packer's installation or construction of nearby structures. A continuous record of head measurement must be kept both before and after the test, in order to filter out these effects. This is especially important in long pumping tests, when head variations due to causes other than the test itself may be important.

A preliminary test interpretation can be made using analytical models (Theis, 1935; Hsieh and Neuman, 1985; Barker, 1988, Papadopoulos et al, 1973, Illman and Tartakowsky, 2005). These are used for interpreting drawdown data, under simplified assumptions, such as homogeneity and infinite extent. For cross-hole tests, drawdown curves are interpreted separately for each observation interval showing a defined response.

Hydraulic tests are not the only actions that can yield information about hydraulic connectivity. Response to other activities that affect head measurements can also be used. These include tunnel excavation, boreholes drilling, ventilation, point inflow measurements at the structures outcrops (tunnel walls, slopes, etc.), and borehole pumping for development purposes or water sampling. Boreholes must be instrumented immediately after drilling to take advantage of these pieces of information.

## **2.3. Selection of conducting features. Geometrical conceptual model.**

Identifying the most conductive structures requires integrating all the above data. Each observation complements the information contributed by the rest. Starting from the structures identified by means of structural geology, hydraulic tests allow determine which are hydraulically active and their main characteristics (position, slopes, etc.).

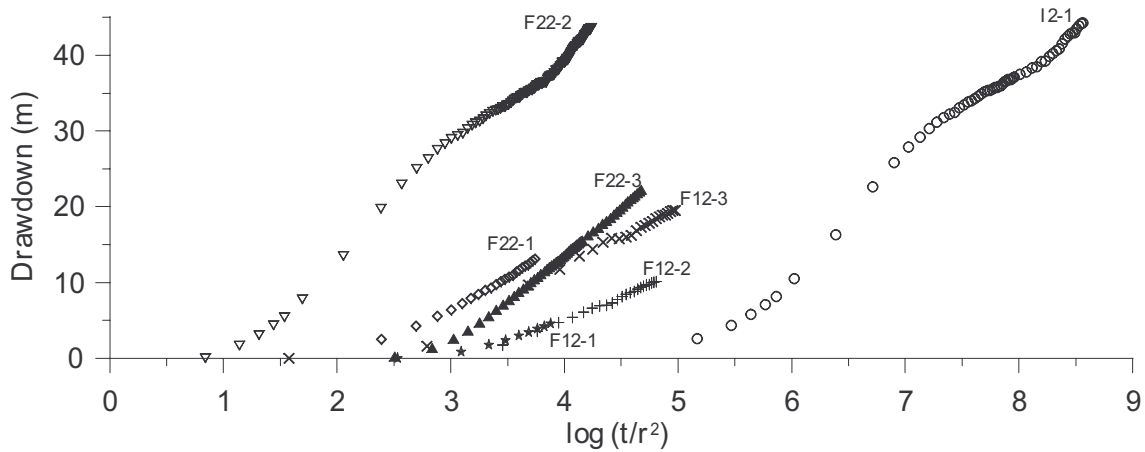


Figure 1: Drawdowns observed in response to pumping interval I2-1. Notice that  $\log(t/r^2)$  is used as horizontal axis (where  $r$  is distance to the pumping point). Fast responses suggest good connectivity. In this case F22-2 is likely to be connected to I2-1 (pumping borehole) through a flowing fracture.

Connectivity between pairs of points can be derived from cross-hole tests. Fractures are zones of high diffusivity, because they can transmit but do not store water. As a result, well connected intervals show a fast response to pumping. Fast response can be evaluated graphically by plotting drawdowns,  $s$ , versus the logarithm of time divided by the distance squared,  $\log(t/r^2)$  (Figure 1). If the medium was homogeneous and isotropic, all curves would become superimposed. An early response (in terms of  $t/r^2$ ) implies good connection. In fact, diffusivity can be used as a measure of connectivity (Knudby and Carrera, 2005b). Since separated interpretation of each drawdown curve results in very similar values of  $K$  (or  $T$  in 2D) for all tested intervals, variations in connectivity are reflected in estimated storativity. That is, estimated storativity is apparent and reflects more the degree of connection between pumping and observation wells than the actual storage properties of the medium (Meier et al., 1998; Sanchez-Vila et al., 1999). A low storativity implies good connection (fast response), and vice versa.

## 2.4. Numerical modeling

The numerical model can be constructed once the conceptual model is defined. The singular feature of the mixed discrete-continuum approach presented here is the need to include all the hydraulic features in the mesh. The background porous media is modelled with 3D elements; fractures are simulated by means of 2D elements, and borehole intervals are assimilated to 1D elements, whenever their length is such that they can provide hydraulic connections. This requires a precise knowledge of the



---

geometry, including the direction and inclination of boreholes, direction and dip of fracture planes, the extent and interception points of fractures, the location of all observation points, etc. Among them, the extent of fractures is the most difficult to evaluate. It has to be defined preliminarily from structural data, and be adjusted during calibration.

### **3. APPLICATION TO FEBEX SITE**

The methodology described above is applied to the FEBEX tunnel located at the GTS.

#### **3.1. FEBEX site description**

The objective of the FEBEX project was to study the behaviour of engineered barriers for the storage of high-level radioactive waste in crystalline rocks. The experiment was based on the Spanish concept of waste storage, which implies the horizontal placement in tunnels of capsules containing the waste. The capsules are surrounded by a clay barrier, built with compacted bentonite blocks. The experiment involves the set-up of two electric heaters, scaled to the dimensions and weights of the capsules in the original concept, placed in a 2.28 m diameter tunnel that was excavated in granite. The volume around the heaters was filled in with compacted bentonite blocks to complete a length of 17.4 m in the testing zone, which was closed with a concrete plug. The monitoring and control system is close to the service area, between the concrete plug and the tunnel entrance (ENRESA 1998).

Within this project, our objective was to characterise the hydrogeology (inflow into FEBEX tunnel and its distribution along the tunnel's wall) of the granite where the heating experiment took place. The aim was to establish a hydrogeologic model of groundwater flow around the FEBEX experiment (Guimerá et al., 1998). The same flow models were used to study any eventual modification of the hydraulic conditions due to the heating.

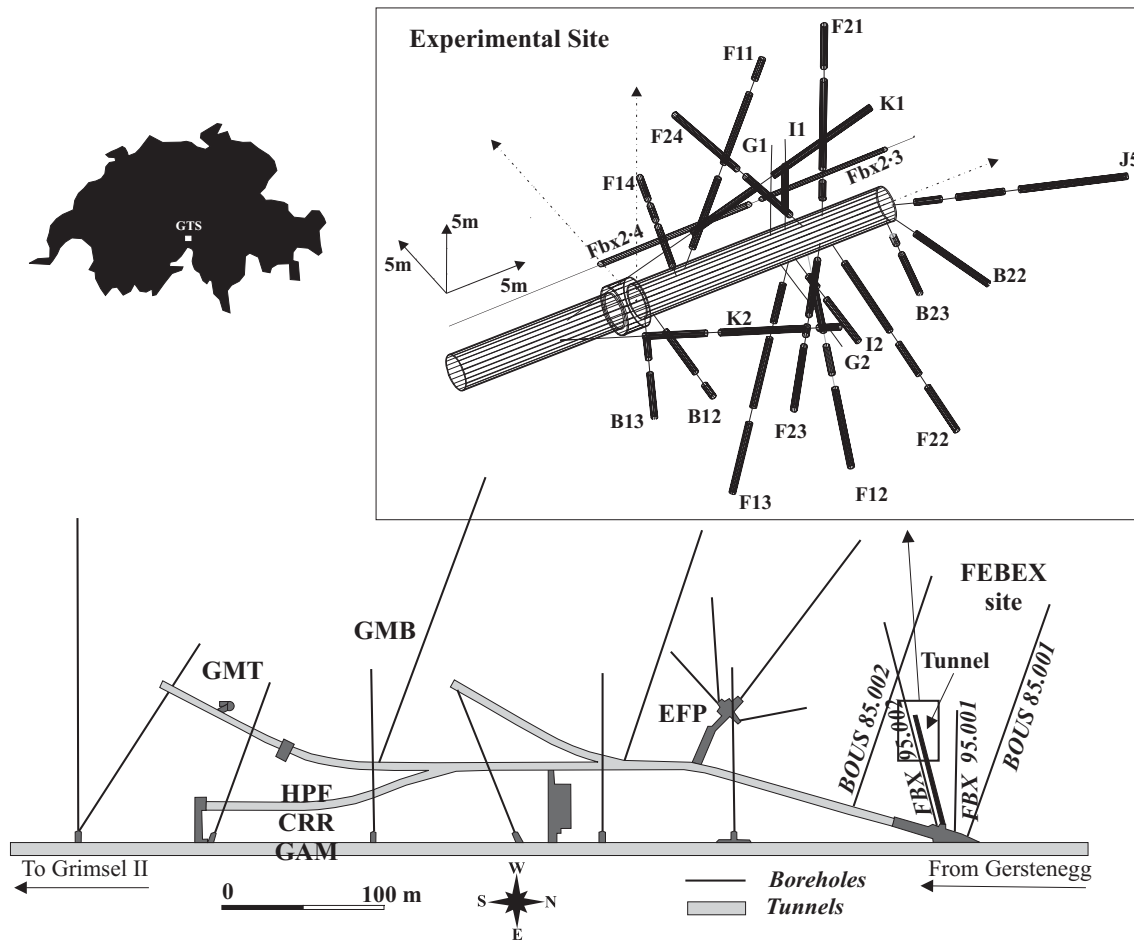


Figure 2: Physical situation of the experiment. The Grimsel Test Site (GTS) is situated in Switzerland; the site corresponds to the Northeast tunnel within the experimental network of galleries. The radial boreholes are located at the end of the FEBEX tunnel, surrounding the experimental site. The cross-hole tests were conducted at these boreholes.

There are 23 boreholes as observation points, at different locations and with different lengths (Figure 2):

- Boreholes BOUS 85-001 and BOUS 85-002 were drilled in 1985 to characterize the GTS geology. They are 148 and 150.3 m long, respectively.
- Boreholes FBX 95-001 and FBX 95-002, drilled in 1995 to search for an adequate place for the experimental FEBEX tunnel, are 76 and 132 m long, respectively.
- 19 radial boreholes were drilled around the FEBEX tunnel to monitor the experiment, with a mean length of about 15 m.

All boreholes are divided into intervals by means of packers (Figure 3), resulting in a total of 64 intervals. Each interval is equipped with pressure transducers and a water re-circulation line to carry out hydraulic tests and hydrochemical sampling.

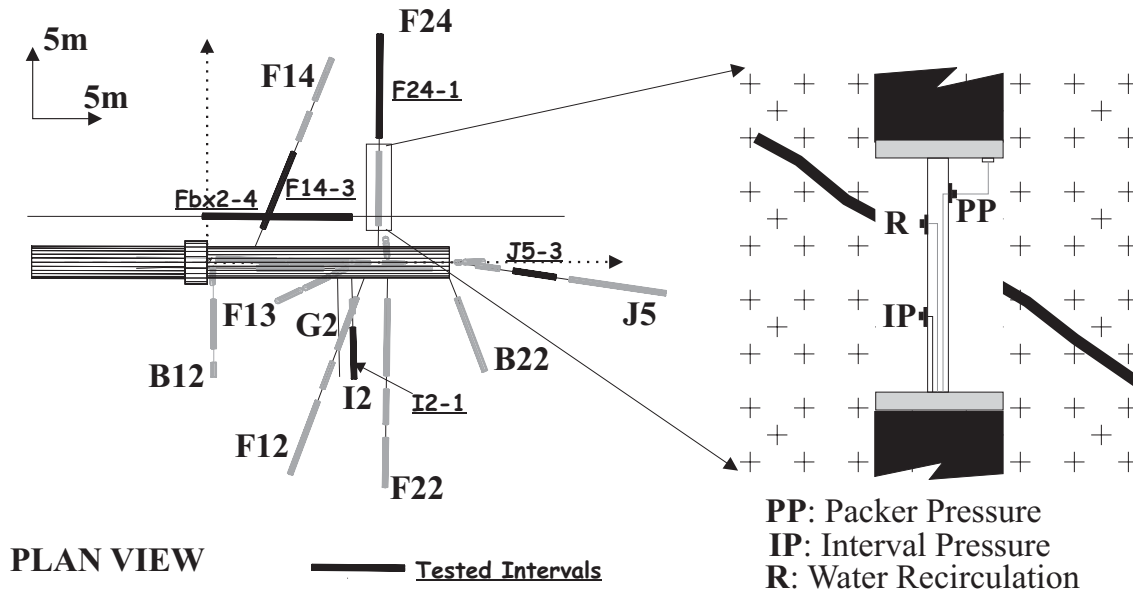


Figure 3: Borehole instrumentation. All the boreholes that surround the FEBEX tunnel are isolated into intervals by means of packers. Each interval is equipped with a packer pressure line, an interval pressure line and a water recirculation line. Pressure lines are connected using a tube with a pressure transducer, which is located at the FEBEX tunnel (outside the experimental zone). The five pumping intervals are drawn in black.

Hydrogeological characterisation at the experiment scale was achieved using geological, geophysical and hydraulic data. Geological data comprise mapping (galleries, tunnels and surface mapping) and borehole core analysis. Geophysical data included seismic tomography and radar. Hydraulic data consisted of pressure measurements at the all borehole intervals during the different phases of FEBEX experiment, including natural conditions, responses to tunnel excavation and hydraulic tests.

### 3.2. Identification of main structures

GTS galleries have been excavated between the Aare granite to the North and Grimsel granodiorite to the South. The FEBEX tunnel is located in the latter.

The main large-scale (500-1000m) geologic structures were detected at GTS using seismic tomography, radar data and structural geology prior to FEBEX project (Blümling and Sattel, 1988; Pratt 1995). The geophysical techniques allow for a good identification of the lamprophyre dykes, due to their differenced electromagnetic behaviour as compared to the granodiorite, but do not have much resolution to detect fractures. Identification of fractures and shear zones at the test site scale was based on

surface mapping, GTS tunnel mapping and the boreholes cores (lithologic descriptions and borehole televiewer) (Pardillo et al., 1997).

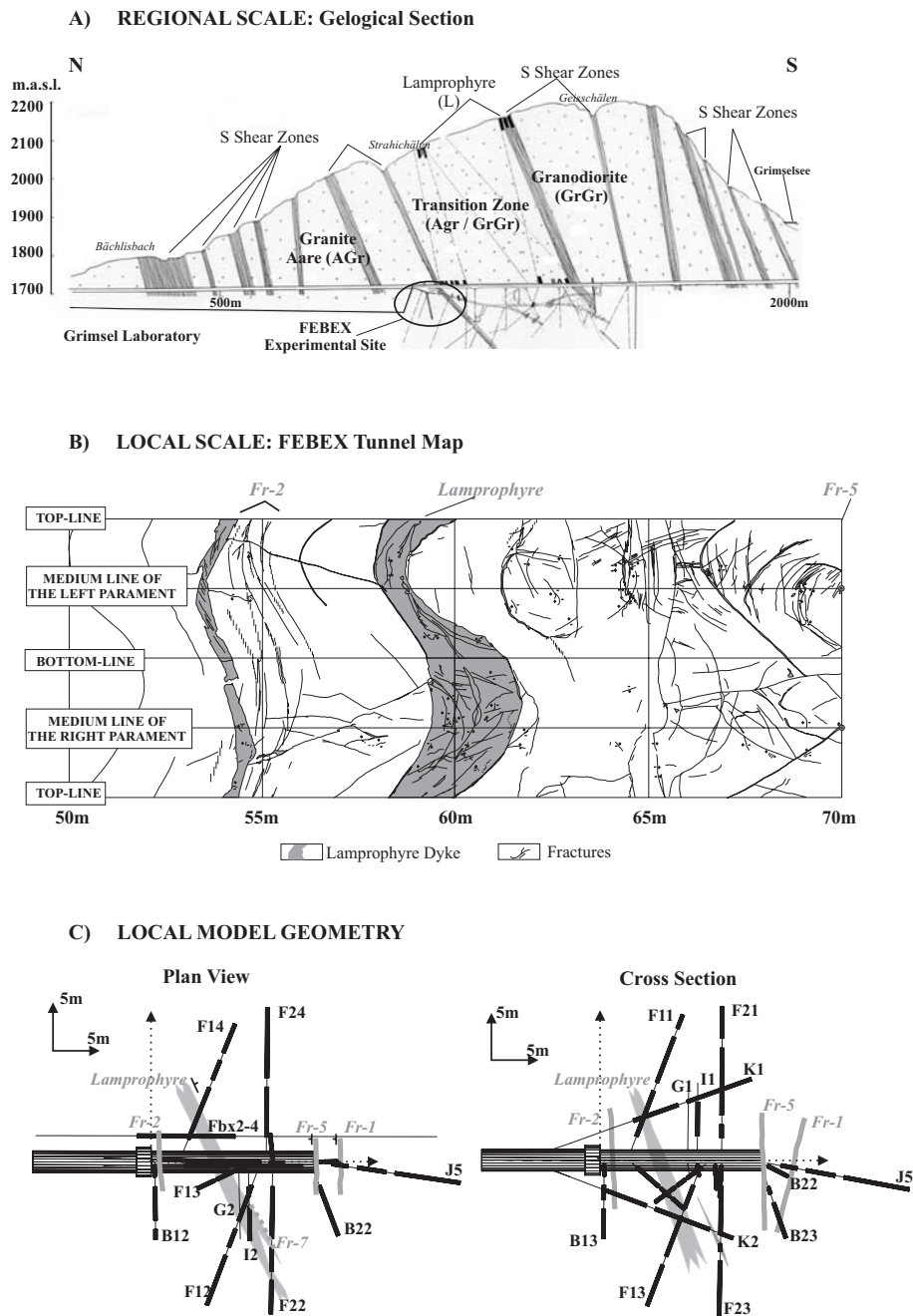


Figure 4: Definition of geometry. This figure shows that just a few of the mapped structures in the tunnel (above, Pardillo et al., 1997) are hydraulically relevant so as to treat them individually. Hydraulically important structures are shown in the lower part of the figure (lamprophyre, Fr-1, Fr-2, Fr-5 and Fr-7). These structures are the only ones included explicitly in the model. The remaining structures are treated as part of an equivalent porous medium.

Once these data have been analysed, it is possible to identify the main geological structures from the hydrogeological standpoint (Figure 4):

- S Shear zones, whose direction is NE-SW and dip subvertically towards the SE. These are high conductivity structures that develop in parallel to the fracture planes and are characterised by a very low perpendicular hydraulic conductivity because of their strong mineral orientation.
- Fracturing direction L, whose direction is WNW-ESE to NW-SE. There are many open fractures, this direction coincides with those of the lamprophyre dykes. The contact surface between the lamprophyre dykes and the granodiorite behaves as a high conductivity zone.

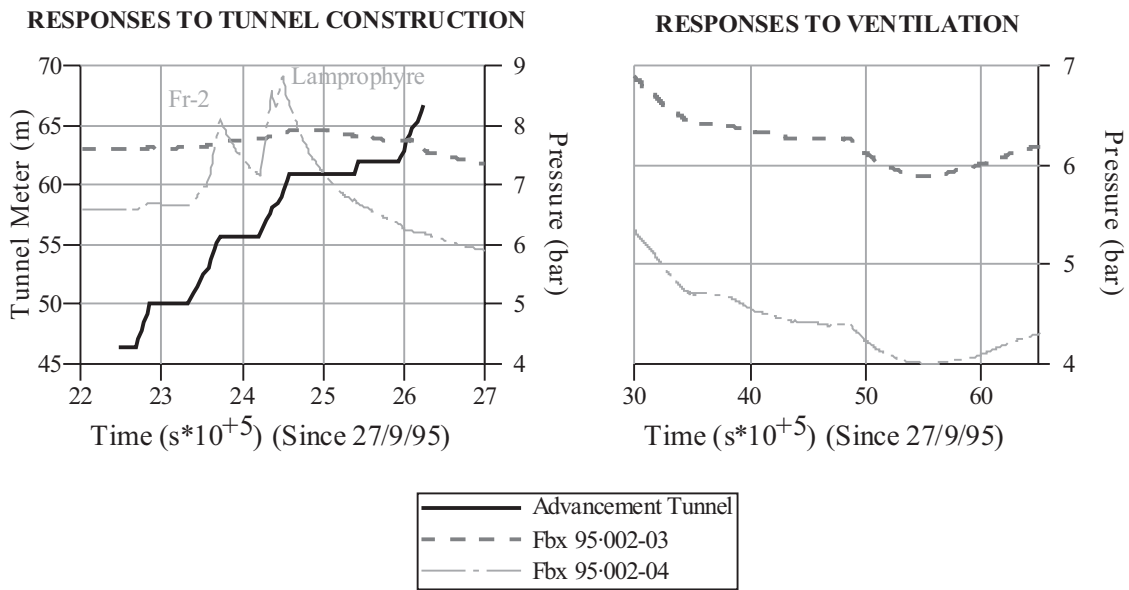


Figure 5: Opportunistic methods to identify hydraulically relevant structures. On the left, pressure variations for intervals 3 and 4 of borehole FBX 95-002 are plotted, representing the response to the tunnel borehole machine (TBM) advance. When the TBM is working, pressure increases at the intervals. If a structure (Fr-2, lamprophyre) connecting the tunnel with the interval is intercepted, then water flows towards the tunnel and pressure diminishes (peaks in pressure curves at borehole FBX 95-002-4). On the right, the response to ventilation of the tunnel are represented. It is not possible to identify any particular structure, because results account for the integrated response of the whole domain (matrix + fractures). Ventilation effects are analogous to a pumping test. The observation points in the picture are located at 2 m-distance from the FEBEX tunnel wall.

The main hydraulic features identified at the local scale (m) are 8 fractures denoted as Fr-1 to 8. They were identified by mapping (surface, galleries, tunnels, borehole cores), response of the intervals pressure to the ventilation and drilling of the experimental tunnel (Figure 5, left and right), and flowrate measurements. Pressure responses to perturbations in the tunnel (ventilation, drilling, etc) are similar to those

produced by the hydraulic tests. So, they provide an idea about the connection between the measurement interval and tunnel. Flowrate measurements at the interception of conductive structures with the tunnel also yield estimates of transmissivity of these features (Ortuño, 2000).

### 3.3. Hydraulic testing

Up to this stage, the main structures have been identified geometrically. However, it is necessary to evaluate their hydraulic role. Single-hole hydraulic tests help in determining the hydraulic parameters of the structures, but it is necessary to conduct cross-hole tests to determine the hydraulic connection between them.

Hydraulic characterisation started by conducting single hole tests at all borehole intervals, including BOUS, FEBEX and radial intervals. These data served to choose intervals suitable for pumping during several hours in cross-hole tests.

Five cross-hole tests were conducted (Figure 3), each with a different pumping point. The applied protocol consisted of pumping from one point and controlling the pressure evolution at the remaining 63 observation points. Tests were sequential in time, with a fixed recovery period to reduce interference with subsequent tests.

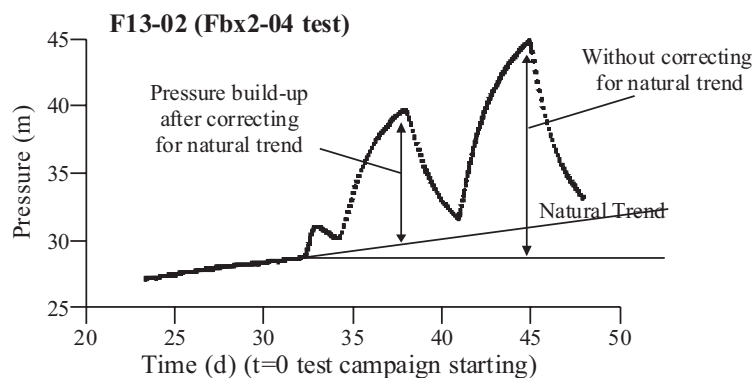


Figure 6: Intervals may need several days to reach equilibrium conditions after borehole instrumentation. Once this happens, pressure is not constant but exhibits a natural evolution. In order to interpret the hydraulic tests at these points, it is necessary to filter any effect that has not been caused by the test.

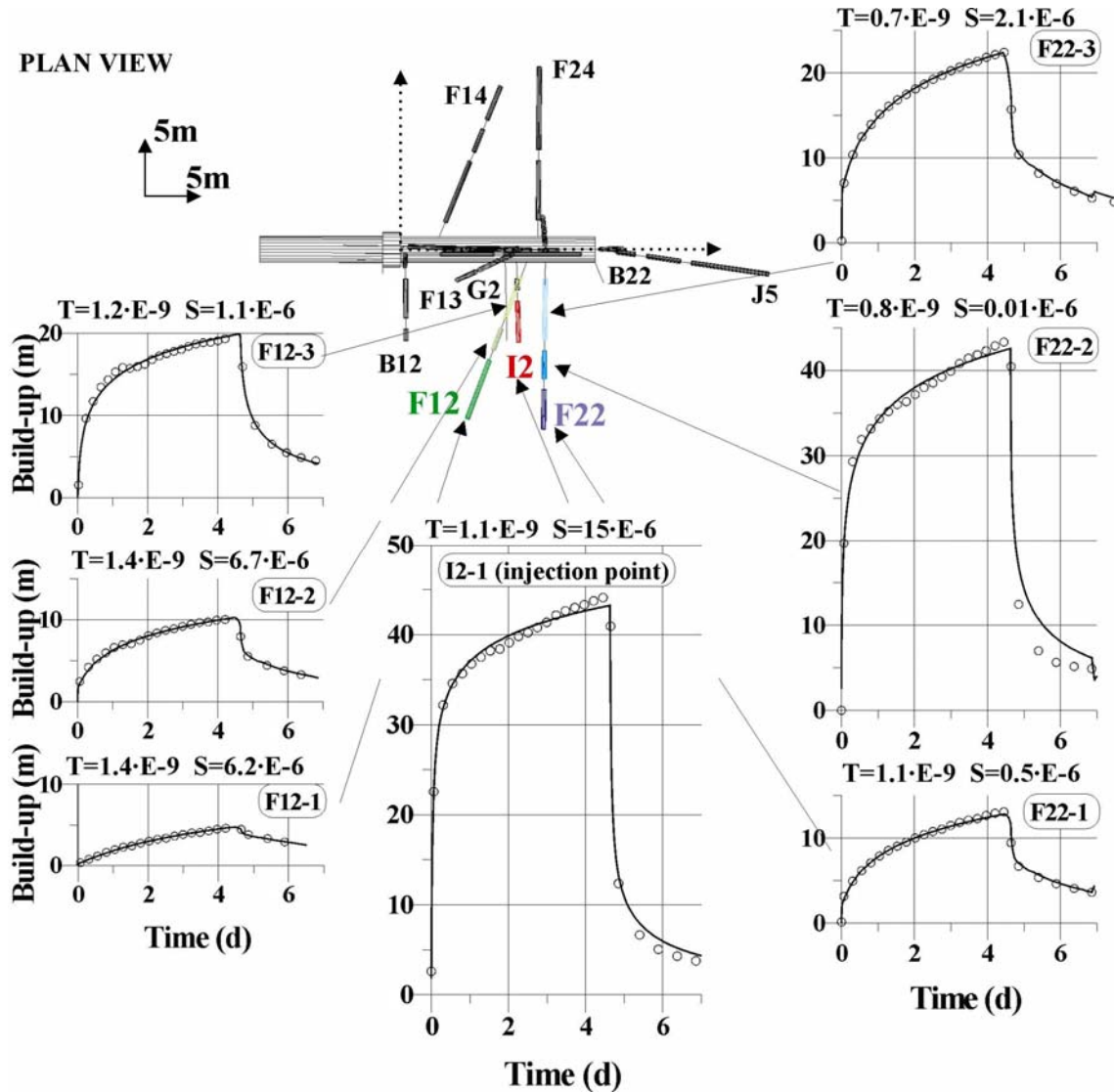


Figure 7: Interpretation of cross-hole test pumping at point I2-1, showing the observation points with a larger response to the test. Transmissivities ( $T$ ) estimated under the hypothesis of a homogeneous model are very similar for all points (from 0.7 up to  $1.4 \cdot 10^{-9} \text{ m}^2 \cdot \text{s}^{-1}$ ), whilst apparent storage coefficients ( $S$ ) are highly variable (from 0.01 up to  $15 \cdot 10^{-6}$ ). This variability reflects the connectivity between pumping and observation points. A high  $S$  is an indication of low connectivity and, conversely, low apparent  $S$  indicates high connectivity (Meier et al., 1998)

Observation points are distributed throughout a 3D rock volume. The hydraulic extent of the fractures is defined by means of the responses to the test of all intervals that intersect them. Accurate description is somewhat ambiguous. We have adopted a rectangular shape for simplicity. Their size is bound by the borehole responses (fractures extend beyond intervals with fast responses, i.e. small  $S$ , and fall short of slowly responding intervals). Within these bounds, the size was adjusted by trial and error during the calibration of cross-hole tests. However, little adjustment was needed.

With this methodology, it is possible to identify some of the heterogeneities that are present on the fracture planes and that behave as preferential flow channels. The connection between the injection (I2-1) and the observation interval (F22-2) is probably due to a flow channel located at the contact plane between the lamprophyre dyke and the granite block.

After integrating all the available information, it is possible to conjecture which is the groundwater flow conceptual model around the tunnel. Figure 4-C summarises the simplified geometry to be implemented in the numerical model, where five main structures can be observed; the remaining identified fractures (Fr-3, Fr-4, Fr-6 and Fr-8) and S shear zone do not lie within the adjacent to the FEBEX tunnel and are not shown in Figure 4-C:

- Lamprophyre dyke. It has been identified through tunnel intersections and borehole cores (Figure 4), as well as the response of interval FBX 95-002-04 to the drilling of FEBEX tunnel (Figure 5, left) and the response to hydraulic testing. It is worth remarking that, according to hydraulic tests, the most conductive zone is at the contact between the granite and the dyke, even though the dike itself displays low permeability. This situation is not unusual ([Babiker and Gudmundsson, 2004](#)).
- Fracture 1 (Fr-1). It was identified based on the cores of boreholes J5 and B23, but its hydraulic connectivity was confirmed during the field tests.
- Fracture 2 (Fr-2). This is an approximation to the group of fractures that were mapped at the tunnel (Figure 4) and the borehole cores. These step-like fractures form a very conductive zone because there are intersections among them. Their connectivity and extent was determined by using hydraulic tests.
- Fracture 5 (Fr-5). It is the simplification of a fractured zone placed at the end of the FEBEX tunnel.
- Fracture 7 (Fr-7). This feature really acts as a preferential flow channel in the lamprophyre-granodiorite contact plane.

### **3.4. Integrated interpretation of cross-hole tests**

Once the geometry and conceptual model have been defined, they are implemented into the numerical model. Figure 8 displays a simplified scheme of the 3D mesh. We built it by generating a 2D mesh, which contains the projections of all the structures of the model (FEBEX tunnel, fractures 1, 2, 5 and 7, lamprophyre, boreholes



and granite). The 3D mesh is then created by replicating all projections along the third dimension with smoothly varying thickness to adapt the 3D grid to the actual fracture planes subparallel to the projection plane. Fractures and boreholes not contained in these planes are modelled by cutting across elements (if the angle is low, which was never the case here, the plane may be approximated by a “stair-case” surface. In this way, fracture planes (2D elements) and boreholes (1D elements) are located exactly (direction, dip, intersection points with boreholes and tunnels); they are surrounded by 3D elements, and connected to them by the shared nodes. This process demands an accurate control of the position, direction and dip of all the structures. Once the geometry is created, the model needs to be calibrated.

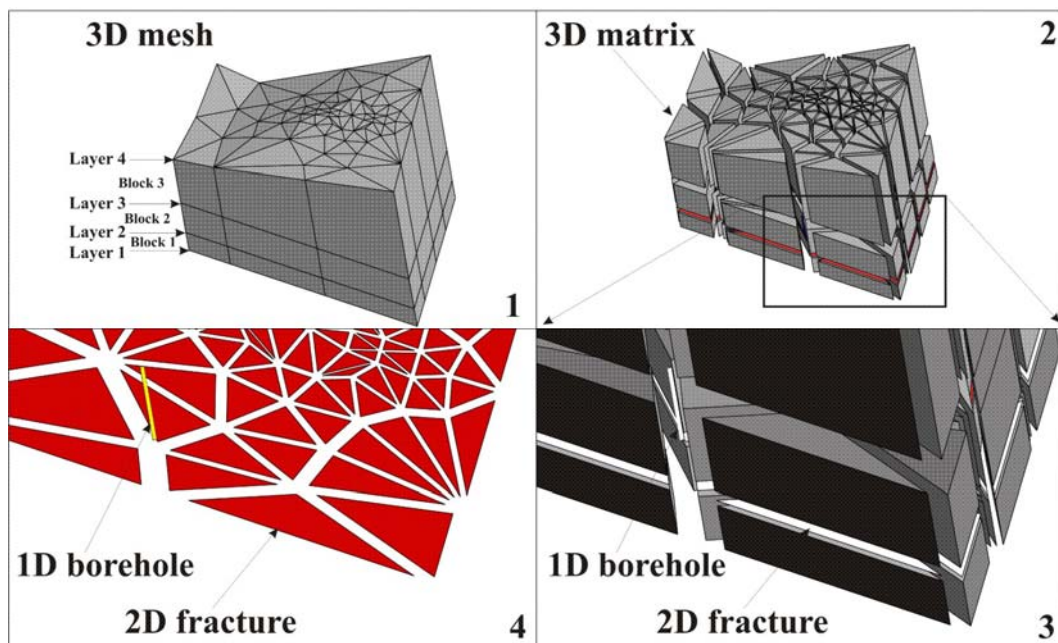


Figure 8: Simplified mesh and three-dimensional geometry. The 3D mesh is built by replicating the 2D mesh along the third dimension (3D blocks delimited by not necessarily parallel layers). Then, all the elements of the geometry are projected onto this 2D mesh. Those geometrical elements –fractures (2D elements), boreholes (1D elements)– are embedded at their true position within the 3D elements (below, right). All of them are connected by the nodes that share with other finite elements of the mesh.

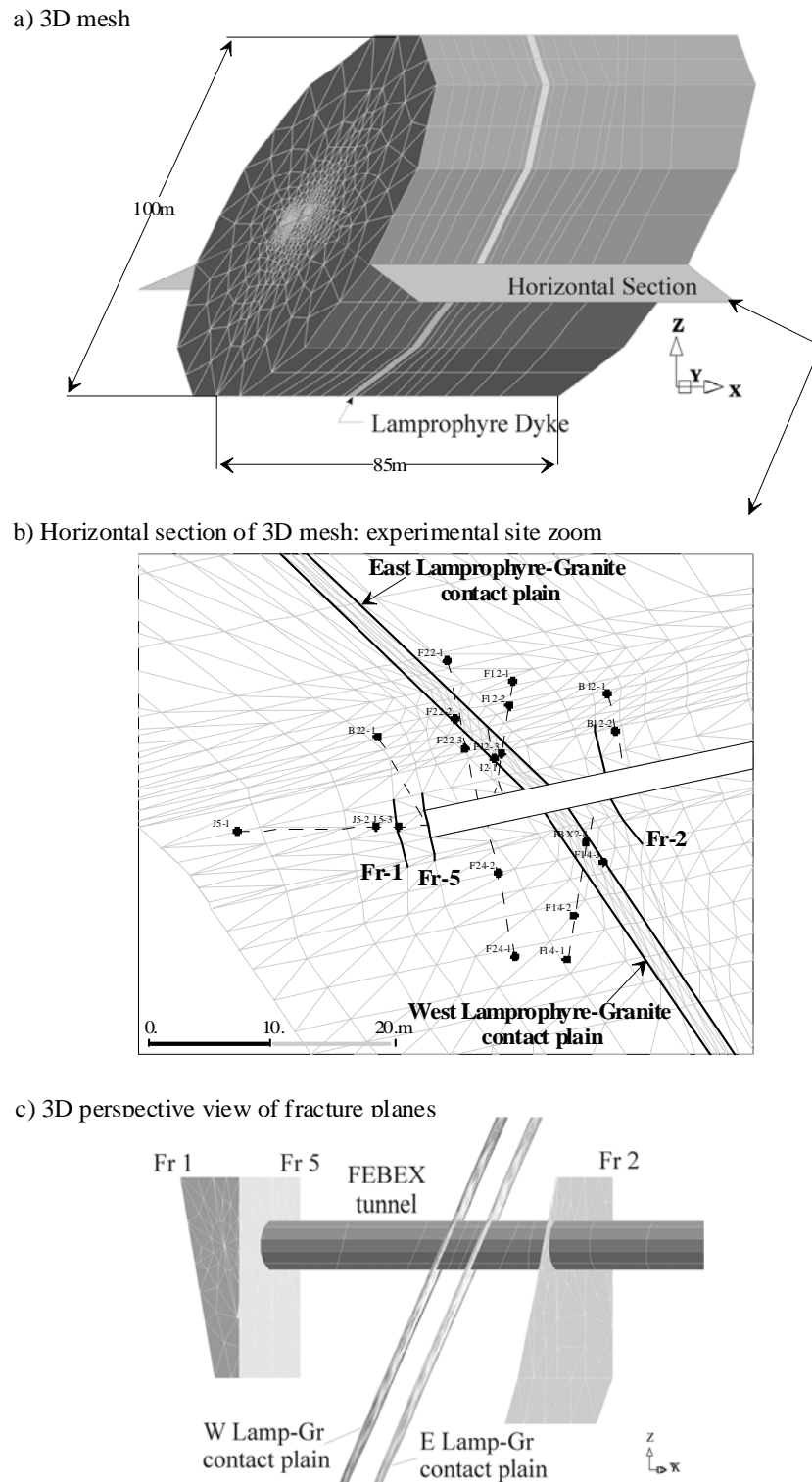


Figure 9: Geometry of cross-hole tests model. a) View of the 3D mesh (notice the lamprophyre dyke). b) Zoom of a horizontal section of the experimental zone (notice the intersections of hydraulically relevant features: lamprophyre, fractures Fr-1, Fr-2 and Fr-5) and the observation points that are situated in the horizontal boreholes. This mesh corresponds to the cross-hole test conducted at the pumping interval I2-1, where the discretization is finer and the size of the elements is of the order of 0.5 m. c) 3D perspective of the main fractures at the experimental scale.

---

The model domain is formed by a 50 m radius and 85 m long cylinder, whose axis is determined by the tunnel (Figure 9a). The end of FEBEX tunnel is placed in the centre of the mesh. The mesh dimensions are conditioned by boundary conditions, which have been taken at a distance large enough to assure that they are not affected by the tests. A no-flow Neumann boundary conditions has been adopted at all outer boundaries to reflect that we work with drawdowns (actually, water flows towards the tunnel, but we assume that the flow rate is not affected by the test, so that drawdowns are simulated with no flow). After running the model, the mass balance has been analysed to confirm that the flow across the boundaries is negligible, that is, to verify that drawdown does not reach the boundaries.

Figure 9b shows an enlargement of a horizontal section of the finite element mesh used to interpret test I2-1. This figure includes a projection of fractures Fr-1, Fr-2, Fr-5 and Fr-7, as well as the contact planes between the lamprophyre and the granite (preferential flow zone), which are represented by 2D elements. The fractures extent lies between  $5 \times 8 \text{ m}^2$  (Fr-1) and  $38 \times 38 \text{ m}^2$  for the lamprophyre-granite contact planes. The mesh elements size increases along the radial direction of the cylinder; in the vicinity of the pumping area, the elements are 0.5 m long, whilst much larger values (15 m) can be found close to the boundaries. The lamprophyre dyke and the granite, modelled by means of 3D elements, can also be visualised. Figure 9c displays a 3D view of the structures shown in this horizontal section.

Each pumping interval has been reproduced by means of 1D elements that are assigned a very high hydraulic conductivity. Flowrate is uniformly distributed among all the nodes that form part of the interval. The background has been treated as homogeneous and anisotropic, because most of the fractures are subvertical, so that conductivity of the equivalent porous media is largest in the vertical direction.

Because transient effects were filtered out, it is implicitly assumed that steady state had been achieved before the start of each test.

The code used to model the tests is TRANSIN-III ([Galarza et al., 1999](#)), which allows automatic calibration of flow and transport parameters. Parameters estimated during the analytical interpretation are used as initial values of the model parameters for calibration. First, each cross-hole test is interpreted separately, without considering the calibrated parameters obtained from the interpretation of the remaining tests. Only the

structures that affect each particular test are calibrated in those individual interpretations. A joint analysis is performed afterwards.

The integration of all parameters implies two possible situations. On the one hand, structures that are only affected by one test (**Table 1**), such as fractures Fr-1, Fr-5 and Fr-7, are assigned the parameter obtained after calibrating that test. On the other hand, the zones and structures affected by more than one test –lamprophyre, Fr-2 and background– are initially assigned the mean value of the estimated parameter from all relevant tests.

**Table 1:** Structures considered in each of the independent calibrations of cross-hole tests, and final parameters obtained from the calibration (units in m and d). Three of these structures were only affected by one test (Fr-1, Fr-5 and Fr-7).

<b>Feature \ Test</b>	<b>SI2-01</b>	<b>SJ5-03</b>	<b>SF14-03</b>	<b>FBX 95-002-04</b>	<b>SF24-01</b>
<b>Lamprophyre</b>	<b>1.5E-10</b>		<b>3.5E-10</b>	<b>1.7E-10</b>	
<b>Fr-1</b>		<b>2.5E-08</b>			
<b>Fr-2</b>			<b>1.3E-09</b>	<b>1.3E-09</b>	
<b>Fr-5</b>		<b>2.3E-08</b>			
<b>Fr-7</b>	<b>1.0E-05</b>				
<b>Background</b>	<b>1.8E-11</b>	<b>1.8E-10</b>	<b>5.9E-12</b>	<b>8.4E-12</b>	<b>8.6E-12</b>

Finally, each cross-hole test model is re-calibrated with the integrated parameters, i.e. a unique set of parameters has been used as initial parameters for the five tests. The resulting parameters are shown in Table 2, along with the standard deviations. Figure 10 shows the fits corresponding to test I2-1, for the same points depicted in Figure 7. The new plot includes those structures that form part of the model geometry. In this test, the most conductive structure is associated to the contact of the lamprophyre with the granite. Within this plane, we have identified a preferential flow channel that enables a better connection between the injection interval (I2-1) and F22-2 interval than the connection with F12-3 interval, despite the fact that the latter is closer to the injection interval and is also placed within the lamprophyre.

This unified calibration of the five cross-hole tests provides a good fit of all observation points. The worst results occur at the injection interval, because skin effect has not been taken into account. The values of calibrated hydraulic parameters are presented in Table 1. Estimation variances are very small (around  $10^{-4}$  in log scale) because they reflect parameter uncertainty, but not model uncertainty, which is much larger. Assessment of overall uncertainty would require a formal error analysis.

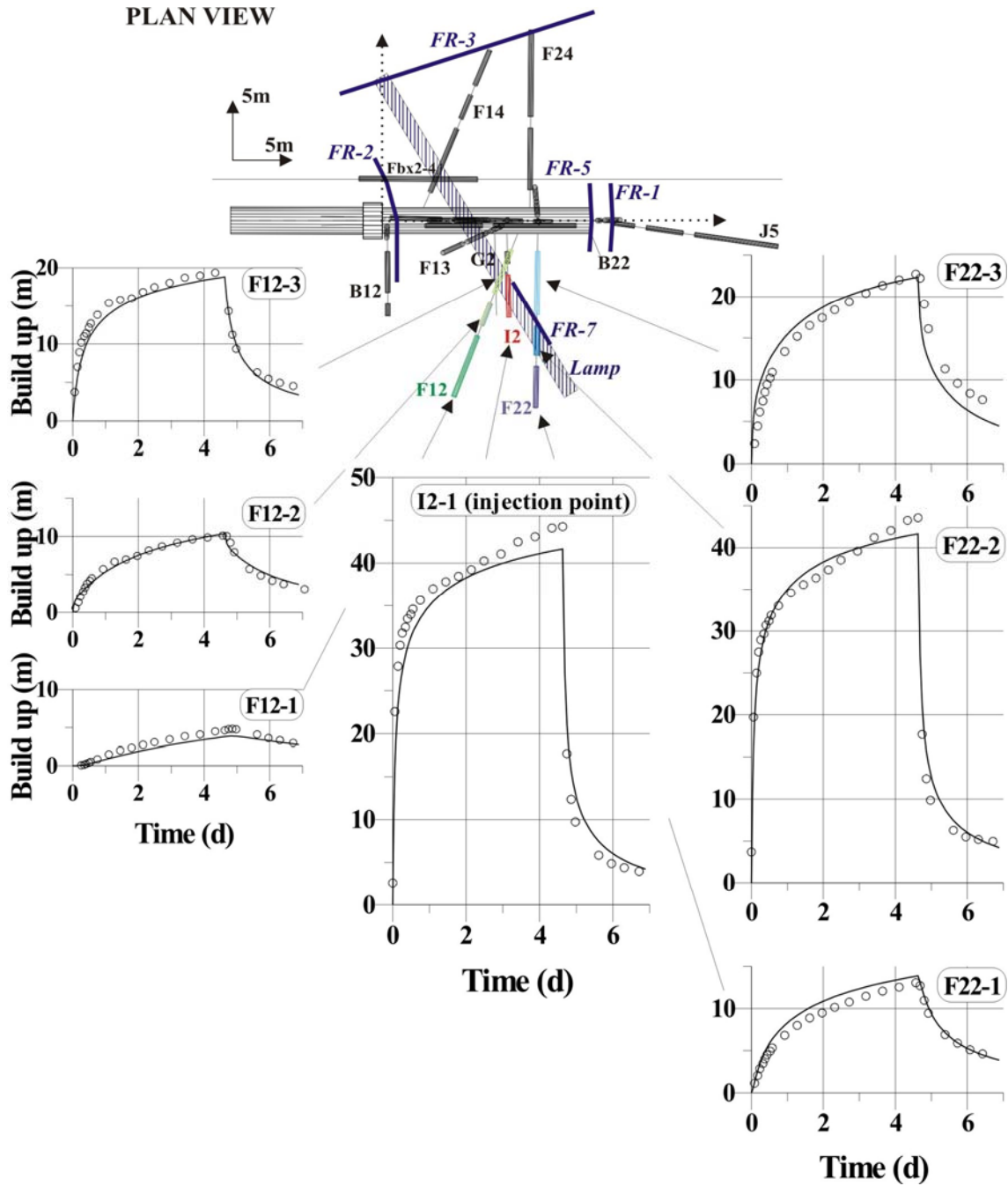


Figure 10: Fits obtained through joint interpretation pressure build-ups in test I2-1 using the grid of Figure 9. Structures included explicitly in the model are shown in the plan view above. It can be seen that injection is channelized by the lamprophyre. Response is marked at intervals intersected by, or close to, the lamprophyre (such as F12-3 or F22-3), specially F22-2, which required a highly conductive channel (Fr-7). The response dies away from the lamprophyre dike (F22-1, F12-2, F12-1). It is distance to the lamprophyre, rather than to the pumping interval, what controls response.

### 3.5. Large scale model

A large scale 3D model has been built to assess long term tunnel inflow and large scale response. This model represents steady state groundwater flow and uses the measurements obtained in the intervals of BOUS, FBX and radial boreholes (Figure 2).

The modelled area domain is approximately cubic and occupies a volume of  $210 \times 230 \times 150 \text{ m}^3$ . The experimental zone of FEBEX tunnel is located in its centre (Figure 11). The domain of each cross-hole test model (experimental site) is contained in this large scale model, which preserves all their geometrical features.

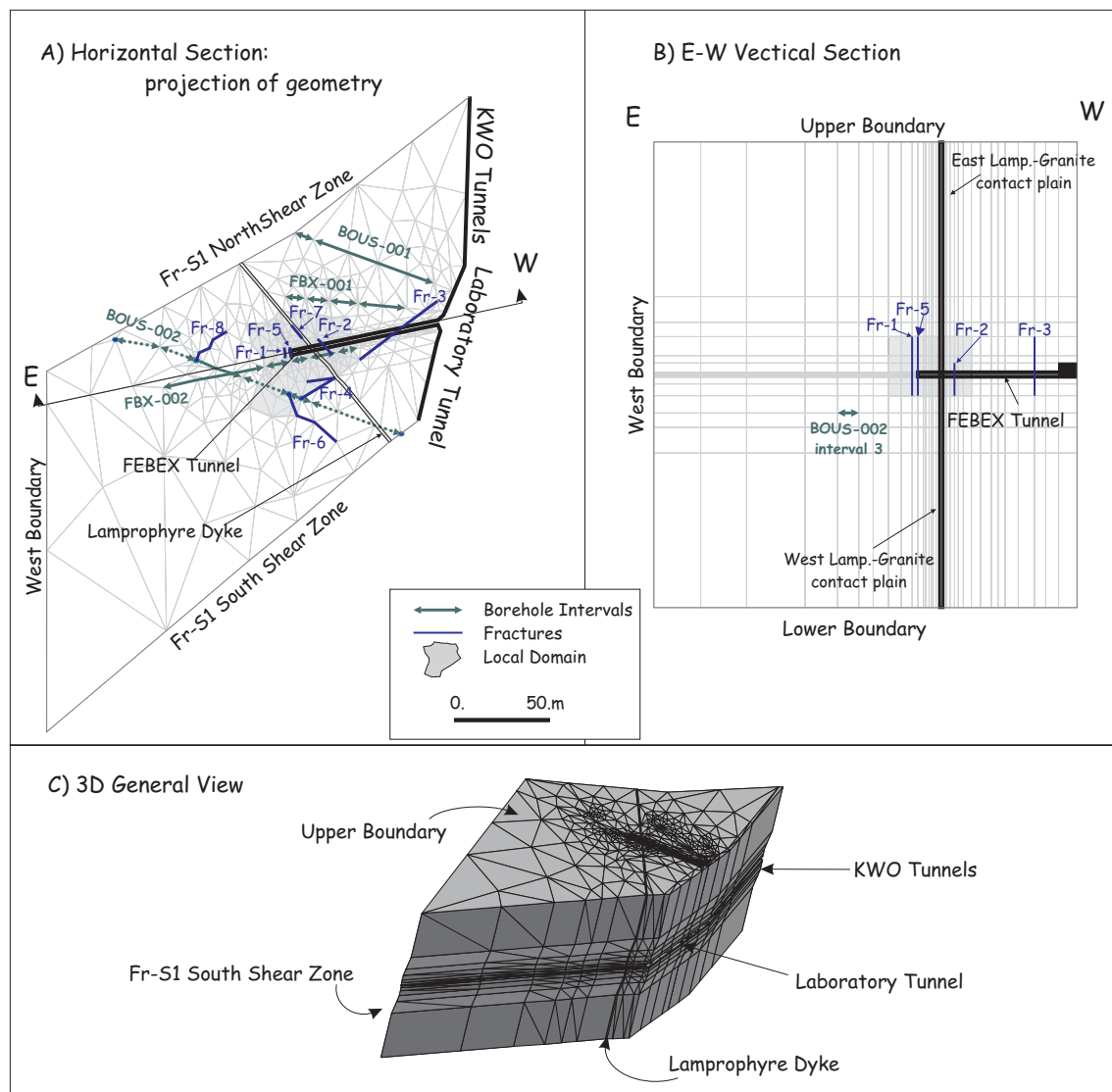


Figure 11: Geometry of the large scale model. The dashed portion represents the area that was characterized in detail. As the effect of relatively small fractures was modeled in detail, the hydraulic conductivity of the 3D blocks in this portion is much smaller than in the remaining.

---

The number of identified fractures increases after enlarging the model domain, resulting in additional conductive structures such as Fr-3, Fr-4, Fr-6 and Fr-8. But the hydraulic characterisation of the additional volume is not exhaustive, which has led to zoning the porous background in two areas, namely the inner background (experimental site) and the outer background, as depicted in Figure 11. Both have been treated in the same way, as a homogeneous and anisotropic equivalent porous medium. Obviously, the poorer characterization of the relevant fractures in the outer background is reflected in a larger value of hydraulic conductivity, since it incorporates structures that may play a role in groundwater flow, but have not been identified.

The upper, lower and Western limits have been considered as prescribed head boundaries, using the heads derived from a regional model by Kiraly (1985). A Cauchy or mixed-type condition has been used for the tunnel. The intersections of fractures Fr-2, Fr-3 and Fr-S1 North and South with the galleries are assigned a prescribed flowrate, determined by in-situ measurements (Ortuño 2000). The Eastern boundary is assumed to behave as a zero flowrate limit, given that it intersects the Grimsel and KWO laboratories tunnels. Since these act like drains, the normal flow through the boundary can be considered negligible. Finally, the Northern and Southern boundaries coincide with two shear zones of family S1, denoted Fr-S1 North and Fr-S1 South. The model has been calibrated against head measurements at every borehole intervals (large and radial boreholes). Flowrate measurements along the tunnel walls were compared with computations *a posteriori*.

The hydraulic conductivity of the outer porous background and the transmissivities of both shear zones are the only calibrated parameters in this large scale model, because the parameters of the remaining structures and areas had been calibrated during the interpretation of cross-hole tests. The initial parameters of structures Fr-S1 North and Fr-S1 South proceed from the interpretation of tests conducted at the intervals of BOUS boreholes, which intercept the shear zones. Shear zones are the larger fractures in the large scale model: 210x240 m<sup>2</sup> each, approximately.

#### **4. DISCUSSION AND CONCLUSIONS**

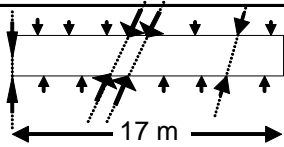
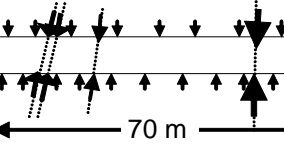
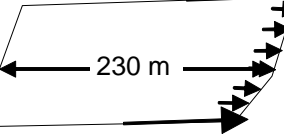
Cross-hole tests allow affecting different rock volumes around the FEBEX tunnel, and therefore deducing the hydraulic parameters of all identified structures: that is, dominant fractures, dyke and background equivalent porous media. Five cross-hole

---

tests were performed and interpreted separately using a 3D numerical model. After integrating all the results and calibrated values, it was possible to obtain a unique set of parameters that can be used to reproduce measured pressures in each test.

A large scale model was then built in order to determine the hydrogeological behaviour of the area and, in particular, groundwater flow to the tunnel. This large scale model allows testing the validity of the small scale models because its hydraulic parameters are fixed to those obtained from the cross-hole tests. Therefore, calibrating this model implies only calibrating the additional parameters that have had to be included in the enlarged domain: the hydraulic conductivity of the outer background and the transmissivities of shear zones Fr-S1 North and Fr-S1 South. The characterization of the outer domain is much coarser than that around the experiment. Therefore, it contains less identified fractures. This is reflected in the value of the hydraulic conductivity of the background porous medium, which is four times larger than in the inner zone.

**Table 2:** Flowrate through the dominant structures at different scales. As the model scale increase, it is likely to intersect longer and more transmissive fractures, causing increasing flow rates

Fracture	Q (m <sup>3</sup> s <sup>-1</sup> )	Dimensions (mxm)	Affecting area
Lamp-Gr Contact Plains	5.2·10 <sup>-8</sup>		FBX gallery end
Total	9.4·10 <sup>-8</sup>		
Fr-3	5.4·10 <sup>-7</sup>		FBX gallery
Total	7.4·10 <sup>-7</sup>		
Fr-S1	0.9·10 <sup>-6</sup>		Whole domain
Total	1·10 <sup>-6</sup>		

The described methodology is based on the assumption that a few fractures carry most of the groundwater flow. Results confirm the validity of this assumption. It must be noticed, however, that the dominant structures will change as the model scale increases (**Table 2**). Flow in the test zone is dominated by the lamprophyre-granite contact planes, which carry more than 60% of the flow rate in this zone (**Table 2**). When increasing the scale to the whole FEBEX tunnel, flow concentrates on a single



---

fracture (Fr-3). Its flow rate is an order of magnitude larger than that of the lamprophyre-granite contact planes. At the large scale model, flowrate is dominated by shear zones Fr-S1 North and Fr-S1 South, while the rest of structures can be viewed as minor fracturing. In summary, flow is dominated by a few fractures at all scales, but they are likely to change as the model scale grows, so that the selection of hydraulically dominant fractures depends on the scale of the study zone.

The validity of the model is supported by the range of data types. The resulting model explains local tests, cross-hole tests, opportunistic observations (response to tunnel excavation and ventilation) and can quantify the spatial distribution of tunnel inflows. Moreover, these are consistent with in-situ measurements.

Both fractures and background equivalent porous medium have been treated as homogeneous. Results suggest that this is sufficient for flow problems. Yet, data would allow simulating heterogeneity. Drawdown fits, such as the one in Figure 10, are not perfect. Also, point measurements of hydraulic conductivity at all intervals suggest small scale variability that it is not honoured by a homogeneous model. The methodology can be extended to stochastic estimation ([Vesselinov et al., 2001](#); [Ando et al., 2003](#); [Alcolea et al., 2005](#)) or simulation ([Gomez-Hernandez et al., 2000](#)). Acknowledging small scale variability may be important to represent channeling which may affect solute transport or multiphase flow.



---

## PAPER II

### **AN ANALYSIS OF HYDRAULIC CONDUCTIVITY SCALE EFFECTS IN GRANITE (FEBEX EXPERIMENT, GRIMSEL, SWITZERLAND)**

Lurdes Martínez-Landa and Jesús Carrera

In press in

Water Resources Research



---

## 1. INTRODUCTION

Heterogeneity is arguably the most singular feature of hydrogeology. It conditions groundwater flow and transport. Hydraulic conductivity can vary by several orders of magnitude within short distances. This is certainly the case of low permeability fractured media, where fractures or fractured zones are embedded in a low permeable matrix. Not all fractures play a relevant role on groundwater flow. In fact, most of the flow takes place through a limited number of major fractures or even planes located within fracture belts. The identification of those relevant features and their connectivity is essential to determine the hydrogeological behaviour of the medium.

Because the effect of heterogeneity is particularly relevant in low-permeability fractured media, results obtained from the interpretation of different types of tests often yield different values of hydraulic conductivity. Moreover, the average or equivalent hydraulic conductivity tends to increase with the involved rock volume. This increase is referred to as scale-effect. Scale-effects are invoked frequently in all types of geological formations, but it is very marked in fractured media (Brace, 1984; Bradbury and Muldoon, 1990; Clauser, 1992; Neuman, 1994; Schlutze-Makuch, 1999; Meier et al, 1998).

The cause, and even the existence, of scale-effects in hydraulic conductivity are controversial. Some authors attribute this scale-effect to factors such as a skin effect around the borehole or an incomplete development of the well (Butler and Healey, 1998; Rovey, 1998; Rovey et al., 2001), or turbulence (Lee and Lee, 1999). These would lead to low local transmissivity values, consistently smaller than the average properties, but may only affect the estimate of hydraulic conductivity in short-range tests (such as pulse and slug-tests). Long range tests are not sensitive to well losses because these are filtered out during interpretation. As a result, they tend to yield transmissivity values larger than short range tests. Other authors attribute the scale effect to the method applied for interpreting the tests (Zlotnik et al., 2000). Meier et al (1999) attribute it to the fact that apparent transmissivities derived from pumping tests reach their equivalent value faster in high transmissive zones than in low transmissive zones. As a result, for a given test duration, more transmissivity estimates will be below than above the average. Guimerà et al (1995), on the other hand, attribute scale effects to the fact that long term hydraulic tests tend to be done in high permeability zones.

---

Even though the factors mentioned above may play a role in certain conditions, the fact is that scale-effect has been observed on data collected at a variety of sites and under diverse fluid flow regimes (Carrera et al., 1990; Schad and Teutsch 1994; Samper-Calvete and García-Vera 1998; Rovey and Cherkauer, 1995). Illman and Neuman (2001, 2003) and Illman et al., (2003) interpreted single-hole and cross-hole tests by means of type-curves and concluded that the conductivity scale-effect is real. The same conclusion was obtained by Vesselinov et al. (2001), who interpreted the same tests using 3-D numerical inversion, while treating the medium as stochastic continuum, randomly heterogeneous. The fact that scale-effects are formed under such a wide set of testing conditions and flow regimes, suggests that the effect is real and cannot be solely attributed to conditions around the well. In fact, Sanchez-Vila et al (1996) found that the large scale equivalent value of transmissivity can be much larger than the geometric average, theoretical value in 2D, whenever points with a high transmissivity value are better connected than points with low transmissivity value. That is, they attribute scale effects to the connectivity of the medium (see also Di Federico and Neuman, 1998; Illman, 2004, Knudby and Carrera, 2005a). This implies that the way the medium is treated during test interpretation may play a role in scale effects.

Two mathematical approaches are applied to the interpretation of hydraulic tests. On the one hand, analytical models provide preliminary interpretations of datasets without taking into account the role of heterogeneities, because the medium is treated as homogeneous. This leads to equivalent hydraulic conductivities that comprise the effect of both the matrix and fractures. On the other hand, numerical models are capable of incorporating heterogeneity to some extent. Two major modelling techniques are available to represent fractured media. Margolin et al. (1998) and others (see Berkowitz, 2002) rely on fracture and channel networks, thereby associating the scale-effect only to the structure of the network. We believe that it is also necessary to take into account the matrix, since the scale-effect can be attributed to the relationship between the main fractures and the matrix. This issue is addressed both by continuum models (Sánchez-Vila et al, 1996; Day-Lewis et al, 2000; Gómez-Hernandez et al., 2000) and mixed-approach models (Carrera and Heredia 1988; Martínez-Landa et al, 2000, Carrera and Martínez-Landa, 2000). Since the conjecture that motivates this paper is that the connectivity between the most conductive structures may explain observed scale effects, it is clear that the latter modelling approaches are needed.

---

In this context, the objective of our work is twofold. First, to test this conjecture from the perspective of the scale-effect by means of hydraulic tests that were performed within the framework of FEBEX project. The FEBEX (Full scale Engineered Barrier Experiment) project is being conducted in the plutonic granite of Aare, at the Grimsel Test Site, Switzerland, to study the viability of engineering barriers to isolate high-radioactivity wastes in deep underground geological repositories. FEBEX hydraulic tests involved different scales (pulse tests, constant head tests, flowrate measurements, cross-hole tests, global steady-state measurements) within the same site. The second objective is to study whether the scale-effect observed at four different scales in FEBEX site may be explained through the mixed numerical modelling approach. This simulates fracture planes as 2D elements embedded in a 3D porous medium that accounts for the matrix and remaining minor fractures (Martinez-Landa and Carrera, 2005a). This approach aims at generating a unique model that is capable of simulating tests that involve a variety of physical scales.

## 2. SITE DESCRIPTION

The FEBEX project was performed to test the Spanish concept of waste storage in crystalline rocks, which implies the horizontal deposition of waste containing capsules in galleries. The capsules are surrounded by a clay barrier consisting of compacted bentonite. The experiment involves the set-up of two electric heaters, scaled to the dimensions and weights of the capsules in the original concept, placed in a 2.28 m diameter and 70 m long tunnel excavated in granite. The volume around the heaters was filled with compacted bentonite blocks to complete a length of 17.4 m (end of the FEBEX tunnel) and closed with a concrete plug. The monitoring and control system is close to the service area, between the concrete plug and the tunnel entrance (ENRESA, 1995; Fuentes-Cantillana and García-Siñeriz, 1998). FEBEX is a long-term project (1994-2004), divided into four stages: pre-operational (planning, design, characterisation, set-up and modelling), operational (heating, cooling), dismantling (removal, inspection, sampling and analysis of the materials) and final assessment of the results and verification of the models.

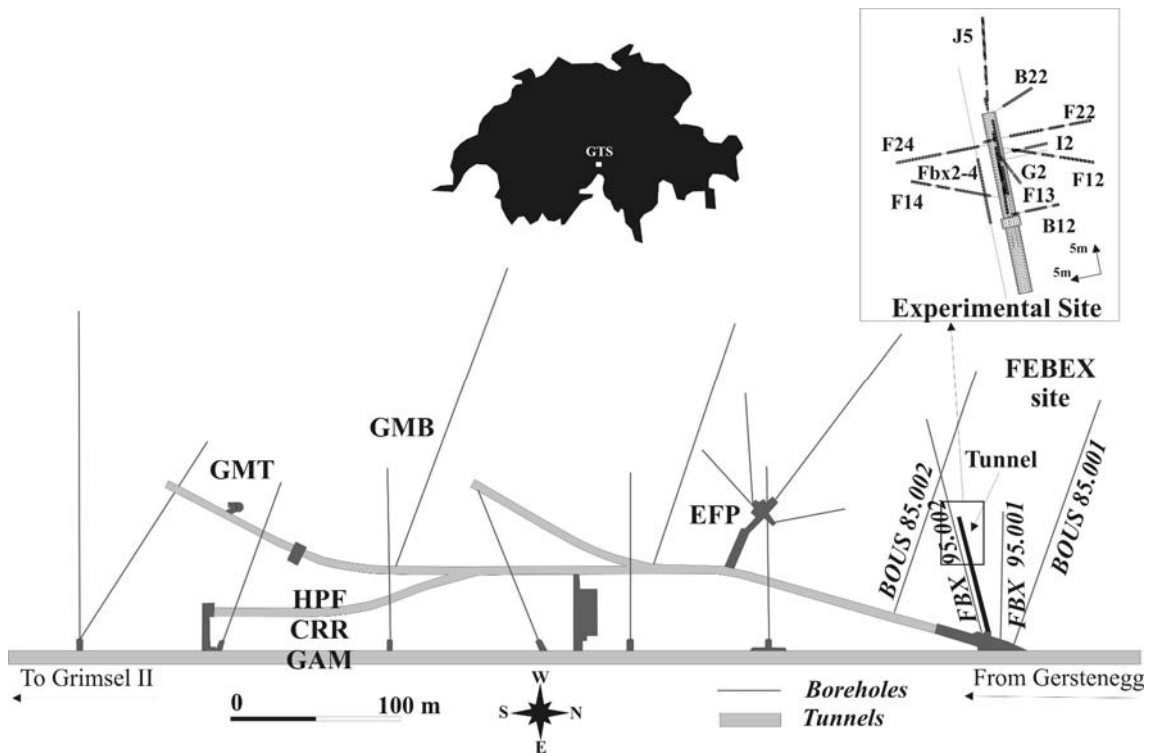


Figure 1: Location of the Grimsel Test Site (GTS), Switzerland, including the tunnel where FEBEX experiments were conducted. Four boreholes (between 70 and 150 m-long) were drilled from the main tunnel around the experimental site (BOUS 85-001 and 002, FEBEX 95-001 and 002). 19 boreholes, averaging 15-m length, were drilled according to a radial distribution from the FEBEX tunnel (inset in the upper right corner).

There are 23 boreholes as observation points, all of them at different positions and with different lengths (Figure 1):

- Boreholes BOUS85-001 and BOUS85-002 were drilled in 1985 to characterise the Grimsel Test Site (GTS) geology, and they are 148 and 150.3 m long, respectively. Their diameter is 101 mm.
- Boreholes FBX95-001 and FBX95-002, were drilled in 1995 to find an adequate place for the experimental FEBEX tunnel. They are 76 and 132 m long, respectively, and their diameter is also 101 mm.
- 19 radial boreholes were drilled around the FEBEX tunnel to control the experiment. These have an average length of 15 m and a diameter of 66 mm.



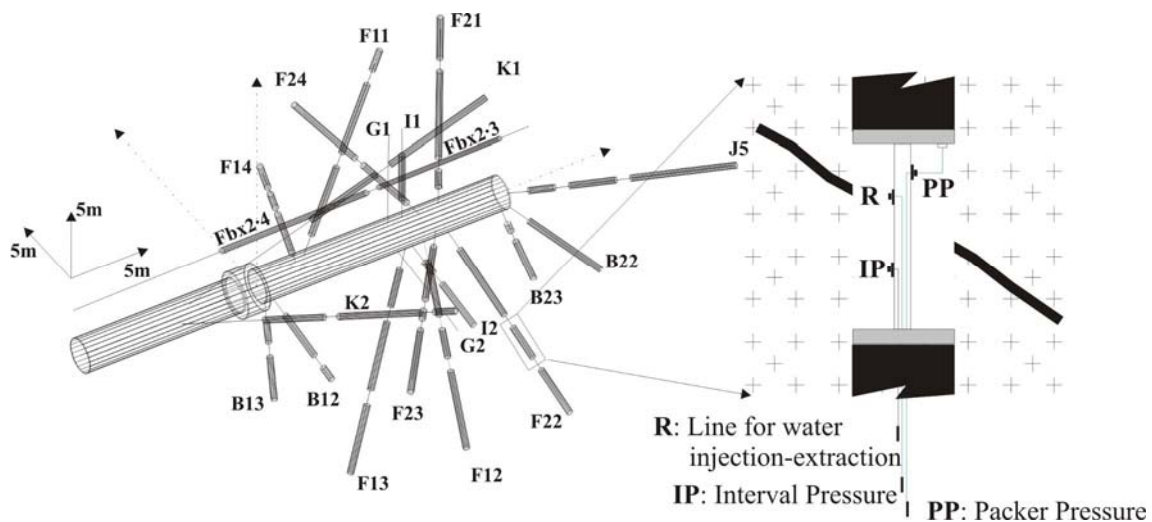


Figure 2: View of the 23 control boreholes in the test area. They are divided into intervals by means of packers. Each interval is equipped with a pressure intake, which is connected to an outer pressure transducer, and with a water recirculation intake for performing hydrochemical sampling and hydraulic tests. This leads to a total of 64 observation points.

These boreholes were divided in intervals using 1 m long packers, in order to characterise the experiment vicinity and to install a control device of the variables to be measured (pressure, temperature, water samples) (Fierz, 1996). This results in a total of 64 observation points. Figure 2 displays a simplified scheme of each interval, which contains a pressure transducer, a water extraction/injection line for sampling purposes, and a water inlet to pressurize the packer itself. All of them were maintained on a yearly basis (Fuentes-Cantillana and García-Siñeriz, 1998). Pressure sensors were connected to a data acquisition system to yield a continuous measurement record from the instrumentation stage through the end of the project. Figure 3 contains the pressure record at observation point FBX95-002-P4 (interval 4 of the FBX95-002 borehole), including its drilling (initial time), instrumentation, successive hydraulic tests and the responses to stresses exerted from other points.

The work presented in this paper was performed with data obtained during the pre-operational stage. The aim was to establish a hydrogeologic flow model around the FEBEX experiment. The same flow models were used in subsequent stages to study modifications of the hydraulic conditions due to the start up of the heating. Data available for the hydrogeological characterisation at the experiment scale comprise geological mapping at galleries and surface, borehole cores, outflow measurements at the tunnel, seismic tomographies and radar (between boreholes BOUS85-001 and BOUS85-002, and between these and the ground surface), pressure measurements at the

intervals during the FEBEX tunnel drilling, and pressure measurements at the borehole intervals during ventilation of the tunnel.

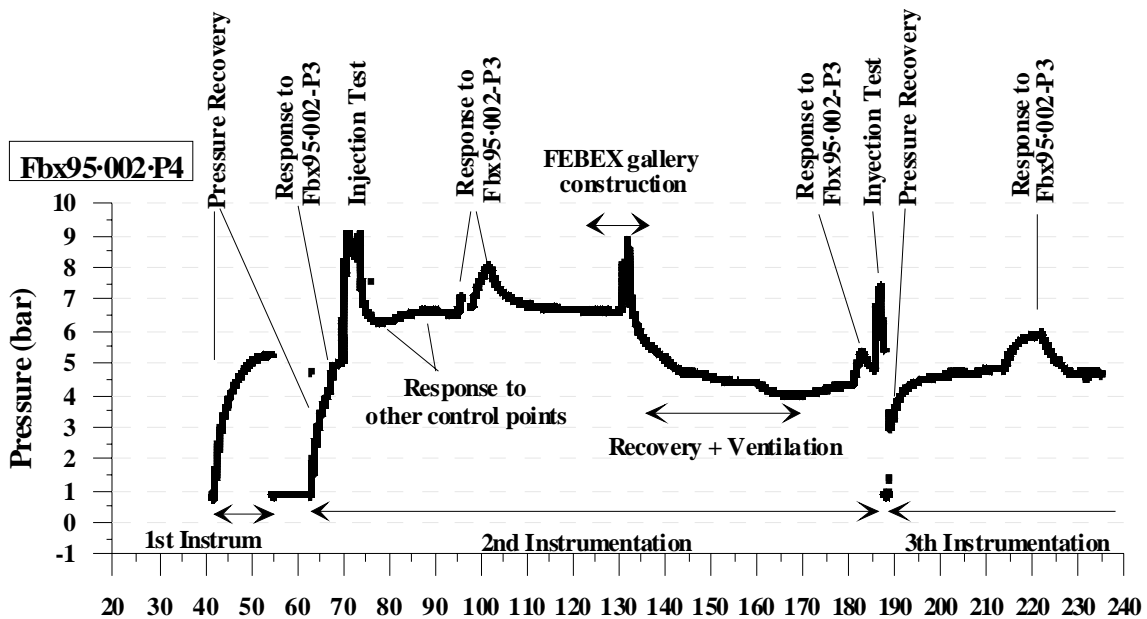


Figure 3: Pressure records at one of the observation points, from the beginning of the borehole instrumentation, displaying the interval history. The packers' position, in this borehole, has been changed three times. The picture shows how pressure recovers within the tested interval after each instrumentation change, and also as a response to tests and other events, such as drilling of FEBEX tunnel, ventilation of the tunnel, hydraulic tests conducted at other points. The effect of pulse-tests can not be identified at this scale (one data point per day), because they cause short-time perturbations.

### 3. HYDRAULIC TESTING AND INTERPRETATION

Hydraulic characterization of the rock around the FEBEX experimental zone consisted of several testing campaigns. First, a pulse test campaign was conducted to achieve a preliminary distribution of the hydraulic conductivity field at the local scale. These were used to select the most conductive intervals, where longer hydraulic tests – cross-hole tests– were carried out to gain insight into the connectivity between pumping and observation points. Data collected during the hydraulic pressure build-up that took place after instrumenting the intervals and both the flowrate data gauged at the tunnel walls were also used as hydraulic tests. All the tests have been interpreted by conventional methods in order to obtain the hydraulic parameters of the medium, as explained below.

---

### 3.1. Pulse tests

Pulse tests consist of isolating a borehole interval, imposing a sudden pressure change on it, and recording pressures up to the recovery of the initial value (Bredehoeft and Papadopoulos, 1980). Therefore, they involve (and thus sample) a small rock volume around the test interval. In FEBEX, the pressure change was imposed by means of water injection or withdrawal. The latter are preferable because chemical properties of water are not perturbed. However, injection tests were performed in those intervals whose initial pressure was so low that the interval could be dried. Pulse tests are scheduled separately in time and space to avoid overlapping in responses. The testing proceeds as follows. First, pressure is recorded at all the intervals for one day prior to the test, to correct potential evolution trends which are independent of the test itself. Second, the pulse is generated. For extraction tests, the valve that connects the interval with atmospheric pressure is left open for a few seconds, which causes an outflow because the tunnel is 450 m underground and water is at a high pressure. A calibrated, 3 mm diameter polyamide tube is placed at the interval outlet to measure the volume of water extracted during the test. For injection tests, the volume has to be determined by the weight difference of a water deposit by means of a precision scale connected to a HPLC pump that injects water into the interval. Finally, pressure recovery is recorded, a period is needed then to recover the interval pressure before starting the next pulse.

All tests have been interpreted with the automatic calibration code MARIAJ-IV (Carbonell et al., 1997) to derive preliminary estimates of hydraulic conductivity. Barker's analytical solution (Barker, 1988), which considers the medium as homogeneous, is used initially. However, intervals that intersect a fracture often exhibit a partial test recovery, followed by a delayed response to achieve full recovery. We attribute the early response to a fracture and the delayed recovery to the matrix. Interpretation of these tests requires modelling both media. MARIAJ-IV has the option to use a numerical model that allows one to represent the medium as radially symmetric with a homogeneous and isotropic matrix, and a horizontal fracture that intercepts the tested interval. Figure 4 displays the fits obtained at three intervals situated in three different boreholes. The responses vary as a function of their position. Point B23-2 is placed within the granite matrix, where permeability is very low which causes a 25 m drawdown. The other two points of Figure 4 (J5-3 and K2-3) intercept transmissive fractures, which results in a much lower drawdown (around 10m). These required using

---

the fracture model. Responses are not identical within the fractures, because their behaviour depends on the heterogeneity of the fracture plane and its hydraulic connection with other structures.

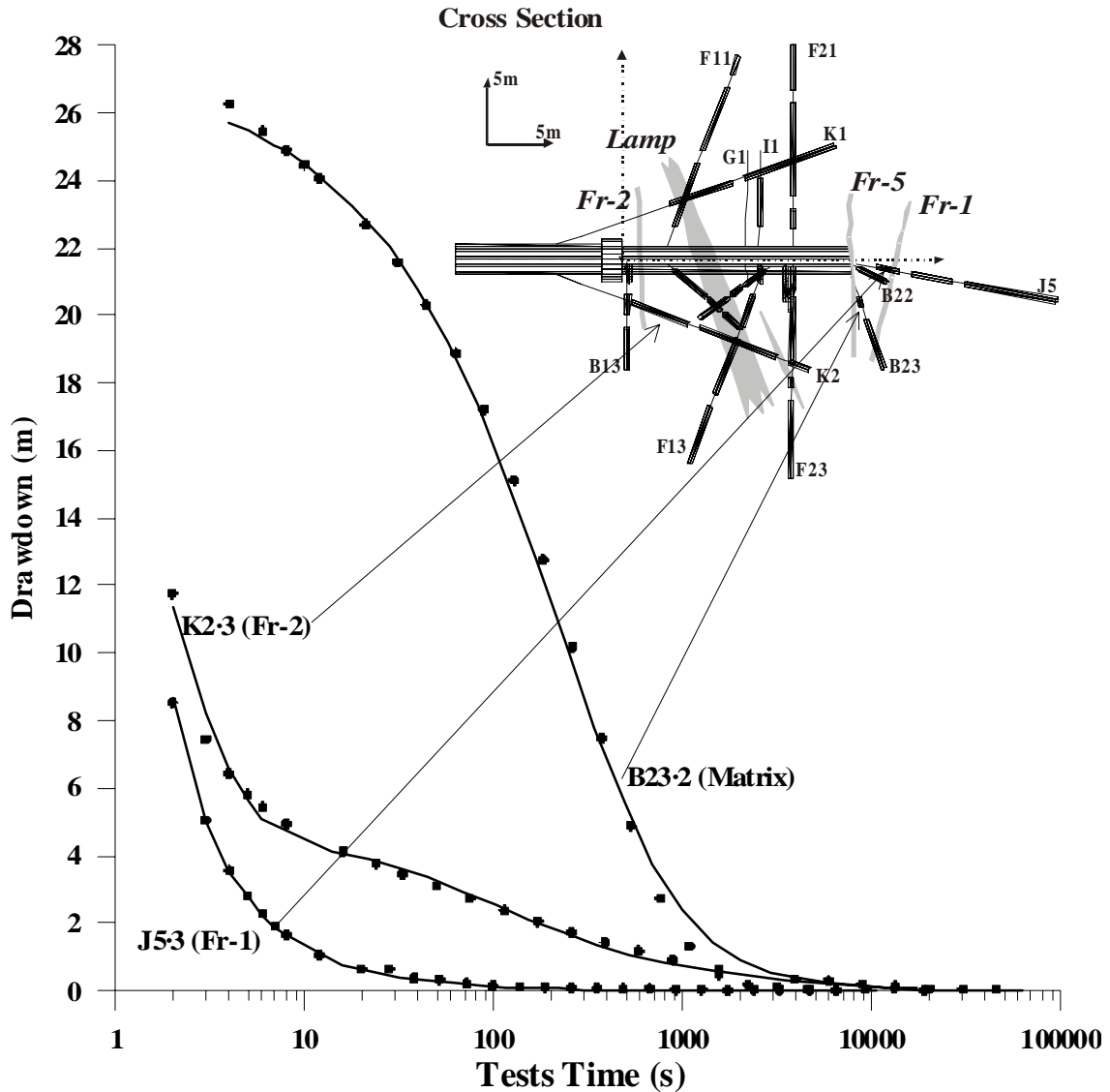


Figure 4: Interpretation of the recovery to three typical pulse tests. Shown are the fitted response (continuous line) and some measured data (dots, most points have been deleted for clarity). Responses depend on the geological structures within the vicinity of the boreholes. B23-2 lies in the rock matrix, thereby presenting a higher drawdown and a slower recovery. The other two tests were performed in intervals intersecting fractures, which imply a lower drawdown and a faster recovery. Notice the difference in the shape of the recovery curves when compared to that of B23-2.

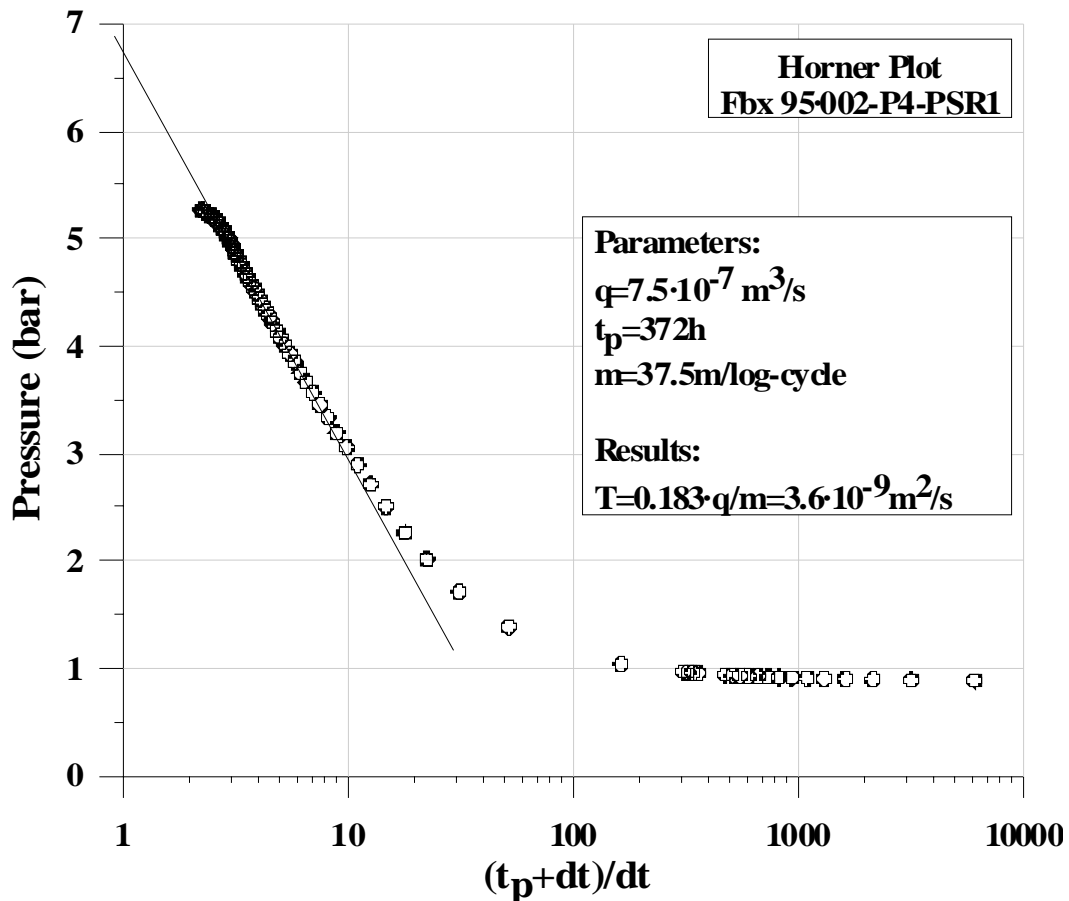


Figure 5: Recoveries in response to the instrumentation of the boreholes were interpreted using Horner's method (Horner 1951).

### 3.2. Recovery tests

Pressure recovery after installing the packers is also used for interpretation (Figure 5). The test consists of measuring the borehole flowrate by locking up the valve placed at the flow line, and then monitoring the pressure recovery. Transmissivity is obtained by means of the Horner (1951) method. The method consist of plotting heads versus  $t_H=(t_p+dt)/dt$  (in log scale), where  $t_p$  (s) is ‘production time’, or time elapsed between the borehole drilling and valve closing, and  $dt$  (s) is the time after the valve is closed. As  $dt$  tends to infinity,  $t_H$  tends to 1 and heads tend to a straight line with a slope  $m=0.183 q_e/T$ , where  $q_e$  ( $\text{m}^3 \cdot \text{s}^{-1}$ ) is the gauged flowrate in the borehole during the production period. Therefore transmissivity is given by  $T=0.183 \cdot q_e/m$ .

The above procedure could not be used at several intervals. Boreholes BOUS85-001 y BOUS85-002, had been drilled in 1985 and later instrumented with a single packer at their mouth. As a result,  $t_p$  was not known. Moreover, water flowed along the boreholes length for several years. This caused a complex transient pressure

profile, which renders the above procedure not applicable. It was not possible to measure the outflow in some radial boreholes during the pressure build-up stage, because they had no water, due to their position within the FEBEX tunnel. Values used in this article were deduced by Meier et al. (1995).

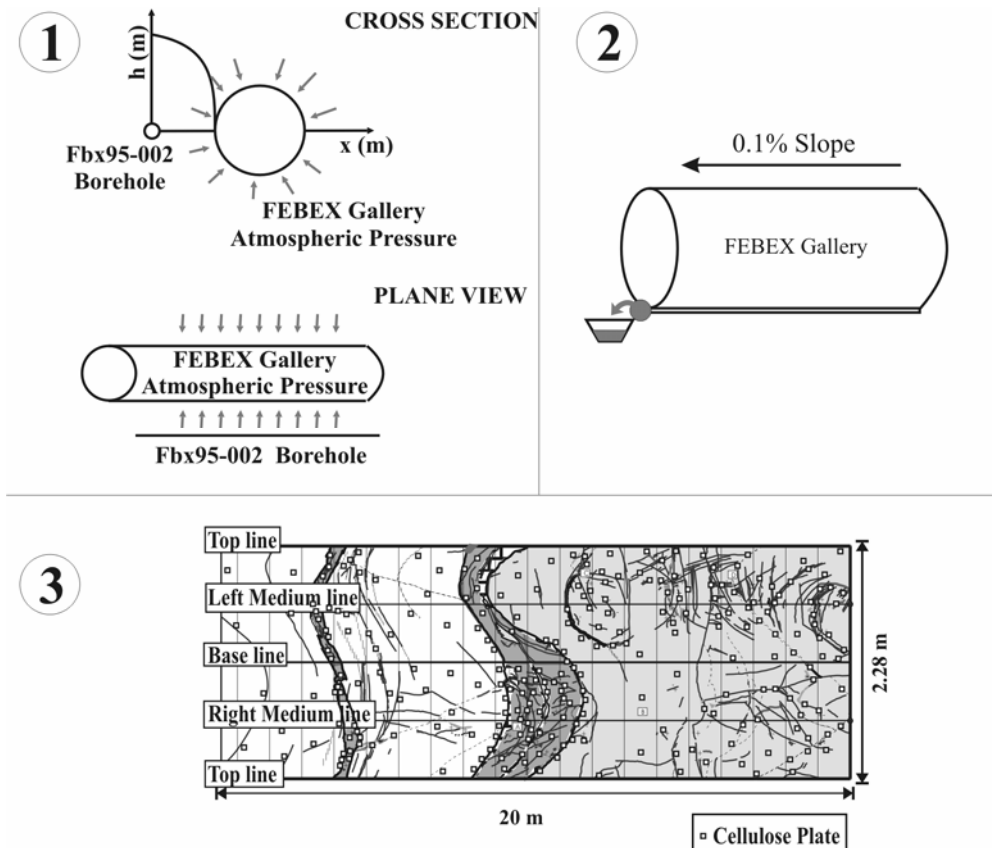


Figure 6: Schematic descriptions of methods used to estimate inflow rates to the experiment zone. (1) pressure values recorded at borehole Fbx95-002 and within the tunnel are used to obtain a pressure gradient, which yields an estimate of the inflow rate under the assumption of radial flow. (2) consists of gauging directly the drainage to the tunnel. Method 3 is represented in the third part of the figure, which contains the geological map after a long period without ventilation of the tunnel (Guimerà et al., 1998). This method consists of placing cellulose plates to quantify the inflow rate towards the tunnel walls. Plates were situated at seepage points within the tunnel.

### 3.3. Integrated flowrate measures

Three methods were used to evaluate tunnel inflows (Figure 6):

1) Borehole FBX95-002 is parallel to the FEBEX tunnel (Figure 1). Since pressure records are available at the borehole, it is possible to calculate the flowrate with Thiem's equation, using the transmissivity derived from this borehole. This yields  $8\text{ml}\cdot\text{min}^{-1}$ .

- 
- 2) The tunnel presents a smooth gradient towards the outlet (0.1%), which allows collecting the water that drains by gravity. This estimate yields a result of  $6.7\text{ml}\cdot\text{min}^{-1}$ .
  - 3) The third method was specifically developed for the project (Ortuño 2000). It consists of installing cellulose plates over the tunnel walls for a given time; the weight difference, before and after the test, can be used to estimate the flowrate, which ranged between  $7.5$  and  $8.5\text{ml}\cdot\text{min}^{-1}$ , according to two different measurements.

Taking into account the uncertainties associated to each method, the three estimates can be considered rather consistent. The equivalent transmissivity is calculated, in this case, under the hypotheses of known drawdown (measured from radial boreholes), 1.14m tunnel radius, and  $8\text{ml}\cdot\text{min}^{-1}$  average flowrate. With these values and Thiem's equation, the result is a transmissivity of  $4.5\cdot 10^{-9}\text{ m}^2\cdot\text{s}^{-1}$  (or, an equivalent hydraulic conductivity of  $2.5\cdot 10^{-10}\text{ m}\cdot\text{s}^{-1}$  for the tunnel length).

### 3.4. Cross-hole tests

Cross-holes tests consisted of 2 day pumping at points strategically distributed with the aim of characterising the whole FEBEX experiment vicinity. Based on the results of pulse-tests, points were selected among the more transmissive intervals to enable a long-term extraction test. Five tests were performed, pumping at J5-3, F22-2, Fbx2-4, F14-3 and F24-1 points. Pumping was done by means of a HPLC pump, which can yield low flowrates, in the range of some  $\text{ml}\cdot\text{min}^{-1}$  (Ortuño et al., 2003). To avoid sudden changes in the interval, both the inner and outer pressure were equilibrated at the beginning of the test by pressuring the line prior to the opening of the pump valve. Pressure was recorded at all observation points (Figure 7), starting one day before the beginning of pumping to correct potential trends. Recovery data were measured until equilibration, when a new test was performed.

The tests have been interpreted first by means of Theis analytical model. Drawdowns at each interval were analyzed independently. We first meant to use Theis' solution as a preliminary step prior to using the method of Hsieh and Neuman (1985), analytical solution for pumping in a homogeneous 3D domain. However we stayed with Theis' solution because the fit was satisfactory (Figure 7). We attribute this to the fact that water flows mostly through the fractures, so that the flow dimension is basically 2D, as assumed by Theis. Still, hydraulic parameters we derived using Hsieh and Neuman model were not very different from those of Theis.

---

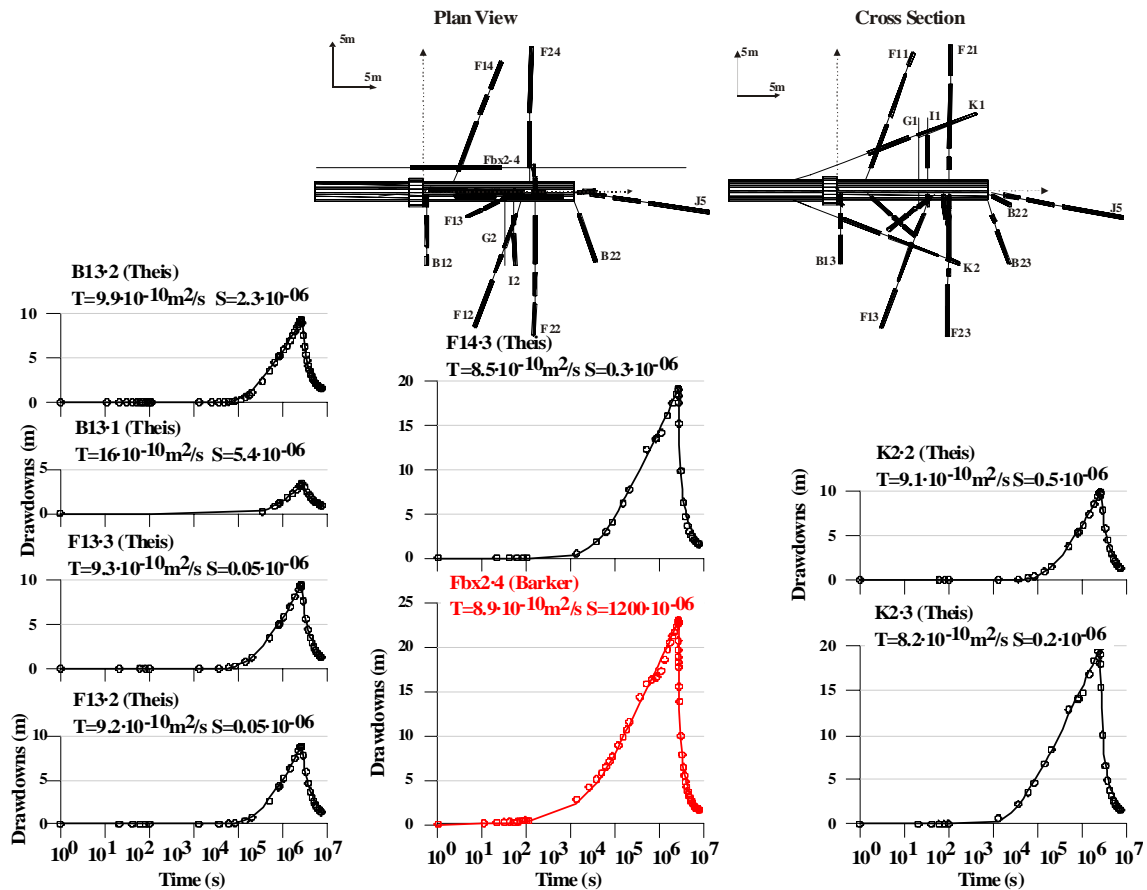


Figure 7: Results of analytical interpretation of the cross-hole test carried out at point Fbx2-4. Responses are interpreted by assuming homogeneous media and fitting the build-up curves for each point separately. The resulting transmissivity and storativity are shown for each interval. Notice that transmissivity variations are minimal (ranging between  $8.3\text{E-}10$  and  $16\text{E-}10 \text{ m}^2 \cdot \text{s}^{-1}$ ), whereas the storage coefficient varies by orders of magnitude (from  $2.6\text{E-}07$  up to  $54\text{E-}07$ ). This gives insight into the heterogeneity of the medium, since intervals that have an apparent low storage coefficient are well connected to the pumping well (Meier et al., 1998; Sánchez-Vila et al., 1999).

### 3.5. Cross-hole numerical interpretation (heterogeneous models)

Numerical three-dimensional models have been used to interpret the five cross-hole tests and also to represent large scale flow in the FEBEX experiment area. The time responses of all observation points and their exact location in the medium with regard to both the pumping interval and the major hydraulic structures were also introduced. This allows us to adjust the responses in all observation points simultaneously for each test (about 40 observation points).

The geometry used to interpret cross-hole tests numerically is identical for all of them, except for the need to refine further the grid around each pumping interval. The



element size is about 1m around the pumping zone, but grows away from them up to 8m. The modelling area consists of a 50-m radius, (almost) 100-m long cylinder, whose axis coincides with FEBEX tunnel. The grid is generated so as to assign its center to the test area. Computed drawdowns do not reach the model perimeter. Still leakage boundary conditions were adopted at outer boundaries and galleries. The mass balance of each calibrated test confirms that groundwater flux through the boundaries is negligible.

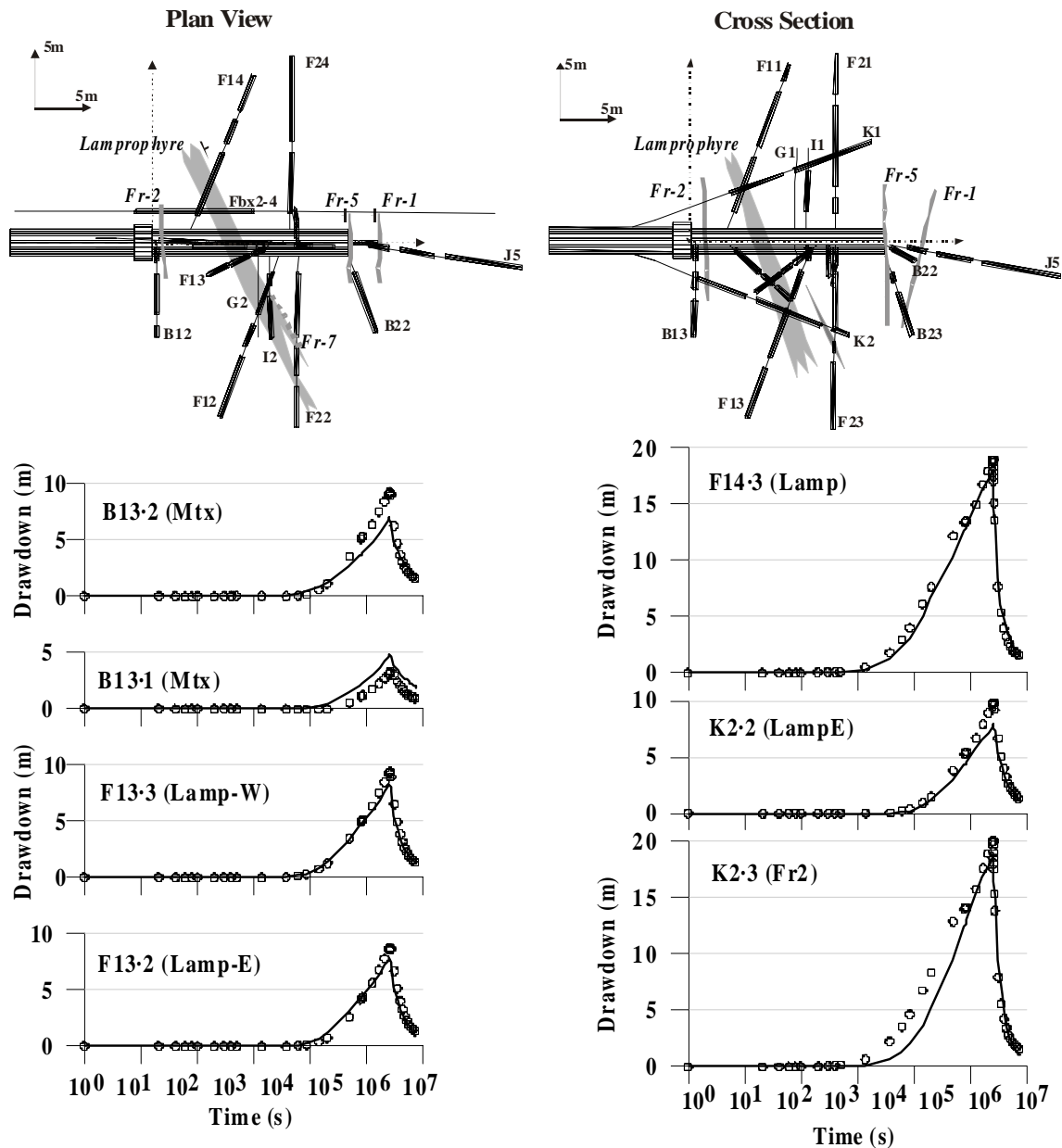


Figure 8: Results of numerical inverse interpretation of Fbx2-4 cross-hole test with a mixed model that includes hydraulically relevant fractures embedded in a 3D homogeneous medium that includes matrix and minor fractures

Fractures are simulated as bidimensional planes embedded in the three dimensional elements that form the matrix. Both fractures and matrix are treated as homogeneous features. The matrix accounts also for the minor fracturing, mainly vertical, that has not been represented explicitly in the model. This effect has been reproduced by considering the hydraulic conductivity of the matrix as anisotropic. As a result, model calibration yields higher matrix conductivity values along the vertical direction than the horizontal axes. The methodology to identify dominant fractures involves integrating structural geology, geophysics, cores descriptions, and the preliminary interpretation of cross-hole tests. Details are provided by (Martinez-Landa and Carrera 2005a). The sizes of fractures included in the model range from 5x8m<sup>2</sup> for Fr-1 to 55x34m<sup>2</sup> for Fr-3. Distances between fractures mid-points range between 5 and 17m. The hydraulic properties of the fractures are also treated as homogeneous (Martinez-Landa and Carrera 2005a).

The fits obtained with this model are shown in Figure 8, which plots the results obtained at the same points where the analytical interpretation was performed.

Table I summarises the statistics of weighted residuals at all the intervals included in the model. All datasets were assigned a unit weight, except for the injection point and intervals F11-3 and K1-2, which were assigned weights of 1/10. For the injection point, this is done to eliminate the effect of the skin. The weight of the other two intervals was lowered because they cut the lamprophyre in an area where connectivity with the pumping point is not significant (the pumping interval intercepts the lamprophyre dyke too).

Table I: Statistics of the Fbx2-4 cross-hole test. The error units are meters.

Sides of Tunnel		Above and End zones of Tunnel		Below of Tunnel	
Interval	RWMSE	Interval	RWMSE	Interval	RWMSE
F22-3	0,81	F21-3	0,24	F23-3	1,49
F22-2	1,46	F21-2	0,13	F23-2	0,41
F22-1	0,23	F21-1	0,25	F23-1	1,24
F12-3	3,08	F11-3	0,37	F13-3	0,76
F12-2	0,43	F11-2	0,08	F13-2	0,69
F12-1	0,20	F11-1	0,62	F13-1	0,71
B12-2	2,58	K1-2	0,40	B13-2	1,61
B12-1	1,06	K1-1	0,15	B13-1	1,25
F14-3	0,69	J5-3	0,11	K2-4	1,00
F14-2	1,71	J5-2	0,07	K2-3	1,27
F14-1	0,15	J5-1	0,07	K2-2	1,37
FBX2-4	2,31	B22-1	0,12	K2-1	1,11
		B23-2	0,10		
		B23-1	0,11		

As for the comparison between computed and measured values, the largest errors occur at interval B12-2 (2-m), which is within the matrix but very close to

---

fracture 2, whose influence is remarkable. The other interval where the average error is high is F12·3 (2.5-m), placed, like intervals F11·3 and K1·2, on the lamprophyre. In general terms, the worst fits take place at the intervals located within this structure, mainly towards the Eastern and upper zones of the FEBEX tunnel. This fact may be due to heterogeneities developed in the lamprophyre dyke, or because of a predominant anisotropic direction within the dyke itself. Representing these effects is what motivates the use of stochastic models to represent small scale variability (see, e.g., [Meier et al, 2001](#); [Vesselinov et al, 2001](#)), but which were not used here for simplicity.

### **3.6. Large scale numerical model**

The main objective of the hydrogeological investigations carried out within the FEBEX project was to achieve a good hydraulic characterization of the granitic block, with the aim of evaluating the inflow towards the tunnel and determining its spatial distribution. These results are being used currently by other research groups.

To achieve these goals, a 3D flow model has been developed at a larger scale (210x230x150 m<sup>3</sup>), its central area being occupied by FEBEX tunnel. The geometry implemented into this large-scale model contains all features described in the previous section (cross-hole tests), but also additional fractures, boreholes (BOUS85-001, BOUS85-002, FEBEX95-001 y FEBEX95-002) and galleries (Figure 1). The procedure to construct this model and to deal with the hydraulic parameters is analogous to the one presented in section 3.5. that the values of hydraulic conductivity derived from the calibration of cross-hole tests have been used as prior information for structures located in the vicinity of FEBEX tunnel ([Martinez-Landa and Carrera, 2005a](#) and [c](#)).

The model simulates steady state groundwater flow. Calibration data include heads measured in the intervals of all instrumented boreholes. A prescribed head condition has been imposed on all external boundaries, and the adopted values have been derived from the large scale model of [Kiraly \(1985\)](#). The galleries boundaries are treated as leakage limits, and so are the intersection points between fractures and the galleries. Flow discharges through the tunnel walls and the fracture intersections with the galleries have been measured by means of the gauging method proposed by [Ortuño \(2000\)](#), which is described in section 3.3. These data have served to contrast the model calibration results.

Four different scenarios were calibrated for the same area, representing heads prior to and after excavation of FEBEX tunnel and to address uncertainty on the boundary shear zones (Guimerà et al., 1998).

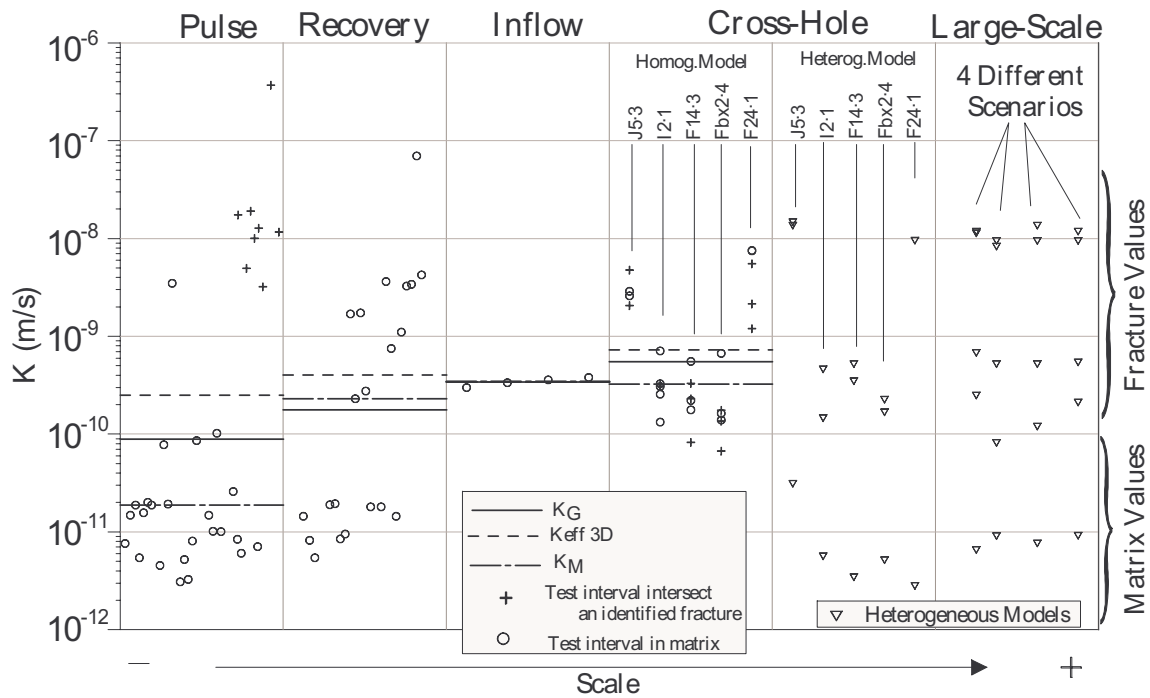


Figure 9: Hydraulic conductivities obtained from interpretation of hydraulic tests versus test scale. The horizontal axis represents a qualitative evaluation of the size of the rock affected by each test type. Within each test type, the ranking is arbitrary. The values of equivalent hydraulic conductivity increase with the volume of rock sampled in the test. Each of the columns (for cross-hole tests) refers to a different test, with a total of 5 tests. The geometric mean ( $K_G$ ), effective 3-D conductivity ( $K_{eff3D}$ ) and the median ( $K_M$ ) have been calculated for each type of test. There is an increase of all these values with the scale of the test. The two last columns represent the results of 3D numerical models used to interpret cross-hole tests and large-scale FEBEX data, respectively. In these columns, symbols identify hydraulically relevant fractures (values between  $10^{-10}$  and  $10^{-7}$  m/s) and minor fractures lumped with the matrix (values below  $10^{-11}$  m/s).

#### 4. RESULTS AND DISCUSSION

All, the values of equivalent hydraulic conductivities obtained from the interpretation of all tests performed along the successive stages of FEBEX project are plotted versus the scale or rock volume affected by the test in Figure 9. Analytical interpretations of hydraulic tests yield values of transmissivity. However, results are presented in terms of hydraulic conductivity for consistency, so as to facilitate comparisons (Neuman, 1987). In this work, K results from dividing the T by the length

---

of the tested interval. The values of  $K$  range between  $10^{-12}$  and  $10^{-6}$   $\text{m}\cdot\text{s}^{-1}$ . It can be observed that  $K$  increases with the scale of the test.

Pulse tests were conducted at all intervals (Figure 9). In general, the hydraulic conductivity is around  $10^{-11}$   $\text{m}\cdot\text{s}^{-1}$  for most intervals, but some displays a higher value. These are the ones that intercept transmissive fractures.

Recovery tests exhibit less dispersion of  $K$  estimates than pulse tests. This can be attributed to involved rock volume, which is larger. Therefore, more conductive structures may be intercepted. However, low values can still be found.

The flowrate measurement (denoted as inflow in Figure 9) is an integrated value at the tunnel scale. The affected rock volume is similar to the one of cross-hole tests. Therefore, it is not surprising that hydraulic conductivities values are also similar.

As discussed above, five cross-hole tests were carried out within the domain to characterise the hydraulic behaviour of the granitic block. Figure 9 shows the results obtained after interpreting these five tests by means of analytical methods. The hydraulic conductivity values are grouped in columns and labelled with the pumping interval name (J5-3, I2-1, F14-3, Fbx2-4 and F24-1). Hydraulic conductivity values derived from analytical interpretation of cross-hole tests do not split into two groups despite the fact that some intervals intercept conductive structures and some do not. Yet, all estimates transmissivity are relatively close to each other for each test (recall also Figure 7) and to the values derived from pulse tests at intervals intersecting fractures.

Cross-hole tests I2-1, F14-3 and Fbx2-4 affect the same structures (lamprophyre, Fr-2 and matrix, Figure 4) and yield rather similar results. The main difference lies in tests J5-3 and F24-1. The former is located in a highly fractured zone (the endpoint of FEBEX tunnel, as shown in Figure 1 and Figure 2). Yet, it is characterized by a much lower fracturing that is not possible to identify with specific fractures. As a result,  $K$  values are grouped and higher than mean values (Figure 9). The latter, on the contrary, intercepts one of the most conductive structures in the zone: a discrete fracture (Fr-3) that is identified through F24 borehole core (in the bottom) and is almost parallel to FEBEX tunnel but does not involve another borehole or test in the zone.

A large number of  $K$  values are available for each test scale. To facilitate the analysis of hydraulic conductivity evolution with scale, statistics such as the median ( $K_M$ ) and the geometric mean ( $K_G$ ) are calculated for each test type. Since the problem

---

is 3-D, it is also represented the 3D effective conductivity ( $K_{\text{eff3D}}$ ) for each test scale.  $K_{\text{eff3D}}$  is defined as (Gutjahr et al 1978):  $K_{\text{eff3D}} = K_G(1 + \sigma_Y^2/6)$  where  $\sigma_Y^2$  is the variance of  $Y = \ln K$ , and was calculated as  $\Sigma(Y_i - \bar{Y})^2/n$  where  $n$  is the number of tests.

All these statistics and equivalent parameters are depicted in Figure 9. If the point values of hydraulic conductivity followed a log-normal distribution, then  $K_G$  should be close to  $K_M$ . Figure 9 shows that this is precisely the case, and also that  $K_{\text{eff3D}}$  is higher than both of them. Still, all of these statistics increase with the tested rock volume, showing a scale-effect.

Results derived from numerical calibrations (cross-hole tests and large scale) are also shown in Figure 9. Five models can be distinguished within cross-hole tests. Parameters shown in the figure correspond to matrix and each of the model fractures. The matrix hydraulic conductivity of model J5-3 is larger than that of the remaining models because the tested area is much more fractured, so that it was not feasible to identify all the main fractures. Therefore, the matrix value increases because it includes some fractures that have not been explicitly included in the model. This plot underscores the difference between the rock matrix and the main hydraulic structures, such as fractures and dykes.

Statistical parameters have been calculated, they increase with scale, except for the interpretation of cross-hole tests with 3D numerical models. The problem lies in the number of values available for the averaging. In recovery tests, there are reliable data only for the long boreholes, as mentioned before. Since only intervals responding clearly to the tests have been represented for the analytical methods, the equivalent conductivities are biased. At the numerical models we have use every observation points, with or without response to the hydraulic test. The consequence of not accounting for all observation points is that statistics of both recovery and cross-hole tests analytical interpretation are higher than expected.

As a result, it can be observed that lowest values (around  $10^{-11} \text{ m}\cdot\text{s}^{-1}$ ) are assigned to the rock matrix equivalent hydraulic conductivity, whilst the values of the fractures depend on their hydraulic properties, such as the heterogeneity in the plane, their extension or their connectivity.

---

When the conductivity values derived from the numerical interpretation of the tests are plotted in Figure 9, it becomes apparent that the scale effect can be attributed to the fractures. Calibrated K values corresponding to fracture zones are comparable to those of the homogeneous model interpretation of cross-hole tests. This suggests that the values derived from these tests represent indeed the major fractures, but are unaffected by the minor fracturing, lumped as matrix in the numerical model.

Results of the numerical model interpretations of the tests also allow us to put the results of short range tests in perspective. High K values correspond qualitative and quantitatively to fractured zones, while small values (around  $10^{-11}$  m/s) correspond to lesser fractured zones (matrix in our model).

## 5. CONCLUSIONS

The objective of this work was to study the scale effect on hydraulic conductivity in fractured granite at FEBEX, Grimsel, Switzerland. A preliminary interpretation of the tests has been done by standard analytical methods that assume a homogeneous medium. The results obtained from these interpretations can be summarised as follows:

- Short-range pulse tests yield point values of hydraulic conductivity. Most of these are low, but there is still a significant range of variation. Low values of average conductivity reflect that the majority of the tested intervals are representative of the matrix hydraulic conductivity, but a few intervals have abnormally high values because they intercept fractures.
- As the test scale grows (recovery, cross-hole tests), the average hydraulic conductivity increases. This can be explained because zones of high hydraulic conductivities are hydraulically well interconnected and therefore control permeability at larger scales.

Using three-dimensional numerical models aids in integrating data and reproducing the effect of heterogeneities, such as fractures and their connections. The use of the measurements registered at all observation points, affected or not by the hydraulic tests, made it possible to better reproduce the response of the medium. This makes it easier to understand the behaviour of the system and to explain the measurements in a consistent way.

The main conclusion of this article is that the equivalent hydraulic conductivity of the medium increases with the scale of the test, but pulse tests (point measurements) already provides relevant information concerning the magnitude of the parameters, as also shown by [Vesselinov et al. \(2001\)](#). To predict hydraulic conductivities at a greater scale, it is necessary to build a large scale model that incorporates point values and the geological information concerning connectivities. This implies a remarkable effort and some complexity. Another alternative consists of conducting long-term hydraulic tests, but this is expensive and not always feasible. Therefore, it would be convenient to revise the current methods to estimate equivalent hydraulic conductivities and to derive a relationship that allows obtaining equivalent hydraulic conductivities based on point conductivity values and connectivity information.



---

## PAPER III

### **A HYDROGEOLOGIC MODEL OF GRANITE ROCK AS A SUPPORT TO A MINE RESTORATION**

Lurdes Martínez-Landa and Jesús Carrera

(Groundwater)



## 1. INTRODUCTION

Low permeability, fractured media are acquiring a more relevant role in hydrogeology due to their suitability to host high radioactivity wastes (deep geologic storage). This interest lies in the intrinsic properties of such media, given the associated low hydraulic conductivity and long travel times for contaminants. However, there is a remarkable contrast between the conductivity of the matrix and the main fractures, which can reach several orders of magnitude. This makes it important to account for heterogeneity when representing the system.

Because of the interest of such geologic environments, there are numerous studies on granites around the world: Stripa (Rouleau and Gale, 1985; Long et al., 1991) and Äspö (Tsang et al., 1996; Svenson, 2001b) in Sweden; Grimsel in Switzerland (Davey Mouldon et al., 1993; Martinez-Landa and Carrera, 2005a); Fanay-Augères in France (Cacas et al., 1990); Mirror Lake in Utah, USA (Shapiro and Hsieh 1991; Day-Lewis et al., 2000). These sites are located in zones affected by the last glaciation, so that their deformational history is different from that of Southern Europe. Only a few studies focus on granites in this area, such as El Berrocal pluton (Guimerà et al., 1995) or Ratonés mine (Martinez-Landa et al., 2005c), both in Spain, thereby contributing to improve the knowledge on this type of media. This article is based on the research work conducted at the Ratonés Mine, in Cáceres province.

Despite those references, there is no a commonly accepted methodology to model low permeability, fractured media. Several approaches hold for modelling these media, but, two main methods have been proposed, depending on the way to represent them: as continuous, porous equivalent media and as fracture networks. The former assimilate the domain to a porous and homogeneous medium, which includes the effect of discrete fractures, and implement the hydraulic conductivity field by means of geostatistical techniques, by conditioning the fields to field measurements, that is, to pressure records in observation points (Gomez-Hernandez et al., 2000; Day-Lewis et al., 2000; Vesselinov et al., 2001; Svenson, 2001a). The later work only with fracture networks that are statistically created. This modelling approach is based on the assumption that fractures behave as preferential paths for water flux through the rock (Long et al., 1987; Cacas et al., 1990; Dershowitz, 1984; Dershowitz et al., 1991; Castaing et al., 2002). An alternative for fracture networks models consists of channel

---

networks models, which only represent the conductive parts of the fractures planes (Moreno and Neretnieks, 1993). Our approach takes advantage of both options: the matrix and minor fractures are simulated as an equivalent porous medium whilst the main fractures are explicitly implemented within the matrix. This allows for a correct positioning of the structures and their associated local effects without refining too much the finite element grid. As a result, the same mesh can be used to interpret hydraulic tests at different work scales, however, as a counterpart, the main structures have to be identified (Martinez-Landa and Carrera, 2005b).

A frequent conclusion when interpreting tests is that a so-called scale effect is observed. This scale effect refers to the apparent increase of hydraulic conductivity or transmissivity as the rock volume increases (Clauser, 1992; Illman and Neuman 2000; Illman and Neuman, 2001; Vesselinov et al., 2001). In a study about field measurements in El Berrocal, Guimerà et al., (1995) argue that the scale effect can be due to the natural selection process that takes place when deciding on the intervals to test, since pulse tests (performed at the cm-scale) are generally conducted in the less conductive points whereas tests that provoke a meter-scale perturbation have to be done in the intervals that can be pumped during longer periods, i.e. from the most conductive points. This hypothesis is valid as concerns the local conductivity around the tested interval, but other authors (Day-Lewis et al., 2000; Meier et al., 1998; Sanchez-Vila et al., 1996) attribute it to the connectivity among structures. Certainly, the hydraulic conductivity derived from interpreting pulse tests yields information about the closer vicinity of the borehole. These results in marked differences between values associated to intervals that intersect any conductive structure and those that are drilled in the matrix (Martinez-Landa and Carrera, 2004). In cross-hole tests, pumping must be carried out from intervals placed in high conductivity zones to maintain a constant flowrate for long time periods, but its effect also affects points located in the matrix. If the interpretation of the tests does not take into account the existence of heterogeneities, their effect can be masked by the value of the effective hydraulic conductivity and it can result in apparently higher values. Implementing the heterogeneities into the model makes that the matrix hydraulic conductivities are similar to the values obtained from pulse tests in intervals placed within the matrix, whilst fractures hydraulic conductivities are close to the highest values obtained in pulse tests (Martinez-Landa and Carrera, 2005b).

---

This discussion shows the discrepancies concerning the preferred approach to model low permeability, fractured media. Illman et al., (2004) elaborated a thorough discussion about scale effect and its origin, pointing to other issues such as poorly developed wells (Butler and Healey, 1998) and turbulences in the boreholes (Lee and Lee, 1999); he concluded that the scale effect is real. In our work within the framework of FEBEX Project in Grimsel, Switzerland (Martinez-Landa and Carrera, 2005a), it is demonstrated that the scale effect can be explained by the heterogeneity that characterise the medium, provided that it is possible to represent the medium together with the major heterogeneities.

Accounting for the heterogeneities makes it possible to use the models to predict other scenarios. This has been done in previous works (Carrera et al., 1990; Carrera et al., 1993) to predict future hydraulic tests by means of hydrogeologic models. The best indicator of model's robustness is being able to apply it to predict changes in flow conditions at scales different from the scale used for calibration.

The objective of this article is threefold. First, it contributes to improving the knowledge of low permeability, fractured media at the Iberian Peninsula, in Southern Europe. Second, it presents a methodology that has been specifically developed for such media and checks its predictive capability as a reliability indicator. Finally, a discussion on the scale effect is presented based on the natural behaviour of these media. Finally, the scale effect on hydraulic conductivity is discussed on the basis of the natural behaviour of low hydraulic conductivity fractured media.

To accomplish these objectives, field datasets from the Ratones Mine (study of the hydrogeology around an old uranium mine excavated in a granitic pluton) are used. Datasets proceed from geochemical, geologic-structural and hydrogeological studies that aid in identifying the main structures (heterogeneities), including their position, direction, dip and extent. A three-dimensional numerical model is constructed then, where the matrix and minor fractures are treated as an equivalent porous medium and the identified fractures are implemented as two-dimensional planes embedded in the matrix. This numerical model is then used to calibrate cross-hole tests and to predict the long-scale pumping tests from the mine.

The article is structured as follows. The first step consists of describing the Ratones mine site, and, afterwards, the hydraulic characterisation and scale-effect issues are explained. Then, the hydrogeological modelling of hydraulic tests and prediction of

a large-scale pumping are presented. The paper ends with a discussion of the model results.

## 2. TEST SITE

The Albalá Granitic Pluton is located in the southwest sector of the Iberian Massif (Central-Iberian Zone of Julivert et al., 1972). The pluton is a concentrically zoned body, elongated in an N-S direction, with porphyric biotite granites in the rim and fine-grained two-mica leucogranites in the core

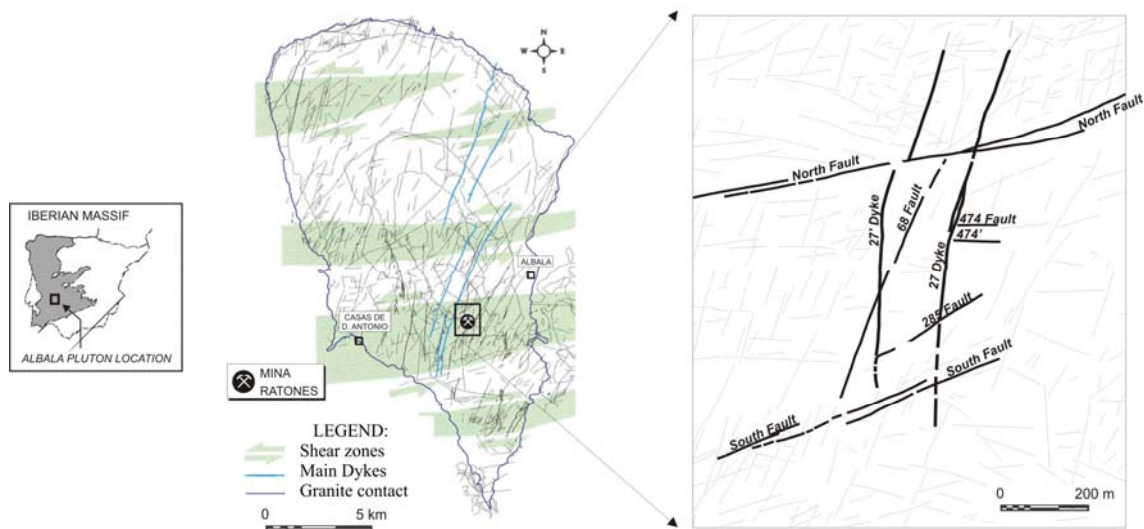


Figure 1: Geological map of Albalá Granitic Pluton with location of the Mina Ratones area (ENRESA, 1996; Escuder Viruete and Pérez Estaún, 1998).

The Ratones mine is located in the central aureoles of the granitic pluton of Albalá (Cáceres, Spain) (Figure 1). Fault zone architecture in the Mina Ratones area has been established on the basis of field geology, structural analysis, seismic experiments, drill cores (SR1 to 5) and sonic well-log data (Escuder Viruete and Pérez-Estaún, 1998; Carbonell et al., 1999; Escuder Viruete, 1999; Jurado, 1999; Jurado, 2000; Pérez-Estaún, 1999; Martí et al., 2002). Surface geology was mapped at 1:5000 and 1:1000 scales in a zone that includes the block where the seismic tomography survey was conducted, and the resulting maps include granitic facies, dykes, ductile-brittle shears, fault zones and granitic soil cover (lehm). The 3-D fault distribution obtained for this area is shown in Figure 2. The main identified structures are the North Fault, the South Fault and the 27 and 27' Dykes. Other relevant brittle structures of minor size are the 474, 478, 285 and 220 Faults. Further, the seismic profiles suggest the existence of the 476 (or SR3 dyke) east of SR3 well.

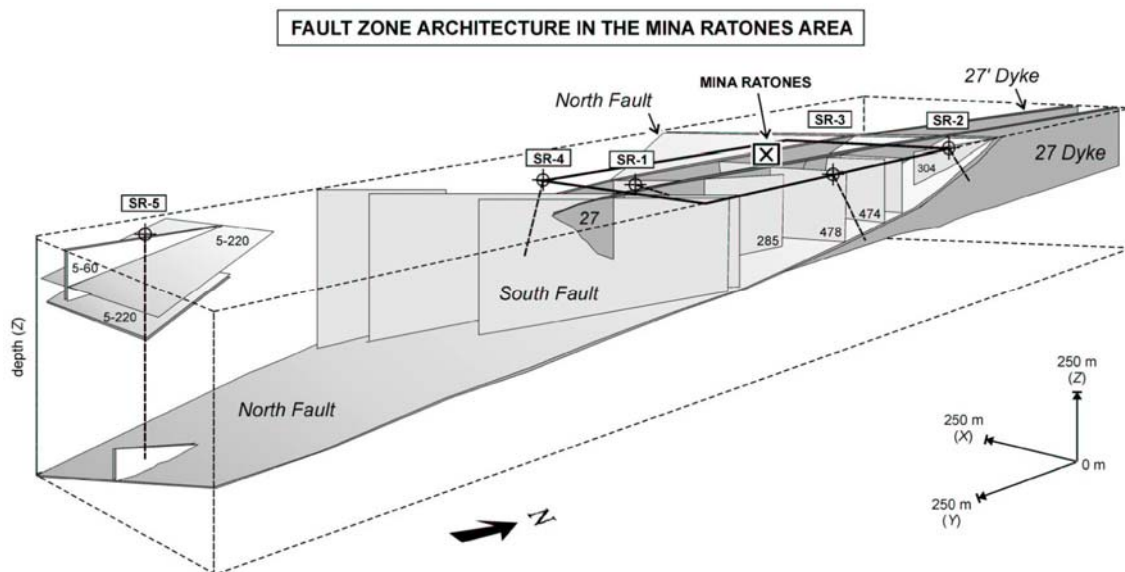


Figure 2: Fault zone architecture of Mina Ratonés area obtained from structural, seismic, core and well log data (Escuder Viruete and Pérez Estaún, 1998; Carbonell et al., 1999; Escuder Viruete, 1999; Pérez Estaún, 1999). The main identified structures are the North Fault, the South Fault and the 27 and 27' Dykes. Other relevant brittle structures of minor size are 474, 478, 285 and 220 Faults.

The 27 dyke trends N028°E and dips E at 80-85°, has a thickness of 0.4-1.8m and is composed of a cataclastic breccia of quartz, cemented by sulphides (Escuder Viruete et al., 2003a; Escuder Viruete et al., 2003b). The 27 and 27' dykes are two mineralized structures of subparallel trend. The 27' dyke trends N014°E and dips W75-80°, and becomes subvertical at 90m depth. The dykes are hosted in an extensively fractured damage zone of hydrothermally altered granite (fractured belts). Drill cores (SR2 and SR3 wells) and geophysical data suggest the North Fault has a N072°E to N080°E trend and an S dip of 55-65°, which decreases with depth to 30-40°. It is defined by a fracturing belt in which the granite is intensively altered from both the chemical and mechanical standpoints. The related fault zone expose at the surface has a width of 12-16m and is characterized by high fracture intensity and extensively altered granite (lehm). The South Fault damage zone is defined by subvertical small faults and kinematically related fracture sets and joints, which form a 14-20m thick brittle shear-zone. Small faults have a N064°E to N078°E trend and N dip 68-82°. The South fault core rocks recovered in the SR4 well are micriobreccias and white clay-rich gouges. The 474 and 474' Faults are two high-dip subparallel structures that trend N064°E to N076°E. Both structures connect toward the W with the 27 dyke. The 285 brittle structure is also a sinistral strike-slip fault with a N052°E to N060°E trend and

subvertical dip. Faults 747 and 285 are younger than the North fault; they cut it and balance it, so that remains hydraulically disconnected.

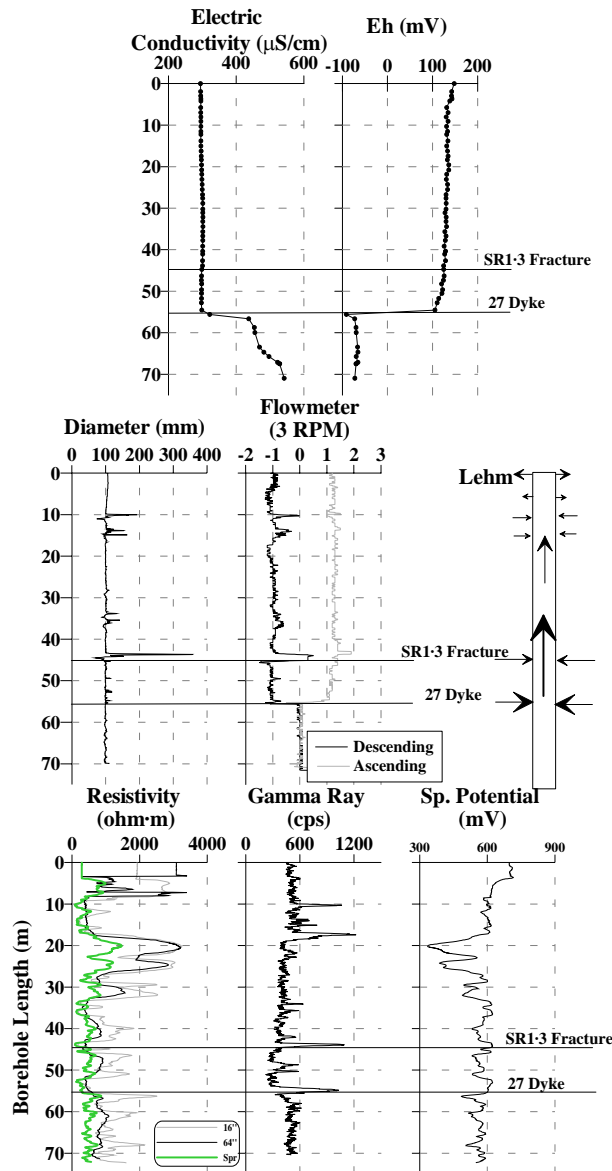


Figure 3: Chemical and geophysical logs at the boreholes. This figure shows some of the records obtained for borehole SR1, which have helped to identify two structures: dyke 27 and fracture SR1-3. The upper logs only display the effect of dyke 27, because water flowing through SR1-3 has circulated previously through the mine, which causes water to acquire the typical properties of mine water. In the lower logs, however, the effect of both structures can be noticed, especially in the gamma log, due to the fractures fillings. Flowmeter measurements at the borehole vertical, with an upwards flow of 3 rpm (pumping) indicate that, below 56 m depth, there is little water movement up to the intersection with dyke 27. This provokes a water inflow with upwards circulation. The same applies to a lesser extent to when intercepting fracture SR1-3.



---

Hydrogeochemical studies aid to identify the fractures. Water flowing through fractures is chemically marked by water-rock interaction along the flowpath within the medium (Perez del Villar et al., 1999; Gomez et al., 1999; Gomez et al., 2001; Gomez, 2002). This enables to identify some fractures and potential connections. Figure 3 shows an example of the diagraphies and records of a multiparametric device (temperature, electrical conductivity, pH, redox potential, dissolved oxygen) in borehole SR1, downgradient the mine. In these data, it can be appreciated the intersection of the borehole with dyke 27, where there is water flowing from the mine, as indicated by chemical parameters and changes in the upwards velocity of flow within the borehole (flowmeter log).

With this information and hydraulic tests performed in a unique borehole (pulse tests, slug test, constant head tests), the location of the structures can be determined. Geology and geophysics can only give insight into the physical configuration of the fracturing network. Local (unique borehole) hydraulic tests serve to identify those intervals with higher conductivities, which may act as conductive structures. Hydrogeochemistry may also inform on connectivity if there is a chemical tracer in the water. But connectivities can only be identified by means of cross-hole tests.

### **3. HYDRAULIC CHARACTERIZATION**

As discussed above, geophysical methods help in identifying the main fractures. To understand the hydraulic conceptual model of the system, it is necessary to know which is the hydraulic extent of the fractures and their connectivities. This is why a hydraulic testing survey was designed.

To achieve a satisfactory hydraulic characterisation of the area, different types of measurements were used:

- a) Development pumping, carried out in all boreholes SR, consisted of pumping with open borehole to withdraw all drilling materials.
- b) Chemical sampling pumping of FN in borehole SR2, of FS in borehole SR4 and some intervals of SR5. Time, flowrate and interval pressure were measured.
- c) Irrigation pumping from the mine to satisfy the water needs of the vegetal cap that was created after restoration of the mine. These data have been used as a cross-hole

test because all the boreholes were instrumented to measure the effect of the pumping stress. Flowrate in the mine and drawdown at all points were recorded.

Also, specifically designed hydraulic tests have been conducted:

- d) Pulse, slug and constant head tests were conducted point by point in boreholes SR3, SR4 and SR5. The three tests were performed with a specially devised instrumentation, which consisted of two packers separated at a constant distance and a system of pipes and valves to allow the injection or extraction of very low water volumes with high precision (Ortuño et al., 2000).
- e) Cross-holes tests. Three of them were planned, called North, East and South. For this purpose, the boreholes were divided into intervals, which were hydraulically isolated by packers. The position of packers was determined to isolate the structures that had to be tested. Each interval is equipped with a pressure outlet and a water injection/extraction point.
  - e.1) North test: pumping interval S14-1. Was designed to characterise the dyke 27 upgradient the mine.
  - e.2) East test: pumping interval SR3-1, which intersects the target North Fault, like SR2-2. After pumping for 9 days, there were no responses at any observation point. Later, it was certified that there is no possible hydraulic connection between these points because the North Fault is cutted and balanced by Faults 474 and 285. This datum was unknown when carrying out the test because it was obtained after interpreting the seismic profiles in a subsequent stage (Pérez-Estaún, 1999; Martí et al., 2002).
  - e.3) South test: pumping interval SR4-1. Located in the discharge zone of the mine, pumping within the South Fault. Only in this test all the observation points reacted to the pumping.

The hydraulic characterisation begins with a one by one test (pulse, slug, and constant head). The calibrated parameters give insight into the transmissivity field around the boreholes, and enable to identify the most conductive intervals. Cross-hole tests are then conducted in these ones to identify connectivities.

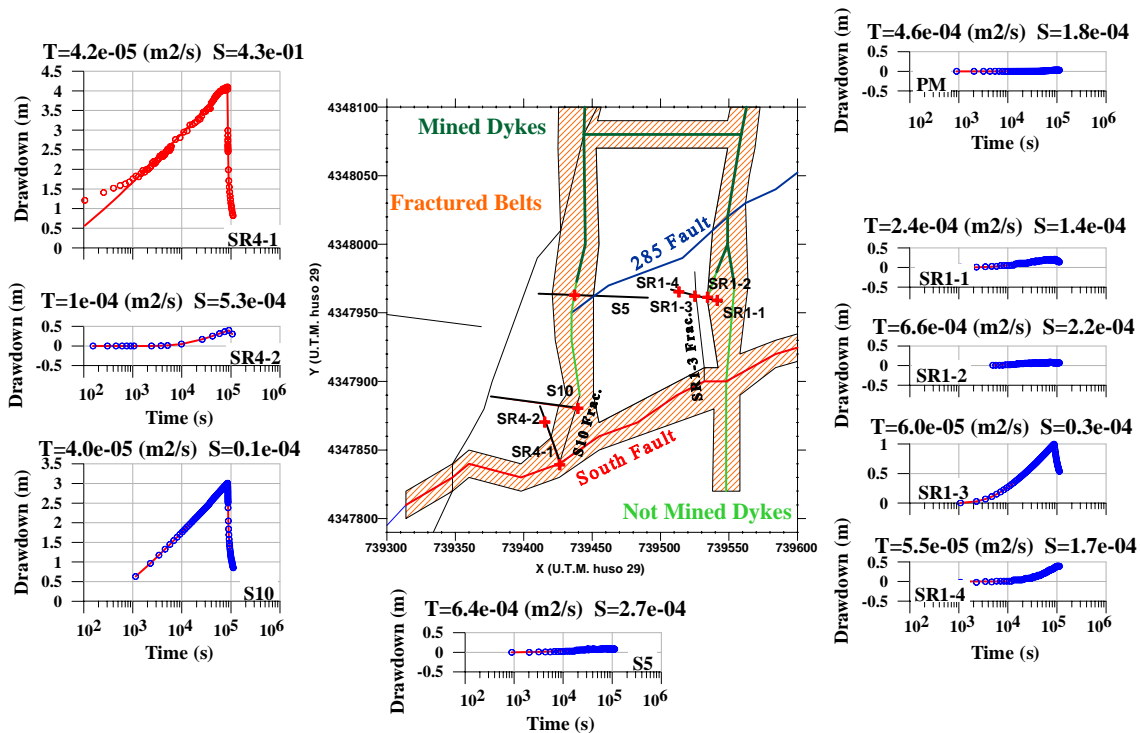


Figure 4: Results from preliminary interpretation of the South cross-hole test (pumping at SR4-1). Transmissivity and storativity are derived by fitting each borehole drawdowns, one-at-a-time, using Theis' model. Degree of connectivity is derived from the estimates of storage coefficients. T varies from 4 to 64-10<sup>-5</sup> m<sup>2</sup>-s<sup>-1</sup>, while S ranges from 1 to 53. We take S estimates to reflect connectivity. A small S (fast response) implies good hydraulic connection between pumping and observation wells. This suggest that best connections take place between the pumping interval and points S10 and SR1-3, whilst points S5 and SR1-2, and, especially point PM, were damped by the mine influence (which behaves as a constant head boundary).

All hydraulic tests have been interpreted with Theis' method (Theis, 1935). This model assumes that the medium is homogeneous and isotropic, thereby integrating the effect of heterogeneities into the matrix. In cross-hole tests, interpretations are done point by point, which yields a couple transmissivity-storage (T-S) for each observation point (Figure 4). These tests provide the connectivity among points through fractures. The storage coefficient values can give an idea of the connectivity between two points: if transmissivity is similar, then the lower the storage coefficient the higher the diffusivity, and the higher the hydraulic connection. The dykes and faults North and South are accompanied by systems of minor fracturing that form part of a higher transmissivity zone situated around these structures. Points S10 and SR1-3 are connected to the pumping point through these fracturing belts that accompany both the dykes and the South fault. In the 3D numerical model, this connectivity has been

simplified by simulating fracture planes referred to as “fracture S10” to connect points S10 and SR4-1, and “fracture SR1-3” to connect points SR1-3 and the pumping point.

The remaining observation points have a lower response to the pumping. Observation points S5 and SR1-2 intersect the dykes 27' and 27, respectively. A priori, it could be thought that these should have a better response to the pumping. Drawdowns between both points are limited by the influence of the mine cavity, which acts as a constant head boundary.

### **3.1. Scale effect**

Figure 5 represents the hydraulic conductivities obtained from all hydraulic tests as a function of the scale. Transmissivities derived from interpreting the datasets are converted into conductivities by dividing by the length of the pumped interval. The scale of the test is determined by the rock volume affected by each test; it can range between a few centimetres (pulse tests) and hundred of meters (cross-hole test SR4-1 and mine pumping).

As commented above, the tested intervals do not coincide in all types of tests. In the case of pulse, slug and constant head tests, they were conducted sequentially with the same interpretation. Instead, the installation of packers for the realization of the cross-hole tests causes the tested points not to be the same, because the main structures are isolated from the matrix and minor fractures. However, it is still possible to compare the calibration parameters with the results of homogeneous and isotropic models (interpreted before using Theis model), since larger scale tests also involve the rock volume of lower scale tests.

The median of hydraulic conductivities increases with the scale. This does not occur with the mine pumping, because all the tests were executed in winter (saturation conditions) but the mine pumping took place in summer, when the upper, more conductive layers (granitic lehm) were dry. This is why calibrated effective hydraulic conductivity are higher in winter than in summer season, when upper more transmissive zones do not play a role in groundwater flow.

The dispersion of hydraulic conductivity values for each test diminished with the scale, due to the fact that, when the medium is treated as homogeneous, it includes the

hydraulic conductivities of the main structures in the effective conductivity, i.e. it is more homogeneous. The mine pumping is the most homogeneous one.

The right part of Figure 5 shows the hydraulic conductivity values obtained after the interpreting the South cross-hole test with a three-dimensional numerical model. This 3D model represents the main features of the medium heterogeneity in an explicit way (fractures, mine and different units of the granite, depending on its hydraulic behaviour). In the next section, the numerical model is presented and their results discussed, but it is included here to compare these results from the perspective of scale effect. Points represented in the Figure 5, for this cross-hole test, do not represent different results at different observation points, but the conductivity of the main fractures, fracturing belts, altered unit, lehm and matrix. Fracture transmissivities are transformed into conductivities by assigning them a unitary width. This results in larger conductivity values for the fractures and dykes, whereas the lower values correspond to the matrix elements, whose conductivity depends on the fracturing index.

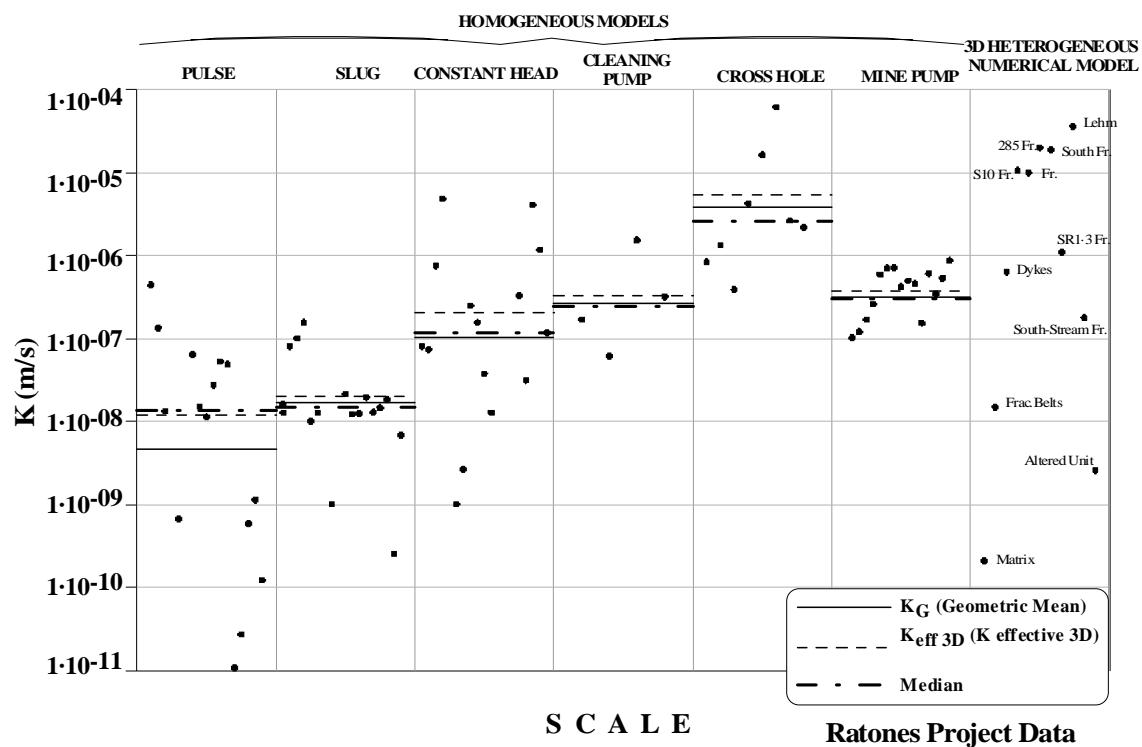


Figure 5: Transmissivity values obtained from interpretation of hydraulic tests performed at varying scales in different holes and intervals. In general, transmissivity grows with the scale, except for the cross-hole test, which was performed in the highly transmissive portion of the site.

In sum, the lower values of hydraulic conductivity are associated to pulse tests for points situated within the matrix. These values are consistent with the conductivity

estimated for the matrix in 3D heterogeneous model. The increase in hydraulic conductivity with scale is due to the contribution of fractures to the effective conductivity when interpreting the tests by means of homogeneous models.

#### 4. NUMERICAL MODEL

A three-dimensional numerical model has been constructed to interpret the South cross-hole test, taking into account the heterogeneities.

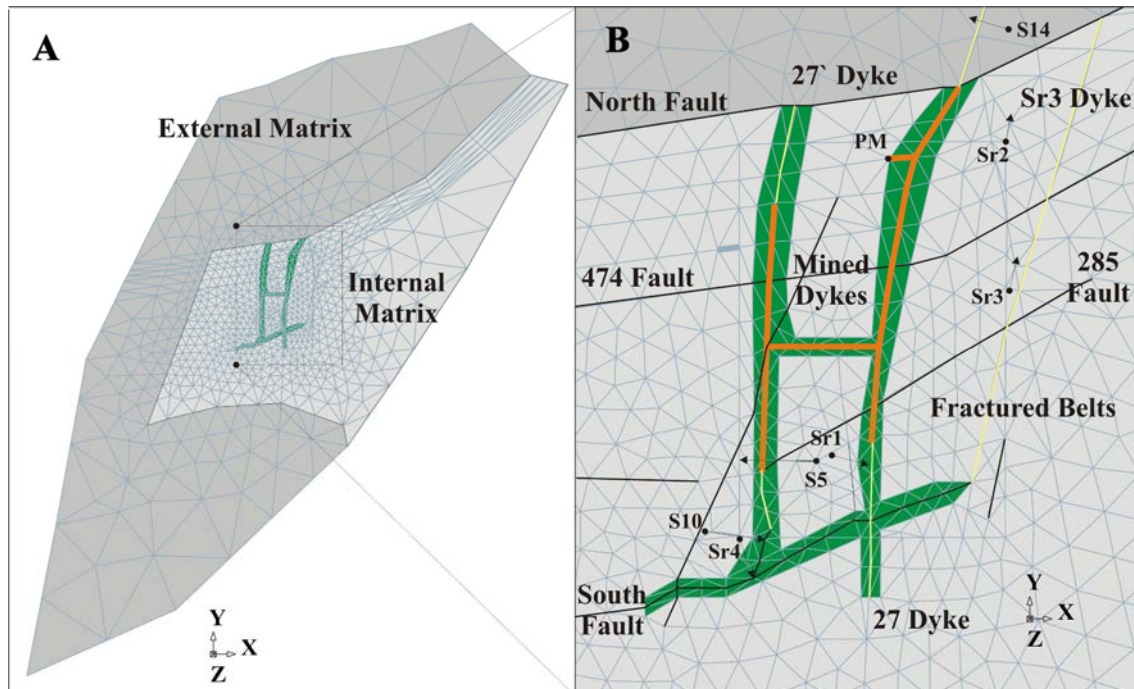


Figure 6: Model geometry. The model consists of two areas The “hydraulic models matrix” is the area where are concentrated the knowledge, the matrix is treated as equivalent porous media with the main structures inside. The “external matrix” is just an extension towards the boundaries, equivalent porous media without identified fractures. The hydraulic conductivity of the latter will be higher, since it is treated as an equivalent porous medium, where the main structures have not been identified. At the local level (right picture), the main structures are explicitly taken into account, including the fractures, dykes 27, 27’ and SR3, and the mine itself, which is excavated in both dykes. The structures are represented by means of two-dimensional elements. The Maderos creek is embedded in the Southern fault. Projections of the boreholes that are closer to the mine are represented by a black dot on surface and by an arrow at the borehole end.

Figure 26 shows a planar view of the geometry introduced in the model. The granitic matrix has been divided into two zones, depending on the degree of characterisation of the whole area. On the one hand, the internal matrix, which belonged to the domain of a previous interpretation model, represents all the fractures identified

around the mine in great detail. On the other hand, the external matrix does include all the structures (because they have not been identified). The conductivity of the external matrix includes the effect of the unidentified fracturing, so it has larger hydraulic conductivities than the internal matrix.

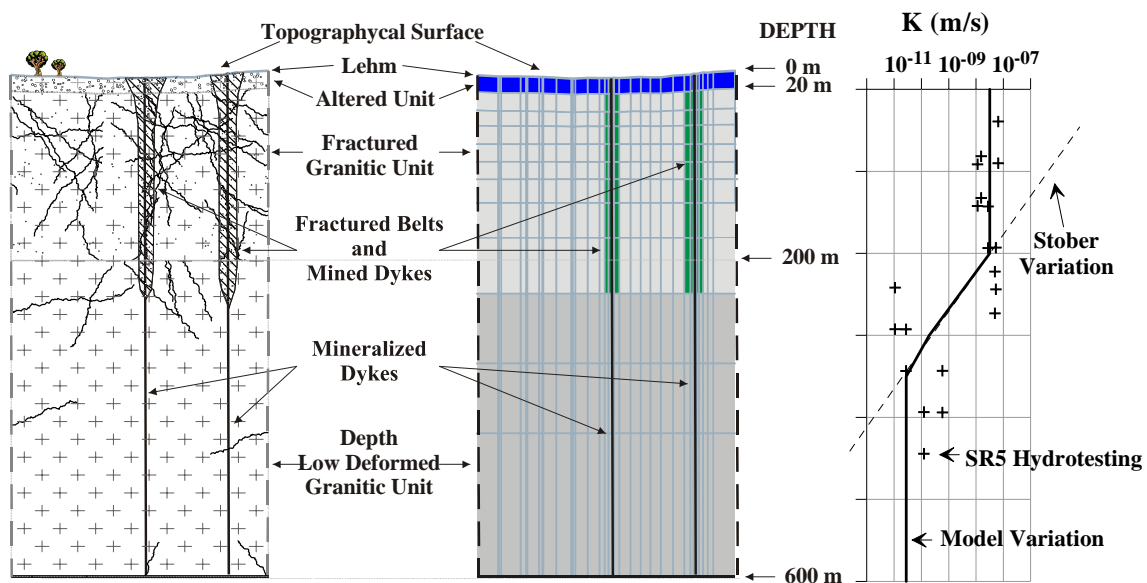


Figure 7: Schematic vertical section representing variations in data derived from the hydraulic characterization of borehole SR5 (500-m deep) indicate that hydraulic conductivity changes with depth. This fact was studied by [Stober \(1997\)](#). The model uses a modification of Stober's equation: hydraulic conductivity is kept constant up to the base of the fractured granitic unit (200 m), then changes with depth down to 350 m. From there, it remains constant down to the model bottom.

The model reaches up to 600m depth to include all measurements (SR5 borehole reached 500m depth) (Figure 7). The different units have been represented in the model. The first, superficial layer is formed by the lehm (two-dimensional elements), which consists of altered, disaggregated and washed granite (like granitic sand) and possess a high hydraulic conductivity. This layer drains rapidly in humid seasons, but, in dry seasons, practically does not carry water. The altered unit reaches 20-m depth, according to geophysics and borehole samples. It is highly weathered, but conserves the granite structure. Their hydraulic conductivity and porosity are higher than those of low-deformed granite, due to the decomposition of feldspar. The fractured granitic unit could be identified by geophysics, and corroborated by the hydraulic characterization of a 500m deep borehole (Figure 7), which was drilled in the matrix, far from the affection originated by the mine. At this depth, there is a reduction in hydraulic conductivity,

which was almost constant up to this horizon. In this unit, the granite does not behave like the altered unit, but its fracturing index is high and, therefore, its effective hydraulic conductivity is higher than the non-deformed granite. Finally, the non-deformed granitic unit, contrarily to the other units, has lower fracturing index and effective hydraulic conductivity.

The gradation in the physical properties of granite with depth is reflected in the reduction of the matrix effective hydraulic conductivity of the model. The upper units (lehm and altered granitic unit) are treated as separated hydraulic conductivity zones, but a unique value is adopted for the fractured and non-deformed units. The behaviour of effective hydraulic conductivity with depth between these two units is represented in the model by means of a lineal relationship proposed by [Stober \(1997\)](#), based on a study on different granites around the world. In this case (Figure 7), conductivity has been kept constant up to 200m, whilst the Stober's equation has been applied between 200 and 350m depth; below 350m, again a constant value has been adopted. This modification is due to the adaptation of Stober's equation to the data obtained in this study area.

The storativity also decreases with depth. In this case, it has been implemented a linear reduction of one order of magnitude between the surface and the bottom (600m deep), based on the results obtained from hydraulic tests.

A zoom in the central part of the model (Figure 26, right) shows the structures included in the model. Both matrix zones and fractured belts are simulated by means of three-dimensional elements; fractures are reproduced with two-dimensional elements (lines in the figure); finally, boreholes are introduced as one-dimensional elements (points in the figure).

Structures included in the model (Figure 28) through two-dimensional elements preserve their azimuth, dip and interception points with the boreholes. In general, they are subverticals, except for the North fault, which is leaned in the surface and cutted, displaced and tilted by fractures 474 and 285. The mine is also treated with two-dimensional elements, because it corresponds to the mining of part of dykes 27 and 27' (planar structures).



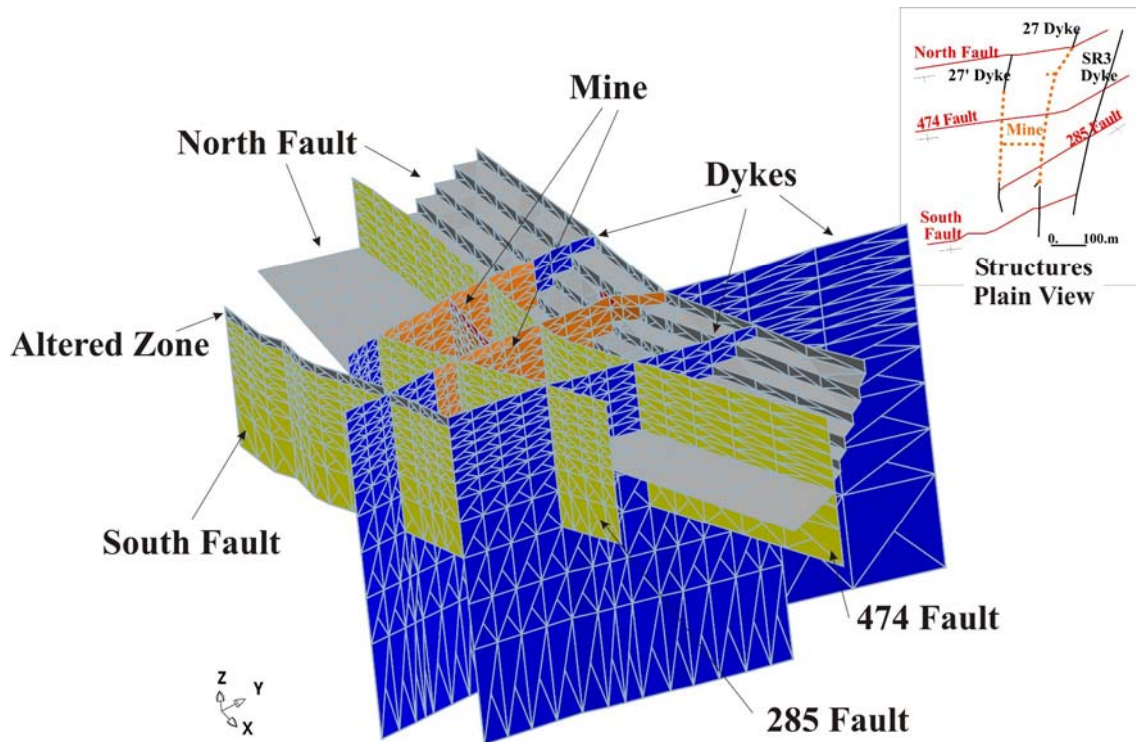


Figure 8: Main structures implemented in the model as planar structures. They are defined by two-dimensional elements. The model honours surface traces and dips. Downwards extension of these structures is performed with the aid of geophysics, structural geology and intersections at boreholes. The Northern fault is the more vertical one at its upper section, and it is cut and disconnected by faults 474 and 285 towards the South. The mine is also represented by means of two-dimensional elements, because it results from the exploitation of the dykes. The Southern fault is zoned at the surface, in order to reproduce the altered zone in which the stream is embedded, where most of the water flows.

#### 4.1. Model calibration of the cross-hole south test

Once the conceptual model is built and the numerical model implemented, a cross-hole test conducted downstream the mine (South test) is calibrated. As initial parameters, those obtained from interpretation of the test with Theis' model are taken. Values of each observation point are assigned to the structure or unit where it is located. The interpretation model of the South cross-hole test works with drawdowns. These are drawdowns are calculated from the measurements registered prior the start of the pumping at each observation point. The model boundaries have been placed at a distance large enough to impose a zero drawdown condition. Table I summarises the results obtained after calibrating the test.

Table I: Parameters obtained after calibration of the South cross-hole test. Units are written in m and sec, but the right dimensions (associated to the scale of each structure in the model) are explicitly defined. Transmissivity values indicate which it changes with depth: the first value holds for the upper 250m (constant parameter), the second value applies to the bottom of the domain –both for the matrix and the fractured belts. The storativity of the “fractured belts lehm” is negligible in the model ( $1.0 \cdot 10^{-30}$ ), to prevent the artifact that water might be withdrawn from that zone.

PARAMETERS (m and s)	DIMENSIONS	TRANSMISIVITY	STORATIVITY
Matrix	3D	$2.1 \cdot 10^{-10} / 7.7 \cdot 10^{-14}$	$1.1 \cdot 10^{-8}$
Fractured Belts	3D	$1.5 \cdot 10^{-8} / 1.5 \cdot 10^{-10}$	$1.0 \cdot 10^{-7}$
Mined Dykes	2D	0.1	$2.7 \cdot 10^{-3}$
Dykes	2D	$6.4 \cdot 10^{-7}$	$1.0 \cdot 10^{-7}$
S10 Fracture	2D	$1.07 \cdot 10^{-5}$	$1.0 \cdot 10^{-7}$
285 Fracture	2D	$2.0 \cdot 10^{-5}$	$1.0 \cdot 10^{-7}$
South Fault	2D	$1.9 \cdot 10^{-5}$	$1.0 \cdot 10^{-7}$
SR1-3 Fracture	2D	$1.1 \cdot 10^{-6}$	$1.0 \cdot 10^{-7}$
Lehm	2D	$1.8 \cdot 10^{-5}$	$3.6 \cdot 10^{-3}$
South Fault-Maderos Str.	2D	$1.8 \cdot 10^{-7}$	$1.7 \cdot 10^{-4}$
S10 Borehole	1D	1	$4.3 \cdot 10^{-6}$
S5 Borehole	1D	1	$4.3 \cdot 10^{-6}$
SR4-2 Borehole	1D	1	$4.3 \cdot 10^{-6}$
Altered Unit	3D	$2.6 \cdot 10^{-9}$	$4.3 \cdot 10^{-6}$
Fractured Belts Lehm	2D	$1.9 \cdot 10^{-4}$	$1.0 \cdot 10^{-30}$

DIMENSION--> 1D: K ( $m \cdot s^{-1}$ ), Ss ( $m^{-1}$ ); 2D: T ( $m^2 \cdot s^{-1}$ ), S (-); 3D: K ( $m \cdot s^{-1}$ ), Ss ( $m^{-1}$ )

Figure 9 represents the resulting fits. Graphs maintain the vertical scale to ease a comparison among the responses. Pumping point is SR4-1, intercepting the South fault. Observation points S10 and SR1-3 respond rapidly to the stress, since they are connected to the pumping point through small structures that form the fractured belts (simplified in the model as fracture S10 and fracture SR1-3), which intercept the Southern fault. The remaining observation points are not that well connected with the pumping point. PM is the mine well, whose response is completely damped by this. Observation points S5 and SR1-2 cut dykes 27' and 27, respectively, close to the mine.

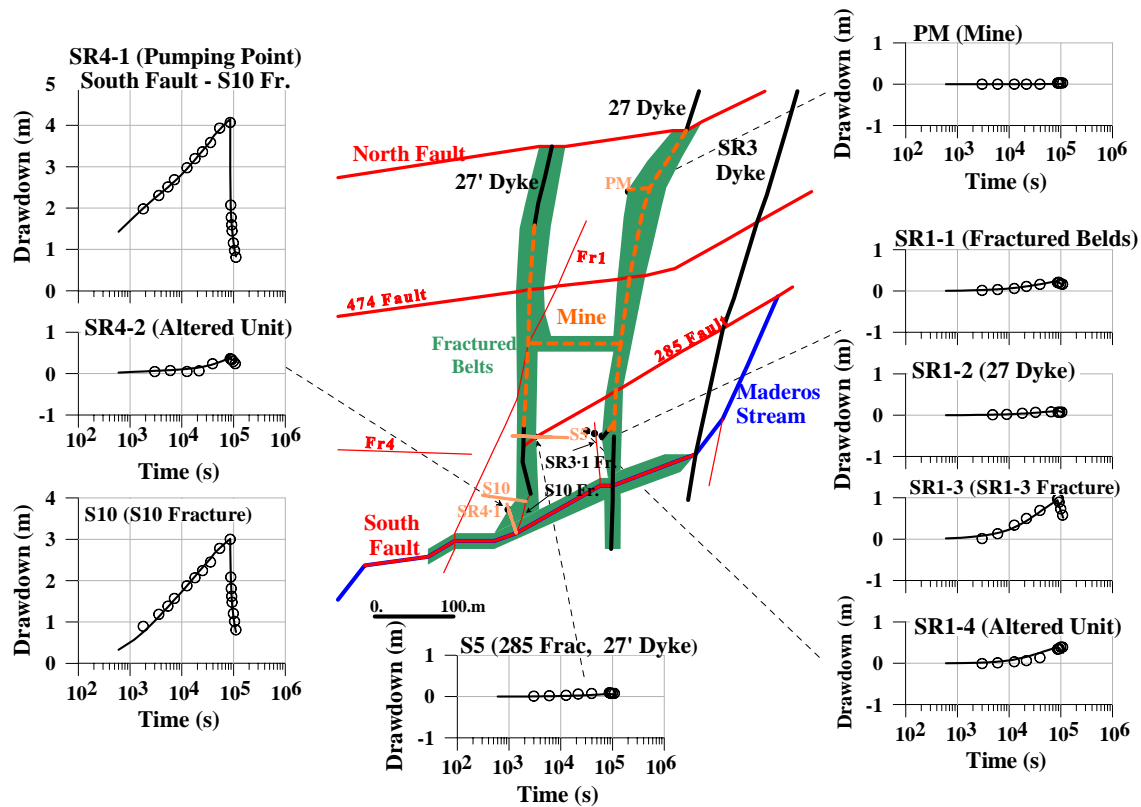


Figure 9: Results (line) obtained after calibrating the SR4-1 cross-hole test data (dots) with the three-dimensional model.

The pumping withdraws water mainly from the superficial layer (lehm), draining it through the bed of Maderos stream, where water flows subsuperficially. Also, water comes from the mine and the altered granitic unit. Flow channels through the fractures (South fault, fractured belts, dykes) towards the pumping point.

#### 4.2. Prediction of pumping from the mine

A four month pumping test from the mine was made, and was carried out at an average flowrate of  $0.0025 \text{ m}^3 \cdot \text{s}^{-1}$ . All boreholes were used as observation points (Figure 10). As for the interpretation of the South cross-hole test, all observations have been introduced as drawdowns calculated from the measurements registered prior the start of the pumping (assumed steady state). Using the calibrated parameters of the analysis of the SR4-1 cross-hole test, a simulation was made to predict the behaviour of this pumping (Figure 10).

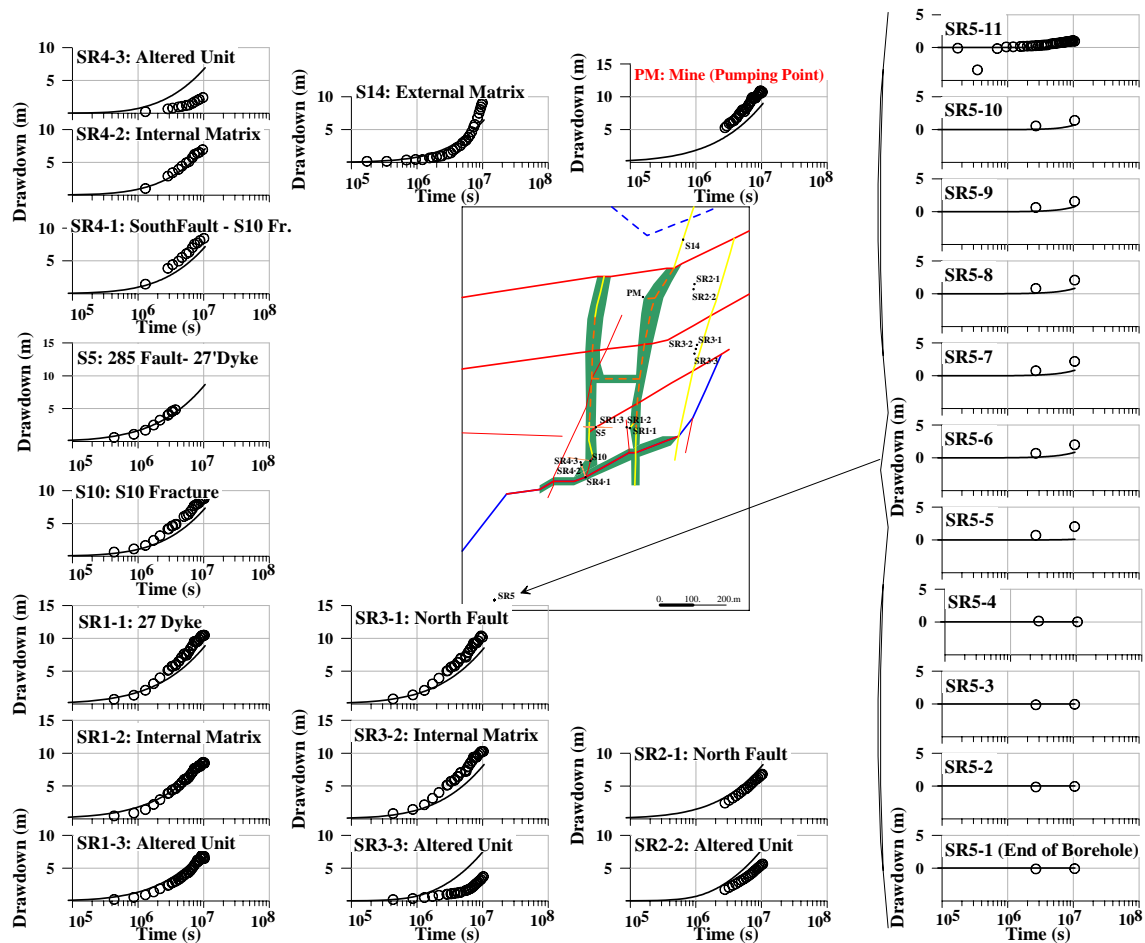


Figure 10: Blind prediction of the long term pumping of the mine (point PM), using calibrated with the SR4-1 cross-hole test. This pumping lasted for four months, and its influence reached all the observation points.

Despite this, it seems that the calculated specific yield for the South cross-hole test model is too. It can be due to the fact that the whole hydraulic characterization of the zone was done during the winter season and within a wet interannual cycle, so that the entire zone was fully saturated. In the prediction, it can be observed that most of the water comes from the lehm, which is a very conductive layer and has a high specific yield ( $3.6 \cdot 10^{-3}$ ), whilst the altered unit specific yield is set at  $4.6 \cdot 10^{-6} \text{ m}^{-1}$ . The mine pumping was carried out in summer, when piezometric heads are lower and the upper units are unsaturated.

A model calibration has also been completed to verify this hypothesis (Figure 11). Numerical results tend to reduce the storage coefficient of the lehm ( $4 \cdot 10^{-5}$ ) and to increase the specific yield of the altered unit ( $1.3 \cdot 10^{-4} \text{ m}^{-1}$ ). This artefact is needed to be able to withdraw water from the altered unit, which is the actual storage unit in dry periods.

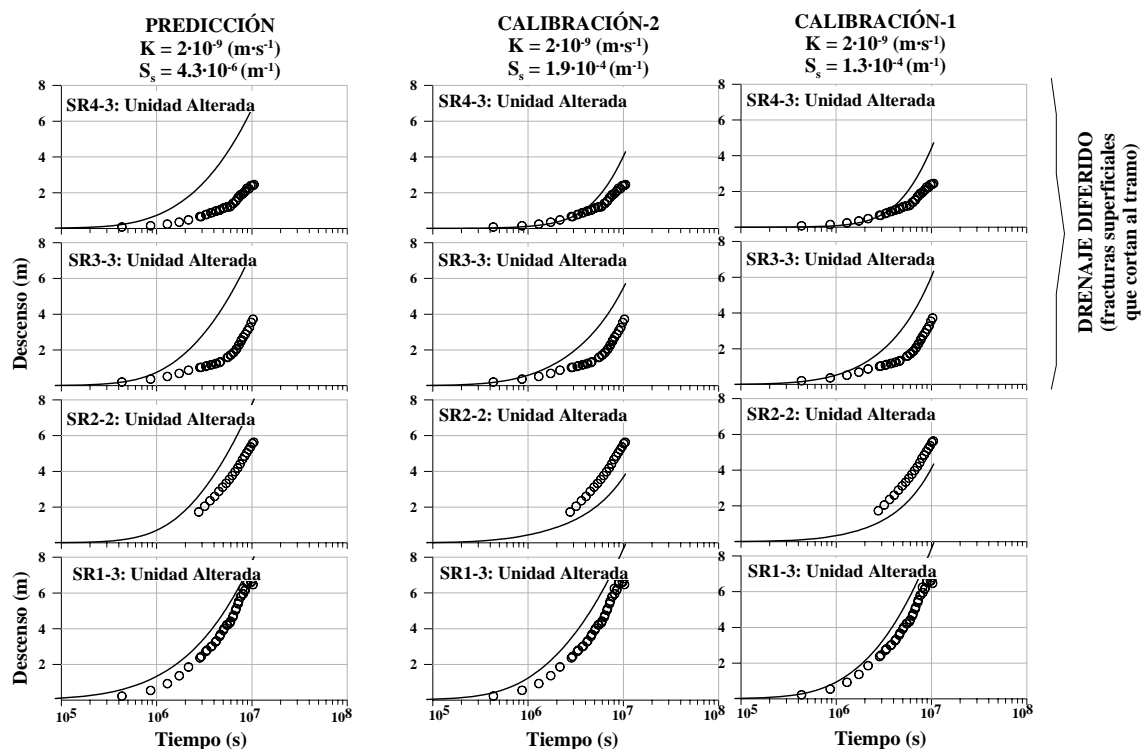


Figure 11: Fits obtained from the pumping test calibration model.

Points with poorer fits are those placed within the altered zone. If we pay attention to the responses measured in those points, it can be deduced that SR4-3 and SR3-3 are subjected to a delayed drainage effect (Figure 12). This fact can be explained by the proximity to a very conductive fracture, which was identified close to the wellhead of borehole SR3 (SR3-3), but it has not been explicitly included in the model because there was not enough information about its direction, dip and connectivities. Borehole SR4 is drilled in one of the most fractured zones, so that there could be one fracture causing this effect in the upper zone of the altered zone.

However, borehole SR2-2 gives a lower drawdown than the measured value, whilst SR1-3 is higher. This may be due to heterogeneities in the altered unit, which is taken as homogeneous in the model.

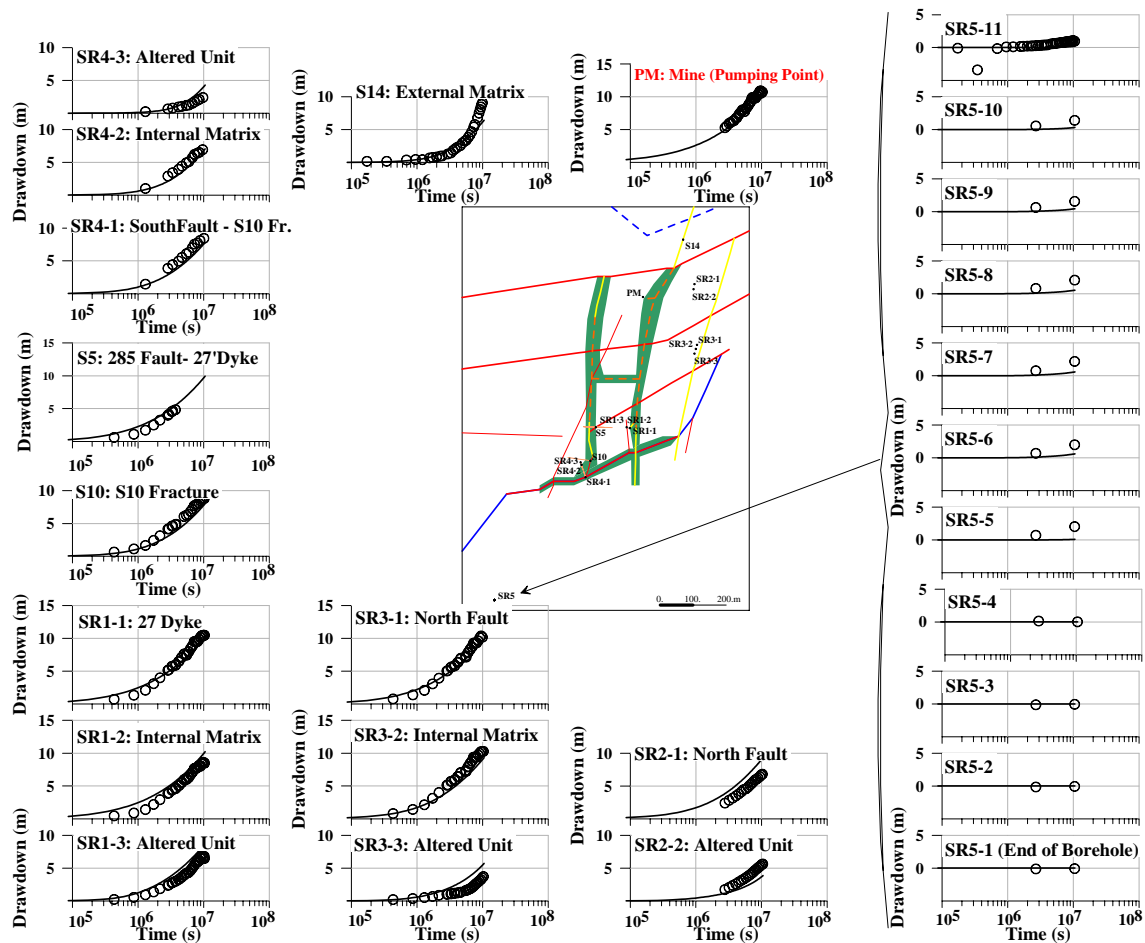


Figure 12: Comparison between altered unit observation points at the prediction and calibration.

## 5. DISCUSSION AND CONCLUSIONS

The main objective of this work is to present the application of the methodology described in [Martinez-Landa and Carrera \(2005a\)](#) to characterize low-permeability fractured media. During the development of this work, values of transmissivity estimated at different scales by considering the medium as homogeneous have been found. When plotting these values against the representative field scale, it can be observed that there is a progressive increment of transmissivity with the scale. If the main heterogeneities of the area are explicitly taken into account, then the scale effect can be explained, because such structures are responsible of the apparent increase in the hydraulic conductivity of the medium. In the lower-scale tests (mine pumping), transmissivities are lower than in the more local cross-hole tests. This can be due to the fact that local-scale tests, which have a shorter duration, withdraw the directly from the more transmissive structures, and, thus, do not affect the matrix. The mine pumping, on the contrary, had a length of 4 months and provoked responses in all observation points

because it integrates the matrix effect, which contributes to decrease the average values of effective transmissivity in the area. Furthermore, the only pumping during summer occurs at the mine, since phreatic levels are below the lehm layer and also below some of the more conductive structures in the altered unit. This causes the effective transmissivities of the test to be lower than those calculated if the test had been performed in winter, as is the case of most of the tests of the project. This explains why the predictive model tends to obtain heads that are lower than the measurements.

Taking that fact into account, together with the results of calibrating the South cross-hole tests, it has been possible to predict a large-scale pumping from the mine. Predicting actions on the medium at scales that are different from the calibration scale supports the reliability of the adopted methodology for modelling low-permeability fractured media, which is based on a mixed approach.





## GENERAL CONCLUSIONS

The methodology presented in this work allows identifying the main fractures through which most of groundwater flows at different scales. To represent these fractures, it has been adopted a mixed modelling approach, which simulate a continuum medium where the dominating fractures are represented explicitly. The main conclusions concerning the advantages of this methodology are the following.

1. Using 3-D numerical models aids in integrating data and reproducing the effect of heterogeneities, such as fractures and their connections. The use of measurements recorded at all observation points, whether or not affected by the hydraulic tests, makes it possible to achieve a better simulation of the medium response. This helps in understanding the behaviour of the system and explaining all measurements in a consistent way.
2. The hydraulic parameters obtained after calibrating hydraulic tests separately with the same conceptual model are consistent among them. A unique conceptual model can thus be used to calibrate problems at different scales. This is due to the bidimensional treatment of the fractures, because their influence is local and refining the mesh around them allows facing scale changes without modifying the geometry.
3. A preliminary interpretation of the tests is needed. This can be done using standard analytical methods that assume a homogeneous medium. The results obtained from these interpretations can be summarised as follows:

-Short-range pulse tests yield point values of hydraulic conductivity or transmissivity. Most of these are low, but there is still a significant range of variation. Low values of average conductivity reflect that the majority of the tested intervals are representative of the matrix hydraulic conductivity, but a few intervals have abnormally high values because they intercept fractures.

-As the test scale grows (recovery, cross-hole tests), the average hydraulic conductivity increases. This can be explained because zones of high hydraulic conductivities are hydraulically well interconnected and therefore control permeability at larger scales.

The equivalent hydraulic conductivity of the medium increases with the scale of the test, but pulse tests (point measurements) may already provide about the magnitude of the parameters. In fact, when hydraulically dominant fractures were identified at the FEBEX site, we could observe that the highest point values were observed at intervals intersected by these fractures. Less permeable intervals (much less permeable) were associated to rock portions that were treated as porous medium, regardless of the actual degree of fracturing.

4. To predict hydraulic conductivities at a greater scale, it is necessary to build a large scale model that incorporates point values and the geological information concerning connectivities. The application to Mina Ratones shows that an adequate characterization of the domain can yield models that are appropriate for scales much larger than that of the initial characterization and even for different flow regime.

---

## REFERENCES

- Alcolea, A., J.Carrera and A.Medina (2005) Pilot points method incorporating prior information for solving the groundwater flow inverse problem, *Submitted*.
- Anderson, J. and R.Thunvik (1986). Predicting mass transport in discrete fracture networks with the aid of geometrical field data, *Water Resour.Res.*, **22**(13): 1942-1950.
- Ando K., A.Kostner and S.P.Neuman (2003). Stochastic continuum modelling of flow and transport in a crystalline rock mass: Fanay-Augères, France, revisited. *Hydrogeol. J.* **11**: 521-535.
- Barker, J.A. (1988). A generalized radial flow model for hydraulic tests in fractured rock, *Water Resour.Res.*, **24**(10): 1796-1804.
- Berkowitz, B. (2002). Characterizing flow and transport in fractured geological media: A review, *Adv Water Resour.*, **25**: 861-884.
- Babiker M. and A.Gudmundsson (2004) The effects of dykes and faults on groundwater flow in an arid land: the Red Sea Hills, Sudan. *J.Hydrol* **297** (1-4): 256-273.
- Blümling, P. and G.Sattle (1988). Tomographic investigations. NAGRA Bull. Spec.Ed. pp. 35-40.
- Bodin J., F.Delay and G.de Marsily (2003). Solute transport in a single fracture with negligible matrix permeability: 1.fundamental mechanisms. *Hydrogeol. J.* **11**:418-433.
- Brace, W.F. (1984). Permeability of crystalline rocks: new in situ measurements. *J Geophys Res*, **89**, B6, 4327-4330.
- Bradbury K.R. and M.A.Muldoon (1990). Hydraulic conductivity determinations in unlithified glacial and fluvial materials, In Nielson D.M. and Johnson, A.I., eds., *Ground Water and Vadose Zone monitoring*, ASTM STP 1053, 138-151.
- Bredehoeft, J.D. and S.S.Papadopoulos (1980). A method for determining the hydraulic properties of tight formations. *Water Resour.Res.*, **16**(1): 233-238.
- Butler, J.J. and J.M.Healey (1998). Relationship between pumping-test and slug-test parameters: scale effect or artefact?, *Ground Water* **36**(2): 305-313.

- 
- Cacas ,M.C., E.Ledoux, G.de Marsily, B.Tillie, A.Barbreau (1990). Modeling fracture flow with a stochastic discrete fracture network: calibration and validation: 1. The flow model, *Water Resour.Res.*, **26**(3): 479-489.
- Clauser C. (1992). Permeability of crystalline rocks. *EOS Trans AGU*, **73**(21): 233-238.
- Carbonell, J.A., A.Pérez-Paricio and J.Carrera (1997). MARIAJ-IV: Programa de calibración automática de ensayos de bombeo. Modelos analíticos y numéricos. ETSECCPB, UPC, Barcelona.
- Carbonell, R. y A.Perez-Estaún (1999). Estudios geológico-estructurales y geofísicos. Tomo II: Caracterización sísmica del entorno de mina Ratones. Proyecto Ratones. ENRESA Internal Report: 10·CJA·IF·03.
- Carrera, J. and J. Heredia (1988). Inverse modelling of the Chalk River Block, HYDROCOIN LEVEL 2/Case3 and Level 3/Case5A. NAGRA TB 88-14. pp.117
- Carrera, J., J. Heredia, S. Vomvoris and P. Hufschmied (1990) Fracture Flow Modelling: Application of automatic calibration techniques to a small fractured Monzonitic Gneiss Block. Hydrogeology of Low Permeability Environments. (Eds.S.P.Neuman\I.Neretnieks), IAHPV, Hydrogeology, Selected Papers, Vol. **2**, pp 115-167.
- Carrera, J., S.F. Mousavi, E. Usunoff, X. Sanchez-Vila and G. Galarza (1993). A discussion on validation of hydrogeological models. *Reliability Engineering and system safety*, **42**, pp. 201-216.
- Carrera, J. and L.Martinez-Landa (1999). Mixed discrete-continuum models: a summary of experiences in test interpretation and model prediction. *Dynamics of Fluids in Fracture Rocks: concepts and recent advances*. (Boris Faybishenko. Paul A. Witherspoon, Sally M. Benson), Berkeley, USA, pp. 251-265.
- Carrera, J. and L. Martínez-Landa (2000). Mixed discrete-continuum models: a summary of experiences in test interpretation and model prediction. Dynamics of Fluids in Fractured Rock, Geophysical Monograph **122**: 251-265, AGU.
- Castaing C., A.Genter, B.Bourgine, J.P.Chilès, J.Wendiling and P.Siegel (2002). Taking into account the complexity of natural fracture systems in reservoir single-phase modelling. *Journal of Hydrology*, **266**: 83-98.
-

- 
- Day-Lewis, F., P.A.Hsieh and S.M.Gorelick (2000). Identifying fracture-zone geometry using simulated annealing and hydraulic-connection data, *Water Resour.Res.*, **36**(7): 1707-1721.
- Davey Mauldon,A., K.Karasaki, S.J.Martel, J.C.S.Long, M.Landsfield and A.Mensch, (1993). An inverse technique for developing models for fluid flow in fracture systems using simulated annealing, *Water Resour.Res.*, **29**(11): 3775-3789.
- Dershowitz, W.S. (1984). Rock Joint System. Ph.D. dissertation, Massachusetts Institute of Technology, Cambridge, Mass.
- Dershowitz W.S. P.Wallmann, J.E. Geier and G.Lee (1991). Discrete Fractured Network Modeling of Tracer Migration Experiments at the SCV Site. SKB Report 91-23, Swedish Nuclear Power and Waste Management Co, Stockholm, Sweden.
- Di Federico, V. and S.P.Neuman (1998). Flow in multiscale log conductivity fields with truncated power variograms. *Water Resour.Res.*, **34**(5), 975-987.
- Dverstorp, B. and J.Anderson (1989). Applicant of the discrete fracture network concept with field data: possibilities of model calibration and validation, *Water Resour.Res.*, **25**(3), 540-550.
- ENRESA (1995) Almacenamiento geológico profundo de residuos radioactivos de alta actividad. Diseños conceptuales genéricos. Publicación técnica nº11/95. Madrid.
- ENRESA (1996). Memoria Cartografía Geológica y Estructural. Rocas Plutónicas, Albalá (G111). ENRESA Internal Report (94-G111-IF), Madrid, Vol.II, 249pp.
- ENRESA (1998) FEBEX Full-scale engineered barrier experiment in crystalline host rock: Final design and installation of the “in situ” test at Grimsel, Pub. Técnica de ENRESA 12/98.
- Escuder Viruete J. y A.Pérez-Estaún (1998). Fracturación en Mina Ratones. Informe Final 1: Estructura, Proyecto Ratones. ENRESA Internal Report: 10·CJA·IF·01.
- Escuder Viruete, J. (1999). Estudios geológico-estructurales y geofísicos. Tomo I: Estudios geológicos. Proyecto Ratones. ENRESA Internal Report: 10·CJA·IF·03.
-

- Escuder Viruete, J., R. Carbonell, D. Martí and A. Perez-Estaún (2003a). 3-D stochastic modeling and simulation of fault zones in the Albalá granitic pluton, SW Iberian Variscan Massif. *Journal of Structural Geology*, **25** (2003): 1487-1506.
- Escuder Viruete, J., R. Carbonell, D. Martí, M.J. Jurado and A. Perez-Estaún (2003b). Architecture of fault zones determined from outcrop, cores, 3-D seismic tomography and geostatistical modelling: example from the Albalá Granitic Pluton, SW Iberian Variscan Massif. *Tectonophysics*, **361**: 97-120.
- Fierz T. (1996). FEBEX Instrumentation of BOUS 85-001 and BOUS 85-002, FBX 95-001 and FBX95-002, and radial boreholes. SOLEXPPTS Report nº 1008, Schwerzenbach.
- Fuentes-Cantillana J.L. and J.L. García-Siñeriz (1998). FEBEX Full-scale engineered barrier experiment in crystalline host rock: Final design and installation of the “in situ” test at Grimsel, Pub. Técnica de ENRESA 12/98, 1998.
- Galarza, G., J. Carrera and A. Medina (1999). Computational techniques for optimization of problems involving non-linear transient simulations. *Int. J. Numer. Meth. Engng.* **45**: 319-334.
- Gómez, P., A. Garralón, M<sup>a</sup>J. Turrero, L. Sánchez, A. Melón, B. Ruiz y F. Fernandez (1999). Impacto medioambiental de la restauración de la Mina Ratones en las aguas subterráneas. Modelo Hidrogeoquímico. Proyecto Ratones. ENRESA Internal Report: 10-CIE-IF-1-99. CIEMAT/DIAE/54211/7/99.
- Gómez, P., A. Garralón, M<sup>a</sup>J. Turrero, L. Sánchez, B. Ruiz y A. Melón (2001). Estudio del efecto de la restauración de la Mina Ratones en las aguas subterráneas. Proyecto Ratones. ENRESA Internal Report: 10-CIE-IF-1-00. CIEMAT/DIAE/54440/1/00.
- Gomez, P. (2002). Estudio del impacto de la mina de uranio “Los Ratones” (Albalá, Cáceres) sobre las aguas superficiales y subterráneas: modelación hidrogeoquímica. Tesis doctoral.
- Gomez-Hernandez, J., H.J.W.M. Hendricks Franssen, A. Shauquillo and J.E. Capilla (2000). Calibration of 3-D transient groundwater flow models for fractured rock. Proceedings Model CARE'99. International Conference on Calibration and reliability in groundwater modeling, Zürich, Switzerland.
-

- 
- Gudmundsson A. (2000). Active fault zones and groundwater flow. *Geophysical Research Letters*, **27**(18): 2993-2996.
- Guimerà, J., L.Vives and J.Carrera (1995). A discussion of scale effects on hydraulic conductivity at a granitic site (El Berrocal, Spain), *Geophysical Research Letters*, **22**(11), 1449-1452.
- Guimerà, J., J.Carrera, L.Martinez-Landa, E.Vazquez-Suñè, F.Ortuño, T.Fierz, C. Bülher, L.Vives, P.Meier, A.Medina, M.Saaltink, B.Ruiz and J.Pardillo (1998). Hydrogeological characterization and modeling. FEBEX project report 70·UPC·M·1·1001. Technical University of Catalonia, Barcelona.
- Gutjhar, A.L., L.W.Gelhar, A.A.Bakr and J.R.MacMillan (1978). Stochastic analysis of spatial variability in subsurface flow, 2. Evaluation and application, *Water Resour.Res.*, **14**, 953-959.
- Gylling B., L.Moreno and I.Neretnieks (1999). The channel network model – a tool for transport simulations in fractured media. *Ground Water* **37**(3): 367-375.
- Hendricks Franssen, H.J.W.M. and J.J.Gomez-Hernández (2002). 3D inverse modelling of groundwater flow at a fractured site using a stochastic continuum model with multiple statistical populations. *Stoch. Envir. Res. and Risk Ass.*, **16**: 155-174.
- Horner D.R. (1951). Pressure build-up in wells. Third world pet. Congress, E.J. Brill, Leiden II, pp. 503-521.
- Hsieh P.A. and S.P.Neuman (1985) Field determination of the three-dimensional hydraulic conductivity tensor of anisotropic media. 1. Theory, *Water Resour.Res.*, **21**(11): 1655-1666.
- Illman, W.A. and S.P.Neuman (2000). Type-curve interpretation of multi-rate single-hole pneumatic injection tests in unsaturated fractured rock, *Ground Water*, **38**: 899-911.
- Illman W.A. and S.P.Neuman (2001). Type curve interpretation of a cross-hole pneumatic injection test in unsaturated fractured tuff. *Water Resour.Res.*, **37**(3), 583-603.
- Illman W.A. and S.P.Neuman (2003). Steady-state analysis of cross-hole pneumatic injection tests in unsaturated fractured tuff. *J.Hydrol.* **281**(1-2), 54-72.
-

- Illman, W. A., S. P. Neuman, V. V. Vesselinov, and A. G. Guzman (2003). Strong evidence for permeability scale effect in fractured rocks, *Groundwater Engineering-Recent Advances*, Kono, I., M. Nishigaki, M. Komatsu (eds), A.A. Balkema Publishers 437-442.
- Illman W.A. (2004). Analysis of permeability scaling within single boreholes. *Geophys Res Lett.*, **31**(5).
- Julivert, M., J.M.Fontbote, A.Ribeiro and L.Conde (1972). Mapa Tectónico de la Península Ibérica y Baleares. E. 1:1000000. IGME, Madrid.
- Jurado, M.J. y A.Perez-Estaún (1999). Estudios geológico-estructurales y geofísicos. Tomo III: Geofísica en sondeos: diagraffías, BHTV, dipmeter y sónicos. Proyecto Ratones. ENRESA Internal Report: 10-CJA-IF-03.
- Jurado, M.J. (2000). Avance sobre evaluación de la testificación geofísica de sondeos adquirida en mina Ratones. Proyecto Ratones. ENRESA Internal Report: 10-CJA-IA-12, CSIC-IJA.
- Kimmeier, F., P.Perrochet, R.Andrews and L.Kiraly (1985). Simulation par Modele Mathematique des Ecoulements Souterrains entre les Alpes et la Foret Noire. NAGRA Technischer Bericht, NTB 84-50.
- Kiraly, L. (1985). FEM301 A three-dimensional model for groundwater flow simulation. NAGRA NTB 84-49, Baden, Switzerland.
- Knudby C. and J.Carrera (2005a) On the Relationship Between Geostatistical, Flow and Transport Connectivity Measures. *Adv Water Resour. In Press*.
- Knudby C. and J.Carrera (2005b) Apparent Hydraulic Diffusivity as an Indicator of Connectivity. *Submitted*.
- Lee J.Y. and K.K.Lee (1999). Analysis of the quality of parameter estimates from repeated pumping and slug tests in a fractured porous aquifer system in Wonju, Korea. *Ground Water* **37**: 692-700.
- Long, J.C.S., S.Remer, C.R.Wilson and P.A.Witherspoon (1982). Porous media equivalents for networks of discontinuous fractures, *Water Resour.Res.*, **18**(3): 645-658.



- 
- Long, J.C.S. and D.M.Billaux (1987). From field data to fracture network modelling: an exemple incorporating spatial structure. *Water Resour.Res.*, **23**: 1201-1216.
- Long, J.C., K.Karasaki, A.Davey, J.Peterson, M.Landsfied, J.Kemeny and S.Martel, (1991). An inverse approach to the construction of fracture hydrology models conditioned by geophysical data, *Intenational Journal of Rock Mechanics and Mining Sciences and Geomechanical Abstracts*, **28**(213): 121-142.
- Margolin, G., B.Berkowitz and H.Scher (1998). Structure, flow and generalized conductivity scaling in fracture networks, *Water Resour.Res.*, **34**(9): 2103-2121.
- Martí, D., R.Carbonell, A.Trygvason, J.Escuder Viruete and A.Pérez-Estaún (2002). Mapping brittle fracture zones in 3-dimensions: high resolution ravel time seismic tomography in a granitic pluton. *Geophysical Journal International*, **149**: 95-105.
- Martínez-Landa, L., J.Carrera, J.Guimerà, E.Vazquez-Suñé, L.Vives, P.Meier and T.Fierz (2000). Methodology for the hydraulic characterization of a granitic block. Model CARE'99. International Conference on Calibration and reliability in groundwater modeling, Zürich, Switzerland. 20-23 September 1999.
- Martinez-Landa, L., A.Alcahud, J.Jordan and J.Carrera (2004). Modelo hidrogeológico del entorno de la mina Ratones (Albalá, Cáceres). Informe de proyecto: 10-UPC-IF-03.
- Martinez-Landa, L. and J.Carrera (2005a). A methodology to interpret a cross-hole tests in a granite block. *Submitted*
- Martinez-Landa, L. and J.Carrera (2005b) A hydrogeologic model of granite rock as a support to a mine restoration. *Submitted*
- Martinez-Landa, L. and J.Carrera (2005c). A hydrogeologic model of granite rock as a support to a mine restoration. *Submitted*
- Meier, P., P.Fernandez, J.Carrera and J.Guimerà (1995). Results of hydraulic testing in boreholes FBX95-001, FBX95-002, BOUS85-001 y BOUS85-002. FEBEX, Phase I. Intering Report. E.T.S.E.C.C.P.B., Universitat Politècnica de Catalunya.
- Meier, P., J.Carrera and X.Sánchez-Vila (1998). An evaluation of Jacob's method work for the interpretation of pumping test in heterogeneous formations, *Water Resour.Res.*, **34**(5): 1011-1025.
-

- Meier, P., J.Carrera and X.Sanchez-Vila (1999). A numerical study on the relation between transmissivity and specific capacity in heterogeneous aquifers. *Groundwater*, **37**(4),pp. 611-617
- Meier, P. and J.Carrera (2001) Geostatistical inversion of cross-hole pumping tests for identifying preferential flow channels within a shear zone. *Groundwater*, **39**(1),pp. 10-17.
- Moreno L. and I.Neretnieks (1993). Fluid flow and solute transport in a network of channels, *J.Contam.Hydrol.* **14**, 163-192.
- Moreno L. and C.F.Tsang (1994) Flow channeling in strongly heterogeneous porous-media - a numerical study. *Water Resour.Res* **30** (5): 1421-1430.
- Neretnieks, I. (1983). A note on fracture flow dispersion mechanisms in the ground, *Water Resour.Res.*, **19**(2): 364-370.
- Neretnieks, I. (1993). Solute transport in fractured rock- application to radionuclide waste repositories. In: J.Bear, C.F.Tsang and G.de Marsily (Eds.). *Flow and Contaminant Transport in Fractured Rock*. Academic Press, NewYork.
- Neuman, S.P. (1987). Stochastic continuum representation of fractured rock permeability as an alternative to the REV and fracture network concepts, in *Rock Mechanics*. In: Farmer IW, Daemen JJK, Desai CS, Glass CE, Neuman SP (eds). *Proceedings of the 28<sup>th</sup> U.S. Symposium*, Tucson, Arizona. Balkema Rotterdam, pp 533-561.
- Neuman S.P. (1994). Generalized scaling of permeabilities: validation and effect of support scale. *Geophys.Res.Lett.*, **21**(5), 349-352.
- Neuman S.P. (2005). Trends, prospects and challenges in quantifying and transport through fractured rocks. *Hydrogeol. J. In Press*.
- Ortuño F. (2000). Medidas de caudales en túneles excavados en medios de baja permeabilidad, Proyecto FEBEX 70·hyd·1·2·001, UPC Barcelona, 82pp.
- Ortuño, F., E. Floría; G. Carretero y J. Suso. (2000). Caracterización hidráulica de Mina Ratones. Proyecto Ratones. ENRESA Internal Report: 10-AIT-IA-04, grupo de hidrogeología de AITEMIN, Toledo.

- 
- Ortuño F., G.Carretero, L.Martinez-Landa and J.Carrera (2003). Hydraulic characterisation of the FEBEX granite: test performance and field interpretation. Symposium Sitges 2003, Large scale field tests in granite: advances in understanding and research needs.
- Papadopoulos, I.S.; J.D.Bredehoeft and H.H.Cooper (1973). On the analysis of slug test data. *Water Resour.Res.*, **9**(4): 1087-1089.
- Pardillo, J., R.Campos and J.Guimerà (1997). Caracterización geológica de la zona de ensayo FEBEX (Grimsel, Suiza). Informe del proyecto FEBEX 70·IMA·M·2·01, CIEMAT/UPC, Madrid/Barcelona, 52pp.
- Pérez Del Villar, L., J.S. Cózar, J. Pardillo, M. Pelayo y M.A. Labajo (1999). Caracterización mineralógica y geoquímica de las harinas de falla y tapices de fractura del proyecto los Ratones (Albalá, Cáceres). Proyecto Ratones. ENRESA Internal Report: 10·CIE·IF·3·99. CIEMAT/DIAE/54211/6-99.
- Pérez-Estaún, A. (1999). Estudios Geológicos-Estructurales y Geofísicos en Mina Ratones. Informe Final: Conclusiones. Proyecto Ratones. ENRESA Internal Report: 10·CJA·IF·03.
- Pratt, R.G. (1995). Anisotropic velocity tomography for “Field 1” tomographic data at the Grimsel Rock Laboratory. NAGRA. Internal Bericht 95-77.
- Rouleau. A. and J.E.Gale (1985). Statistical characterization of the fracture system in the Stripa granite, Sweden. *Int.J.Rock.Mech.Min.Sci.Geomech.Abstr.* **22**:353-367
- Rovey C.W. and D.S.Cherkauer (1995). Scale dependency of hydraulic conductivity measurements. *Ground Water* **33**(5), 769-780.
- Rovey C.W. (1998). Digital simulation of the scale effect in hydraulic conductivity. *Hydrogeol.J.* **6**, 216-225.
- Rovey C.W. and W.L.Nieman (2001). Wellskins and slug tests: where’s the bias? *J.Hydrol* **243**, 120-132.
- Samper-Calvete J and M.A.García-Vera (1998). Inverse modelling of groundwater flow in the semiarid evaporitic closed basin of Los Monegros, Spain. *Hydrogeol.J.* **6**(1), 33-49.
-

- Sanchez-Vila, X., J. Carrera and J.P. Girardi (1996). Scale effects in transmissivity, *J. Hydrol.*, **183**: 1-22.
- Sanchez-Vila, X., P.M. Meier and J. Carrera (1999). Pumping tests in heterogeneous aquifers: An analytical study of what can be obtained from their interpretation using Jacob's method, *Water Resour. Res.*, **35**(4): 943-952.
- Schad H. and G. Teutsch (1994). Effects of the investigation scale on pumping test results in heterogeneous porous aquifers. *J. Hydrol.*, **159**, 61-77.
- Schulze-Makuch, D., D.A. Carlson, D.S. Cherkauer and P. Malik (1999). Scale dependency of hydraulic conductivity in heterogeneous media, *Ground Water*, **37**(6): 904-919.
- Selroos, J.O., D.D. Walker, A. Ström, B. Gylling and S. Follin (2002). Comparison of alternative modeling approaches for groundwater flow in fractured rock. *J. Hydrol.*, **257**, 174-188.
- Shapiro, A.M. and P.A. Hsieh (1991). Research in fractured-rock hydrogeology: characterizing fluid movement and chemical transport in fractured rock at the Mirror Lake drainage basin. *Proceedings of the Technical Meeting of U.S. Geological Survey Toxic Substances Hydrology Program*, Monterey, Calif., March 11-15, edited by G.E. Mallard and D.A. Aronson (also, Water Resources Investigation Report 91-4034, U.S. Geological Survey), Reston, Va.
- Smith, L. and F.W. Schwarz (1984). An analysis of the influence of fracture geometry on mass transport in fractured media, *Water Resour. Res.*, **20**(9): 1241-1252.
- Stober, I. (1997). Ergebnisse geohydraulischer und hydrochemischer Untersuchungen im Kristallinen Grundgebirge des Schwarzwaldes und seiner Randgebiete. Tübingen.
- Svenson, U. (2001a). A continuum representation of fracture networks. Part I: Method and basic test cases, *J. Hydrol.*, **250**, 170-186.
- Svenson, U. (2001b). A continuum representation of fracture networks. Part II: application to the Äspö Hard Rock laboratory, *J. Hydrol.*, **250**, 187-205.
- Talbot C.J. and M. Sirat (2001). Stress control of hydraulic conductivity in fracture-saturated Swedish bedrock. *Engineering Geology* **61**: 145-153.
-

- 
- Theis, C.V. (1935). The relation between the lowering of the piezometric surface and the rate and duration of discharge of a well using ground-water storage. *Trans.Am.Geophysical Union*, **16**, 519-524.
- Tsang, Y.W., C.F.Tsang, F.V.Hale and B.Dverstorp (1996). Tracer transport in a stochastic continuum model of fractured media, *Water Resour.Res.*,**32**(10), 3077-3092.
- Tsang C.F. and I.Neretnieks (1998). Flow channelling in heterogeneous fractured rocks. *Reviews of Geophysics*, **36**(2): 275-298.
- Vesselinov V.V., S.P Neuman and W.A.Illman (2001). Three-dimensional numerical inversion of pneumatic cross-hole tests in unsaturated fractured tuff. 2. Equivalent parameters, high-resolution stochastic imaging and scale effects. *Water Resour.Res.*, **37**(12), 3019-3041.
- Zlotnik V.A., B.R.Zurbuchen, T.Ptak and G.Teutsch (2000). Support volume and scale effect in hydraulic conductivity: Experimental aspects. Theory, Modeling, and Field Investigation in Hydrogeology. A Special Volume in Honor of Shlomo P.Neuman's 60<sup>th</sup> Birthday. Dongxiao Zhang and C.Larry Winter, Editors.
- Zoback M.D., C.A.Barton, M.Brudy, D.A.Castillo, T.Finkbeiner, B.R.Grollmund, D.B.Moos, P.Peska, C.D.Ward and D.J.Wiprut (2003). Determination of stress orientation and magnitude in deep wells. *International Journal of Rock Mechanics and Mining Sciences* **40**: 1049-1076.